Title
Improving entomological predictions of human West Nile virus disease risk

Author
Stiles, Pascale

Publication Date
2021

Peer reviewed|Thesis/dissertation

Improving entomological predictions of human West Nile virus disease risk

By

PASCALE CLAIRE STILES

DISSERTATION

Submitted in partial satisfaction of the requirements for the degree of

DOCTOR OF PHILOSOPHY

in

Epidemiology

in the

OFFICE OF GRADUATE STUDIES

of the

UNIVERSITY OF CALIFORNIA

DAVIS

Approved:

Christopher Barker, Chair

William Reisen

Woutrina Smith

Committee in Charge

2022

Table of Contents

Acknowledgements

This dissertation has truly been borne from the contributions of countless individuals. First and foremost, Dr. Chris Barker, thank you for your unwavering support and mentorship while pushing me out of my comfort zone and helping me to ask the right questions and become a better scientist and communicator. I am eternally grateful that you gave me the opportunity to join the DART team and have relished the experiences and friendships I've built up over the past 5+ years.

I also wouldn't be at this point without the support of my dissertation committee. Dr. William Reisen and Dr. Woutrina Smith, thank you both for your invaluable feedback and advice, and for keeping me grounded in epidemiology. Thank you also to the other UC Davis professors who have supported me with advice, mentorship, and opportunities along the way, especially Dr. Danielle Harvey, Dr. Irva Hertz-Picciotto, Dr. Geoff Attardo, Dr. Rob Atwill, and Dr. Beatriz Martinez-Lopez.

To my fellow DARTians, especially Karen, Marisa, Sarah, Ania, Olivia, Matteo, and Brad, thank you for making the group such a fun and dynamic place to work. You were always ready to help when I had questions about code, stats, or mosquitoes, and I cherished every conference we attended as a group. My presentations were always better after our late-night hotel practice sessions. Gurman, thank you for spending so many hours driving around the Sacramento Valley in the old, rickety truck with me to collect and count mosquitoes. I'm sure you could have envisioned better ways to spend your summer, and I truly appreciate that you chose to work with us. Emma, thank you for all your help gathering and formatting data and for taking over as the Data Steward – VectorSurv is in good hands.

Jody, Kurt, Shawn, and Mathew, thank you for your patience answering my database questions and helping me navigate the VectorSurv help email. I learned so much about

computer programming through working with you. When I first started working with VectorSurv, it often felt like you were speaking a foreign language, and although sometimes it still felt that way after a few years, at least I knew what an API was.

Thank you to everyone at the MVCAC and CDPH who have given me the opportunity to participate in WNV planning meetings. Those conversations were invaluable to framing my dissertation. Mary Sorensen, Jake Hartle, Joel Buettner, Marcia Reed, and Sarah Wheeler, thank you for all of your advice and input on my chapters. It is because of your feedback that I know my research will have value for mosquito control.

Dr. Cyril Caminade and Prof. Matthew Baylis, thank you for welcoming me into your group in Liverpool for a month-long lab exchange. It was lovely to experience a different research perspective and I learned a great deal about spatial and meteorological data that I have carried with me since.

Thank you to my fellow GGE students and friends for making my time in Davis so enjoyable. I especially want to shout out Laura, Eric, Esther, Gad, Lorie, and Emily. Laura and Eric, thank you for being our California ambassadors and making us fall in love with Mendocino County. Esther and Gad, thank you for your incredible friendship and for being the best TV watching companions (although we still haven't finished Vikings). Lorie, thank you for the great conversations before our Avengers theater nights. Emily, thank you for being the best travel companion and flatmate in Liverpool.

Last but certainly not least, thank you to my partner and absolute rock throughout this crazy adventure, Jerome. You've been by my side from coast to coast and across oceans (literally) and it's not an exaggeration to say that this dissertation would not have been possible without you. And to my loving parents, Bruce and Chantal, thank you for your unwavering encouragement. I wouldn't have gotten to this point if not for the values of perseverance and problem-solving you've instilled since I can remember.

Finally, thank you, reader, for delving into this labor of love (and blood, sweat, and tears) to which I have dedicated the last 5 years.

Abstract

West Nile virus (WNV; family *Flaviviridae*) has been an annual public health concern in the continental United States since its introduction in 1999. It is particularly difficult to determine when and where human infections will occur because WNV is highly focal and amplifies in bird-mosquito cycles with incidental spillover to humans. WNV is transmitted by female mosquitoes in the genus *Culex*, most commonly *Cx. tarsalis*, *Cx. pipiens*, and *Cx. quinquefasciatus*. The mosquitoes' capacity to transmit WNV depends on the environment, particularly temperature, resulting in seasonal cycles with most human cases occurring between July and September. WNV prevention is predominantly through vector management, consisting of a combination of larval and adult control. Integrated vector management programs in California conduct surveillance to monitor mosquito abundance and mosquito infection prevalence as a means for targeting control strategies, but these estimates are not adjusted for biases that could be induced by short-term variation in weather. This dissertation investigates the complicated relationship between environmental factors, entomological surveillance observations, and human WNV disease.

Chapter 1 focused on the relationship between entomological surveillance indicators and risk for human WNV disease. In particular, we evaluated the ability of the vector index (VI), the product of mosquito abundance and infection prevalence, to predict periods of above-average WNV incidence. We used receiver operating characteristic (ROC) curves to identify the VI threshold that maximized sensitivity and specificity of these predictions and found that these thresholds were highly dependent on the dominant vector species in an area and the trap type used for targeting surveillance. We also used statistical models with observed entomological surveillance and human disease data aggregated to different spatial scales to examine the effect of spatial scale on the ability of the VI to predict human WNV disease incidence. These results

found cities to be the best balance between being small enough to be operationally relevant but large enough to have adequate predictive accuracy during high-risk periods.

Chapter 2 considered short-term weather variability as a potential source of bias in entomological surveillance that may affect estimates of WNV disease risk. We collected mosquitoes and gathered weather data from 10 field sites equipped with devices to record mosquito counts, temperature, and wind speed every 15 minutes in the rice-growing region of northern California. We used the 15-minute mosquito data to estimate four outcomes for the primary WNV vector in the study area, *Cx. tarsalis*: the total overnight count, the onset time of evening host-seeking activity, the median time of nightly host-seeking activity, and the hour of peak host-seeking activity. We related each of these outcomes to the wind speed and temperature recorded at a range of times in the afternoon leading to the host-seeking night through statistical models and found both wind speed and temperature at 20:00, or just prior to the onset of host-seeking, to be the best predictors of all four outcomes. These predictable factors will help guide the timing of vector control applications to maximize their effects on the local vector population, thus reducing the overall risk of WNV transmission.

Chapter 3 applied spatio-temporal predictive models that accounted for ecological factors and were capable of highlighting gaps in surveillance coverage for estimating risk of WNV transmission. We used a generalized additive model (GAM) to model the nonlinear weekly seasonal trends of *Cx. tarsalis* abundance in a range of land use types using trap count data for the years 2008-2020 collected by 20 Central Valley mosquito and vector control districts in California. Overall, the model captured strong seasonal patterns in abundance, modified by local land use and ephemeral spatio-temporal anomalies. Models maintained a similar predictive accuracy for out-of-sample data compared to that for the training data set. To determine the ability of the model to extrapolate from known surveillance locations, we then used the GAM to predict weekly *Cx. tarsalis* abundance at unmeasured locations across a 2.5-km grid of the

Central Valley. We found that these predictions were most accurate when the nearest observed trap was within 2 km and one week prior.

Taken together, these three chapters provide a basis for improving WNV risk estimation through entomological surveillance. These chapters will inform efforts to prevent human WNV disease through a more complete understanding of the link between WNV vector dynamics and the risk of human disease, improving the ability to predict risk and target mosquito control.

Introduction: West Nile virus in the United States

History

West Nile virus (WNV) is an arbovirus of the family *Flaviviridae* and is a member of the Japanese encephalitis subgroup (Calisher et al. 1989). It was first isolated from the blood of a febrile woman in the West Nile District of Uganda in 1937 and experiments at that time found it to be neurotropic and immunologically related to Japanese B encephalitis and Saint Louis encephalitis (SLE) viruses (Smithburn et al. 1940). Throughout much of its recorded history, WNV outbreaks were mainly limited to the Mediterranean basin, particularly in Israel, Egypt, and Eastern Europe (Sejvar 2003, Zeller and Schuffenecker 2004, Kramer et al. 2008), until the first identification of WNV in North America in 1999 (Nash et al. 2001). Genetic analyses revealed that these initial North American viral isolates were most closely related to isolates from a goose in Israel the prior year, pointing to the Eastern Mediterranean as the likely source of the virus causing this initial outbreak, possibly through the transport of infected birds or mosquitoes (Lanciotti et al. 1999). WNV then spread rapidly across the continental United States, reaching California by 2003 (Reisen et al. 2004, Murray, Mertens, et al. 2010, Roehrig 2013, Hadfield et al. 2019, Kramer et al. 2019). It is now the most commonly reported arboviral disease in humans in the United States (McDonald et al. 2019). WNV also has the widest geographic range of any arbovirus, being found in both temperate and tropical regions on every continent except Antarctica (Kramer et al. 2008, Ciota and Kramer 2013, Reisen 2013, Ciota 2017).

In California, WNV invaded an area supporting endemic arboviruses including SLE and western equine encephalomyelitis (WEE) viruses (Howitt 1939, Sudia et al. 1971, Reisen, Hardy, et al. 1992, 1995). SLEV is a member of the Japanese encephalitis virus subgroup of the genus *Flavivvirus* and is very closely related to WNV. Both viruses are maintained in an enzootic

transmission cycle among similar avian hosts and mosquito vectors (Gruwell et al. 2000, Hollidge et al. 2010). Additionally, viral challenge studies found evidence of cross protection against infection in birds (Fang and Reisen 2006). However, WNV appears to be more virulent in birds. SLEV has not been associated with avian mortality unless modified to more closely resemble WNV (Kramer and Bernard 2001, Lord and Day 2004, Fang and Reisen 2006, Maharaj et al. 2018). Subsequent to the invasion of WNV in California, there were no environmental detections of SLEV in California after 2003 as WNV emerged as the dominant arbovirus in the state until its reappearance in 2015 (Reisen, Lothrop, et al. 2008, White et al. 2016, Swetnam et al. 2020). Although WEEV is an alphavirus, it also maintains an enzootic transmission cycle similar to WNV and SLEV (Reisen et al. 2003).

Transmission and ecology

WNV is an enzootic virus that maintains a transmission cycle between mosquito vectors and avian reservoir hosts (McLean et al. 2001). Although WNV is primarily vectored by mosquitoes in the genus *Culex*, vector competence studies have found other genera, including *Aedes*, to be competent when experimentally infected with different WNV strains (Sardelis et al. 2001, 2002, Turell, O'Guinn, et al. 2001, Turell, Sardelis, et al. 2001, Goddard et al. 2002, Tiawsirisup et al. 2008). Many passerine birds develop sufficiently elevated levels of viremia when infected with WNV to be infective to mosquitoes, particularly American crows, house finches, house sparrows, jays, American robins, and grackles (Komar et al. 2003, Wheeler et al. 2009, 2012, Lampman et al. 2013, Reisen et al. 2013). Given the role of birds in the transmission cycle, only mosquito species that frequently take bloodmeals from competent avian host species are relevant to transmission in nature. Of particular importance are *Cx. tarsalis* and the *Cx. pipiens* complex (*Cx. pipiens* and *Cx. quinquefasciatus*), which are both competent vectors that frequently feed upon avian species (Mclver 1968, Turell, Sardelis, et al. 2001, Kilpatrick, Daszak, et al. 2006, Hamer et al. 2009, Molaei et al. 2010, Farajollahi et al. 2011, Montgomery et al. 2011, Savage and Kothera 2012, Thiemann et al. 2012, Fitzpatrick et al.

2019, Kothera et al. 2020). Furthermore, these mosquito species are important bridge vectors for spillover transmission events to mammals, as there is evidence of shifting blood feeding behavior towards mammals after the preferred avian host species migrate (Tempelis et al. 1965, Reisen and Reeves 1990, Kilpatrick, Kramer, et al. 2006, Kent et al. 2009, Thiemann et al. 2011). Additionally, it has been demonstrated that WNV infection risk is lower in areas with higher avian biodiversity, diverting bloodmeals towards less competent hosts (Ezenwa et al. 2006, Johnson et al. 2012, Campbell et al. 2013, Levine et al. 2017).

The *Cx. pipiens* complex is comprised of several genetically distinct but morphologically similar species, of which the primary species of medical importance are *Cx. pipiens* and *Cx. quinquefasciatus* (Mattingly et al. 1951, Fonseca et al. 2004, Farajollahi et al. 2011, Turell 2012). These mosquitoes thrive in urban areas, breeding in small, stagnant pools produced by urban infrastructure, often exploiting underground storm drains (Metzger et al. 2008, Reisen 2012). *Cx. pipiens* are generally found in the north whereas *Cx. quinquefasciatus* are found in the south, although a wide zone of cohabitation extending over most of California exists where the two species interbreed and form hybrids (Barr 1957, Urbanelli et al. 1997, Kothera et al. 2009, 2012, Nelms, Kothera, et al. 2013). The primary distinction between *Cx. pipiens* and *Cx. quinquefasciatus* is the ability to undergo reproductive diapause during winter, which is a period of inactivity induced by the cooling temperature and shortening daylength during which reproduction is paused while mosquitoes shelter in thermo-insulated areas (Eldridge 1987a). *Cx. pipiens* is able to enter reproductive diapause, enabling it to survive harsher winter climates, whereas *Cx. quinquefasciatus* cannot, thereby limiting its northern range (Barr 1957, Eldridge 1987a, Farajollahi et al. 2011, Meuti et al. 2015). Hybrids of the two species are able to diapause, but at different rates depending on the species of the female (Meuti et al. 2015). Hybrids are also potentially more efficient vectors of WNV than either pure species (Vaidyanathan and Scott 2007, Ciota et al. 2013). Similar to *Cx. pipiens*, *Cx. tarsalis* are able to enter reproductive diapause to survive in harsh winter climates (Reisen, Smith, et al. 1995, Nelms, Macedo, et al.

2013). However, unlike the *Cx. pipiens* complex, *Cx. tarsalis* are generally associated with irrigated agriculture, particularly rice fields, where they can breed in open clean water sources (Bailey et al. 1965, Reisen et al. 1989, Reisen and Reeves 1990, Walton et al. 1990, Reisen 2012)

Temperature has a significant effect on WNV ecology through two main mechanisms. The first is its effect on the mosquito life cycle. As temperatures increase, the length of time between a blood meal and oviposition, known as the gonotrophic cycle, decreases (Reisen and Reeves 1990, Reisen, Milby, Presser, et al. 1992). This shortening of the gonotrophic period means that mosquitoes take more frequent blood meals, increasing the odds of becoming infected with WNV (Hartley et al. 2012), particularly among mosquitoes unable to undergo autogenous development (Reisen and Reeves 1990, Hartley et al. 2012). Furthermore, larval development time is shortest at warmer temperatures, although mortality increases when average temperatures exceed 30°C (Reisen et al. 1989, Rueda et al. 1990, Ciota et al. 2014). The combination of a faster gonotrophic period and shorter larval development time contributes to increased mosquito abundance associated with higher temperatures both at short time lags of one to two weeks and longer seasonal time lags (Reisen, Cayan, et al. 2008, Chuang et al. 2011, Wang et al. 2011, Poh et al. 2019, Ripoche et al. 2019). Thus, mosquito abundance tends to peak during the summer months, with some regional variability among species (Reisen, Milby, and Meyer 1992, Reisen, Milby, Presser, et al. 1992, Barker et al. 2010).

The second important effect of temperature on WNV transmission is shortening the extrinsic incubation period (EIP), which is the length of time necessary for a mosquito to become infectious following an infective blood meal (Dohm et al. 2002, Reisen et al. 2006, Kilpatrick et al. 2008, Richards et al. 2008, Danforth et al. 2015, 2016). At a basic level, mosquitoes require at least two blood meals to be able to transmit virus to host: one blood meal to become infected and one blood meal to transmit. A short EIP means that mosquitoes are more likely to survive long enough to become infectious, leading to greater infection prevalence in mosquito populations and increased WNV disease incidence in humans (Reisen, Lothrop, et

al. 1995, Ruiz et al. 2010, Keyel et al. 2019). The primary mechanism for this is the increased blood meal frequency at higher temperatures rather than mosquito survival, which is negatively associated with temperature (Eldridge 1968, Reisen and Reeves 1990, Reisen 1995, Ciota et al. 2014). The temperature dependence of the EIP is an established property for many vector-borne pathogens, including dengue, Zika, and malaria (Tjaden et al. 2013, Shapiro et al. 2017, Winokur et al. 2020).

Mosquito populations and WNV transmission dynamics are further impacted by variations in seasonal precipitation. There is an inconsistent pattern in the relationship between *Culex* spp. vector population dynamics and precipitation depending on larval ecology, with some studies showing a positive association after the creation of rural surface pools (DeGaetano 2004, Reisen, Cayan, et al. 2008, Chuang et al. 2011, Karki et al. 2016) whereas others showed mixed results, especially for species exploiting urban drainage system (Deichmeister and Telang 2011, Wang et al. 2011, Day et al. 2015). However, drought periods have been associated with increased mosquito infection rates as well as increases in human WNV disease incidence, possibly through higher contact rates between mosquitoes and birds or because, counterintuitively, mosquito breeding sites are not readily washed out through rainfall events (Shaman et al. 2005, Ruiz et al. 2010, Wang et al. 2010, Johnson and Sukhdeo 2013, Paull et al. 2017).

Epidemiology

Between the first outbreak in the New York City area in 1999 and 2019, the most recent year for which data are official, 51,801 cases of WNV disease and 2,390 deaths have been reported in the United States, with 7,131 cases and 332 deaths reported in California (Centers for Disease Control and Prevention et al. 2020, California Department of Public Health 2021). Approximately 80% of infections result in asymptomatic cases, while the majority of symptomatic cases involve a mild febrile illness characterized by fever, head and body aches, joint pain, and rash after an incubation period of 2-14 days (Hubálek 2001, Murphy et al. 2005,

Sejvar and Marfin 2006, Zou et al. 2010, Rudolph et al. 2014, Ronca et al. 2019). Fewer than 1% of infections develop into West Nile neuroinvasive disease (WNND), which occurs when the virus enters the central nervous system and can involve encephalitis, meningitis, or other nervous system symptoms and has a 10% fatality rate (Mostashari et al. 2001, Davis et al. 2006, Sejvar and Marfin 2006, Lindsey et al. 2010, Carson et al. 2012, Betsem et al. 2017). The risk of experiencing WNND increases in elderly individuals and individuals with immunocompromising pre-existing conditions (Lindsey et al. 2010, Snyder, Cooksey, et al. 2020, McDonald et al. 2021). WNND may involve long-term sequelae up to one decade after the initial infection and have a high estimated economic burden for affected individuals (Carson et al. 2006, Sejvar 2007, Sejvar et al. 2008, Barber et al. 2010, Murray, Walker, et al. 2010, Barrett 2014, Murray et al. 2014, Staples et al. 2014, Patel et al. 2015, Weatherhead et al. 2015). The mild, non-specific symptoms of non-neuroinvasive disease cases are often underreported due to patients not seeking medical care or to misdiagnoses if WNV testing is not conducted, leading to approximately 60% of reported cases being of WNND (Silk et al. 2010, Zou et al. 2010, Vanichanan et al. 2016, McDonald et al. 2021). However, WNND can also be underdiagnosed, making it difficult to accurately determine the overall WNV burden in the United States (Lindsey et al. 2016). Studies of blood donors attempt to elucidate this problem, with one study estimating that approximately 7 million people were infected between 1999 and 2016 (Busch et al. 2006, Planitzer et al. 2009, Petersen et al. 2013, Ronca et al. 2019).

Because of the nature of mosquito population and viral dynamics, transmission is highly seasonal with most cases occurring during the summer months (Zeller and Schuffenecker 2004, Cruz-Pacheco et al. 2009, Lindsey et al. 2010, McDonald et al. 2021). There is strong spatial heterogeneity for WNV transmission as well, with the highest incidence observed in agricultural Midwestern counties (Eisen et al. 2010, Lindsey et al. 2010, Bowden et al. 2011, Chuang et al. 2012, McDonald et al. 2021). *Cx. tarsalis* is associated with WNV transmission in these rural areas whereas the *Cx. pipiens* complex, among other *Culex* species, is implicated in urban areas

of the United States (Molaei et al. 2006, 2010, Reisen et al. 2009, Kwan, Kluh, Madon, and Reisen 2010, Trawinski and Mackay 2010, Deichmeister and Telang 2011, Schurich et al. 2014, Dunphy et al. 2019, Rochlin et al. 2019, Poh et al. 2020). Year-to-year variability in incidence also appears to be dependent on immunity levels in avian populations (Kwan, Kluh, et al. 2012).

California presents a microcosm of WNV transmission cycles in the United States, where *Cx. tarsalis* is found in large numbers around irrigated agriculture in the Central Valley and the *Cx. pipiens* complex dominates the transmission cycle in the more urbanized and densely populated Southern California (Sudia et al. 1971, Kwan, Kluh, Madon, and Reisen 2010, Kovach and Kilpatrick 2018). The highest case numbers are found in the Southern California region, although the highest incidence is observed in the Central Valley, similar to the spatial patterns observed in the contiguous United States (Snyder, Feiszli, et al. 2020, Danforth et al. 2021).

Prevention and control

Although there are several effective equine vaccines against WNV licensed for veterinary use, no such vaccine yet exists for humans (Ng et al. 2003, Gardner et al. 2007, Kaiser and Barrett 2019). Protection of the public health relies on WNV prevention through a combination of personal protective actions and local vector control districts enacting integrated vector control (Gubler et al. 2000, Gujral et al. 2007, Nasci and Mutebi 2019). The capacity for vector-borne disease prevention has greatly increased since the first detection of WNV in the United States (Hadler et al. 2015, Ramírez et al. 2018), although funding for these programs is highly variable despite increasing trends in vector-borne disease incidence (Beard et al. 2019, Kading et al. 2020, Ronca et al. 2021). Vector control efforts range from routine biological or chemical larvicidal treatments of breeding habitats to aerial applications of adulticide in response to elevated risk indicators (California Department of Public Health Vector Borne Diseases Section 2005, California Department of Public Health et al. 2020). Such measures have been shown to be effective at reducing mosquito populations, thereby limiting the opportunity for contact between mosquitoes and people, as well as WNV infection rates in mosquitoes (Carney et al.

2008, Elnaiem et al. 2008, Holcomb et al. 2021). Furthermore, there is no evidence of adverse human health effects to insecticide applications (Macedo et al. 2010, Geraghty et al. 2013) and peripheral effects on nontarget insects appears to be limited to small-bodied arthropods (Boyce et al. 2007, Pokhrel et al. 2018).

Tools for risk estimation

Because of the enzootic transmission cycle and potential delay in recognizing mild WNV disease cases, it is often too late to prevent further disease once the first cases are detected. Thus, entomological surveillance to monitor for increases in WNV activity in local mosquito populations is critical for prevention of human infection with WNV. In California, a network of vector control districts was established during the first half of the 20th century and enhanced in order to prevent infections with circulating arboviruses such as WEEV (Stead and Peters 1953, Eldridge 1987b, Mosquito & Vector Control Association of California 2021). Arboviral risk is often best estimated through the entomological inoculation rate (EIR), which originally was defined for malarial transmission systems and represents the average number of infectious bites per person during a defined time period (Hay et al. 2005). The EIR is the product of the vector to human density ratio, the mosquito biting rate, the proportion of mosquitoes biting humans, and the proportion of mosquitoes that are infectious. In practice, the vector to human density ratio and proportion of mosquitoes that are infectious components of this equation are approximated through routine surveillance estimates of mosquito abundance and mosquito infection prevalence, respectively, and are widely used as entomological indicators for risk of WNV transmission (California Department of Public Health et al. 2020). The product of these quantities is the vector index (VI), which is the number of infected female mosquitoes in an area (Gujral et al. 2007).

Studies of WNV outbreaks across the United States have demonstrated links between these specific mosquito indices and human WNV infection risk. In Maricopa County, Arizona, in 2010, epidemiologists found increased abundance of *Cx. quinquefasciatus* in the outbreak area,

with abundance peaking approximately 1-2 weeks before human infections (Godsey Jr. et al. 2012, Colborn et al. 2013). In Davis, California, a study during the peak transmission season showed spatial and temporal associations between WNV-infected vectors and human WNV infections, similar to results observed in an outbreak in Texas (Nielsen et al. 2008, Martinez et al. 2017). In the 2012 WNV epidemic in Dallas, Texas, elevated VIs were associated with high-incidence areas (Chung et al. 2013). Further, numerous retrospective statistical models have identified associations between each of the commonly used entomological risk indicators and human WNV disease incidence across a variety of WNV transmission settings (Andreadis et al. 2004, Gujral et al. 2007, Bolling et al. 2009, Liu et al. 2009, Kilpatrick and Pape 2013, Fauver et al. 2016, Giordano et al. 2017, Karki et al. 2017, 2020, Talbot et al. 2019).

Risk assessments for WNV typically include both mosquito abundance and mosquito infection prevalence and often include environmental information (i.e., temperature). Many states also use dead bird reports and sentinel chicken seroconversions as early warning indicators for potential WNV transmission to humans. Clusters of dead birds have been linked to human cases up to several months in advance (Eidson et al. 2001, Mostashari et al. 2003, Julian et al. 2004, Carney et al. 2008, Nielsen et al. 2008, Carney et al. 2011, Kwan, Park, et al. 2012) while sentinel chicken seroconversions can serve as a proxy for WNV activity in an area, although by the time seroconversions are detected it is often too late to prevent human infections (Kwan, Kluh, Madon, Nguyen, et al. 2010). In California, these elements are incorporated into the Mosquito-Borne Virus Surveillance and Response Plan, which assigns risk levels to surveillance observations during the prior two weeks and assigns appropriate measures to take in response. The three risk levels range are normal season, with the recommendation of maintaining normal vector control operations with an emphasis on larval control; emergency planning, with the recommendation to increase adult mosquito surveillance and viral testing and implement localized adult mosquito control; and epidemic conditions, with the

recommendation to broaden the scope of mosquito surveillance and initiate area-wide ground- and/or air-based adult mosquito control (California Department of Public Health et al. 2020).

Dissertation scope

This dissertation research focuses on the relationship between entomological surveillance data and human WNV disease in California. The first chapter explores this relationship empirically through receiver operating curve analyses and statistically at a variety of course and fine control-relevant spatial scales to identify the entomological threshold at which human disease risk increases. This chapter helps to fill a gap in vector control knowledge by utilizing information already collected by districts to identify optimal entomological "trigger points" for enacting mosquito control. The second chapter examines the relationship between daily weather conditions and nightly mosquito host-seeking activity through statistical models to identify potential biases in mosquito abundance estimation and identify optimal time frames for control to have maximum impact on host-seeking mosquito populations. This chapter improves interpretation of mosquito abundance estimates, and by extension risk assessment. Finally, the third chapter evaluates a spatio-temporal modelling approach for estimating risk where surveillance coverage is limited and applies this method to predict mosquito abundance. This chapter enhances tools for spatial risk estimation already in place by evaluating mosquito abundance at a fine spatial scale in the near-term future. Taken together, these chapters will improve the use of entomological surveillance data for risk estimation and WNV disease prevention in California.

References

Andreadis, T. G., J. F. Anderson, C. R. Vossbrinck, and A. J. Main. **2004**. Epidemiology of West Nile virus in Connecticut: a five-year analysis of mosquito data. Vector-Borne Zoonotic Dis. 4: 360–378.

Bailey, S. F., D. A. Eliason, and B. L. Hoffmann. **1965**. Flight and dispersal of the mosquito *Culex tarsalis* Coquillett in the Sacramento Valley of California. Hilgardia. 37: 73–113.

Barber, L. M., J. J. Schleier, and R. K. D. Peterson. **2010**. Economic cost analysis of

West Nile virus outbreak, Sacramento County, California, USA, 2005. Emerg. Infect. Dis. 16: 480–486.

Barker, C. M., B. F. Eldridge, and W. K. Reisen. **2010**. Seasonal abundance of *Culex tarsalis* and *Culex pipiens* complex mosquitoes (Diptera: Culicidae) in California. J. Med. Entomol. 47: 759–768.

Barr, A. R. 1957. The distribution of *Culex p. pipiens* and *C. p. quinquefasciatus* in North America. Am. J. Trop. Med. Hyg. 6: 153–165.

Barrett, A. D. T. 2014. Economic burden of West Nile virus in the United States. Am. J. Trop. Med. Hyg. 90: 389–390.

Beard, C. B., S. N. Visser, and L. R. Petersen. **2019**. The need for a national strategy to address vector-borne disease threats in the United States. J. Med. Entomol. 56: 1199.

Betsem, E., Z. Kaidarova, S. L. Stramer, B. Shaz, M. Sayers, G. LeParc, B. Custer, M. P. Busch, and E. L. Murphy. **2017**. Correlation of West Nile virus incidence in donated blood with West Nile neuroinvasive disease rates, United States, 2010–2012. Emerg. Infect. Dis. 23: 212–219.

Bolling, B. G., C. M. Barker, C. G. Moore, W. J. Pape, and L. Eisen. **2009**. Seasonal patterns for entomological measures of risk for exposure to *Culex* vectors and West Nile virus in relation to human disease cases in northeastern Colorado. J. Med. Entomol. 46: 1519–1531.

Bowden, S. E., K. Magori, and J. M. Drake. **2011**. Regional differences in the association between land cover and West Nile virus disease incidence in humans in the United States. Am. J. Trop. Med. Hyg. 84: 234–238.

Boyce, W. M., S. P. Lawler, J. M. Schultz, S. J. McCauley, L. S. Kimsey, M. K. Niermela, C. F. Nielsen, and W. K. Reisen. **2007**. Nontarget effects of the mosquito adulticide pyrethrin applied aerially during a West Nile virus outbreak in an urban California environment. J. Am. Mosq. Control Assoc. 23: 335–339.

Busch, M. P., D. J. Wright, B. Custer, L. H. Tobler, S. L. Stramer, S. H. Kleinman, H. E. Prince, C. Bianco, G. Foster, L. R. Petersen, G. Nemo, and S. A. Glynn. **2006**. West Nile virus infections projected from blood donor screening data, United States, 2003. Emerg. Infect. Dis. 12: 395–402.

California Department of Public Health. **2021**. Human Reports. (https://westnile.ca.gov/resources_reports.php?report_category_id=1).

California Department of Public Health, Mosquito & Vector Control Association of California, and University of California. **2020**. California mosquito-borne virus surveillance & response plan. Sacramento, CA.

California Department of Public Health Vector Borne Diseases Section. **2005**. Overview of mosquito control practices in California.

Calisher, C. H., N. Karabatsos, J. M. Dalrymple, R. E. Shope, J. S. Porterfield, E. G. Westaway, and W. E. Brandt. **1989**. Antigenic relationships between flaviviruses as determined by cross-neutralization tests with polyclonal antisera. J. Gen. Virol. 70: 37–43.

Campbell, R., T. C. Thiemann, D. Lemenager, and W. K. Reisen. **2013**. Host-selection patterns of *Culex tarsalis* (Diptera: Culicidae) determine the spatial heterogeneity of West

Nile virus enzootic activity in Northern California. J. Med. Entomol. 50: 1303–1309.

Carney, R. M., S. C. Ahearn, A. McConchie, C. Glaser, C. Jean, C. Barker, B. Park, K. Padgett, E. Parker, E. Aquino, and V. Kramer. **2011**. Early warning system for West Nile virus risk areas, California, USA. Emerg. Infect. Dis. 17: 1454.

Carney, R. M., S. Husted, C. Jean, C. Glaser, and V. Kramer. **2008**. Efficacy of aerial spraying of mosquito adulticide in reducing incidence of West Nile virus, California, 2005. Emerg. Infect. Dis. 14: 747–754.

Carson, P. J., S. M. Borchardt, B. Custer, H. E. Prince, J. Dunn-Williams, V. Winkelman, L. Tobler, B. J. Biggerstaff, R. Lanciotti, L. R. Petersen, and M. P. Busch. **2012**. Neuroinvasive disease and West Nile virus Infection, North Dakota, USA, 1999–2008. Emerg. Infect. Dis. 18: 684–686.

Carson, P. J., P. Konewko, K. S. Wold, P. Mariani, S. Goli, P. Bergloff, and R. D. Crosby. **2006**. Long-term clinical and neuropsychological outcomes of West Nile virus infection. Clin. Infect. Dis. 43: 723–730.

Centers for Disease Control and Prevention, National Center for Emerging and Zoonotic Infectious Diseases, and Division of Vector-Borne Diseases. **2020**. Final Cumulative Maps and Data. (https://www.cdc.gov/westnile/statsmaps/cumMapsData.html).

Chuang, T., M. B. Hildreth, D. L. Vanroekel, and M. C. Wimberly. **2011**. Weather and land cover influences on mosquito populations in Sioux Falls, South Dakota. J. Med. Entomol. 48: 669–679.

Chuang, T. W., C. W. Hockett, L. Kightlinger, and M. C. Wimberly. **2012**. Landscape-level spatial patterns of West Nile virus risk in the northern Great Plains. Am. J. Trop. m. 84: 724–731.

Chung, W. M., C. M. Buseman, S. N. Joyner, S. M. Hughes, T. B. Fomby, J. P. Luby, and R. W. Haley. **2013**. The 2012 West Nile encephalitis epidemic in Dallas, Texas. J. Am. Med. Assoc. 310: 297–307.

Ciota, A. T. 2017. West Nile virus and its vectors. Curr. Opin. Insect Sci. 22: 28–36.

Ciota, A. T., P. A. Chin, and L. D. Kramer. **2013**. The effect of hybridization of *Culex pipiens* complex mosquitoes on transmission of West Nile virus. Parasites and Vectors. 6: 2–5.

Ciota, A. T., and L. D. Kramer. **2013**. Vector-virus interactions and transmission dynamics of West Nile virus. Viruses. 5: 3021–3047.

Ciota, A. T., A. C. Matacchiero, A. M. Kilpatrick, and L. D. Kramer. **2014**. The effect of temperature on life history traits of *Culex* mosquitoes. J. Med. Entomol. 51: 55–62.

Colborn, J. M., K. A. Smith, J. Townsend, D. Damian, R. S. Nasci, and J.-P. Mutebi. **2013**. West Nile virus outbreak in Phoenix, Arizona—2010: Entomological observations and epidemiological correlations. J. Am. Mosq. Control Assoc. 29: 123–132.

Cruz-Pacheco, G., L. Esteva, and C. Vargas. **2009**. Seasonality and Outbreaks in West Nile Virus Infection. Bull. Math. Biol. 71: 1378–1393.

Danforth, M. E., M. Fischer, R. E. Snyder, N. P. Lindsey, S. W. Martin, and V. L. Kramer. **2021**. Characterizing areas with increased burden of West Nile virus disease in

California, 2009–2018. Vector-Borne Zoonotic Dis.

Danforth, M. E., W. K. Reisen, and C. M. Barker. **2015**. Extrinsic incubation rate is not accelerated in recent California strains of West Nile virus in *Culex tarsalis* (Diptera: Culicidae). J. Med. Entomol. 52: 1083.

Danforth, M. E., W. K. Reisen, and C. M. Barker. **2016**. The impact of cycling temperature on the transmission of West Nile virus. J Med Entomol. 53: 681–686.

Davis, L. E., R. DeBiasi, D. E. Goade, K. Y. Haaland, J. A. Harrington, J. A. B. Harnar, S. A. Pergam, M. K. King, B. K. DeMasters, and K. L. Tyler. **2006**. West Nile virus neuroinvasive disease. Ann. Neurol. 60: 286–300.

Day, J. F., W. J. Tabachnick, and C. T. Smartt. **2015**. Factors that influence the transmission of West Nile virus in Florida. J. Med. Entomol. 52: 743–754.

DeGaetano, A. T. 2004. Meteorological effects on adult mosquito (*Culex*) populations in metropolitan New Jersey. Int. J. Biometeorol. 49: 345–353.

Deichmeister, J. M., and A. Telang. **2011**. Abundance of West Nile virus mosquito vectors in relation to climate and landscape variables. J. Vector Ecol. 36: 75–85.

Dohm, D. J., M. L. O'Guinn, and M. J. Turell. **2002**. Effect of environmental temperature on the ability of Culex pipiens (Diptera: Culicidae) to transmit West Nile virus. J. Med. Entomol. 39: 221–225.

Dunphy, B. M., K. B. Kovach, E. J. Gehrke, E. N. Field, W. A. Rowley, L. C. Bartholomay, and R. C. Smith. **2019**. Long-term surveillance defines spatial and temporal patterns implicating *Culex tarsalis* as the primary vector of West Nile virus. Sci. Rep. 9: 6637.

Eidson, M., L. Kramer, W. Stone, Y. Hagiwara, K. Schmit, and New York State West Nile Virus Avian Surveillance Team. **2001**. Dead bird surveillance as an early warning system for West Nile virus. Emerg. Infect. Dis. 7: 635.

Eisen, L., C. M. Barker, C. G. Moore, W. J. Pape, A. M. Winters, and N. Cheronis. **2010**. Irrigated agriculture is an important risk factor for West Nile virus disease in the hyperendemic Larimer-Boulder-Weld area of North Central Colorado. J. Med. Entomol. 47: 939–951.

Eldridge, B. F. 1968. The effect of temperature and photoperiod on blood-feeding and ovarian development in mosquitoes of the *Culex pipiens* complex. Am. J. Trop. Med. Hyg. 17: 133–140.

Eldridge, B. F. 1987a. Diapause and related phenomena in *Culex* mosquitoes: Their relation to arbovirus disease ecology, pp. 1–28. *In* Harris, K.F. (ed.), Curr. Top. Vector Res. Springer, New York, NY, New York.

Eldridge, B. F. 1987b. Strategies for surveillance, prevention, and control of arboviruses in western North America. Am. J. Trop. Med. Hyg. 37: 77S-86S.

Elnaiem, D. A., K. Kelley, S. Wright, R. Laffey, G. Yoshimura, M. Reed, G. Goodman, T. Thiemann, L. Reimer, W. K. Reisen, D. Brown, and D. A. Elnaiem. **2008**. Impact of aerial spraying of pyrethrin insecticide on Culex pipiens and Culex tarsalis (Diptera: Culicidae) abundance and West Nile virus infection rates in an urban/suburban area of Sacramento County, California. J. Med. Entomol. 45: 751–757.

Ezenwa, V. O., M. S. Godsey, R. J. King, and S. C. Guptill. **2006**. Avian diversity and West Nile virus: Testing associations between biodiversity and infectious disease risk. Proc. R. Soc. B Biol. Sci. 273: 109–117.

Fang, Y., and W. K. Reisen. **2006**. Previous infection with West Nile or St. Louis encephalitis viruses provides cross protection during reinfection in house finches. Am. J. Trop. Med. Hyg. 75: 480–485.

Farajollahi, A., D. M. Fonseca, L. D. Kramer, and A. M. Kilpatrick. **2011**. "Bird biting" mosquitoes and human disease: A review of the role of *Culex pipiens* complex mosquitoes in epidemiology. Infect. Genet. Evol. 11: 1577–1585.

Fauver, J. R., L. Pecher, J. A. Schurich, B. G. Bolling, M. Calhoon, N. D. Grubaugh, K. L. Burkhalter, L. Eisen, B. G. Andre, R. S. Nasci, A. LeBailly, G. D. Ebel, and C. G. Moore. **2016**. Temporal and spatial variability of entomological risk indices for West Nile virus infection in northern Colorado: 2006-2013. J. Med. Entomol. 53: 425–434.

Fitzpatrick, D. M., L. M. Hattaway, A. N. Hsueh, M. E. Ramos-Niño, and S. M. Cheetham. **2019**. PCR-based bloodmeal analysis of *Aedes aegypti* and *Culex quinquefasciatus* (Diptera: Culicidae) in St. George Parish, Grenada. J. Med. Entomol. 56: 1170–1175.

Fonseca, D. M., N. Keyghobadi, C. A. Malcolm, C. Mehmet, F. Schaffner, M. Mogi, R. C. Fleischer, and R. C. Wilkerson. **2004**. Emerging vectors in the *Culex pipiens* complex. Science (80-.). 303: 1535–1538.

Gardner, I. A., S. J. Wong, G. L. Ferraro, U. B. Balasuriya, P. J. Hullinger, W. D. Wilson, P.-Y. Shi, and N. J. MacLachlan. **2007**. Incidence and effects of West Nile virus infection in vaccinated and unvaccinated horses in California. Vet. Res. 38: 109–116.

Geraghty, E. M., H. G. Margolis, A. Kjemtrup, W. Reisen, and P. Franks. **2013**. Correlation between aerial insecticide spraying to interrupt West Nile virus transmission and emergency department visits in Sacramento County, California. Public Heal. Rep. 128: 221–230.

Giordano, B. V., S. Kaur, and F. F. Hunter. **2017**. West Nile virus in Ontario, Canada: A twelve-year analysis of human case prevalence, mosquito surveillance, and climate data. PLoS One. 12: e0183568.

Goddard, L. B., A. E. Roth, W. K. Reisen, and T. W. Scott. **2002**. Vector competence of California mosquitoes for West Nile virus. Emerg. Infect. Dis. 8: 1385–1391.

Godsey Jr., M. S., K. Burkhalter, G. Young, M. Delorey, K. Smith, J. Townsend, C. Levy, and J.-P. Mutebi. **2012**. Entomologic investigations during an outbreak of West Nile virus disease in Maricopa County, Arizona, 2010. Am. J. Trop. Med. Hyg. 87: 1131.

Gruwell, J. A., C. L. Fogarty, S. G. Bennett, G. L. Challet, K. S. Vanderpool, M. Jozan, and J. P. Webb. **2000**. Role of peridomestic birds in the transmission of St. Louis encephalitis virus in southern California. J. Wildl. Dis. 36: 13–34.

Gubler, D. J., G. L. Campbell, R. Nasci, N. Komar, L. Petersen, and J. T. Roehrig. **2000**. West Nile virus in the United States: Guidelines for detection, prevention, and control. Viral Immunol.

Gujral, I. B., E. C. Zielinski-Gutierrez, A. LeBailly, and R. Nasci. **2007**. Behavioral risks for West Nile virus disease, northern Colorado, 2003. Emerg. Infect. Dis. 13: 419–425.

Hadfield, J., A. F. Brito, D. M. Swetnam, C. B. F. Vogels, R. E. Tokarz, K. G. Andersen, R. C. Smith, T. Bedford, and N. D. Grubaugh. **2019**. Twenty years of West Nile virus spread and evolution in the Americas visualized by Nextstrain. PLoS Pathog.

Hadler, J. L., D. Patel, R. S. Nasci, L. R. Petersen, J. M. Hughes, K. Bradley, P. Etkind, L. Kan, and J. Engel. **2015**. Assessment of arbovirus surveillance 13 years after introduction of West Nile virus, United States. Emerg. Infect. Dis. 21: 1159.

Hamer, G. L., U. D. Kitron, T. L. Goldberg, J. D. Brawn, S. R. Loss, M. O. Ruiz, D. B. Hayes, and E. D. Walker. **2009**. Host selection by *Culex pipiens* mosquitoes and West Nile virus amplification. Am. J. Trop. Med. Hyg. 80: 268–278.

Hartley, D. M., C. M. Barker, A. Le Menach, T. Niu, H. D. Gaff, and W. K. Reisen. **2012**. Effects of temperature on emergence and seasonality of West Nile virus in California. Am. J. Trop. Med. Hyg. 86: 884–894.

Hay, S. I., C. A. Guerra, A. J. Tatem, P. M. Atkinson, and R. W. Snow. **2005**. Urbanization, malaria transmission and disease burden in Africa. Nat. Rev. Microbiol. 3: 81–108.

Holcomb, K., R. Reiner, and C. Barker. **2021**. Spatio-temporal impacts of aerial insecticide applications on West Nile virus vectors. Parasit. Vectors. 14: 120.

Hollidge, B. S., F. González-Scarano, and S. S. Soldan. **2010**. Arboviral encephalitides: Transmission, emergence, and pathogenesis. J Neuroimmune Pharmacol. 5: 428–442.

Howitt, B. F. 1939. Viruses of equine and of St. Louis encephalitis in relationship to human infections in California 1937-1938. Am. J. Public Health. 29: 1083–1097.

Hubálek, Z. 2001. Comparative sympomatology of West Nile fever. Lancet. 358: 254–255.

Johnson, B. J., K. Munafo, L. Shappell, N. Tsipoura, M. Robson, J. Ehrenfeld, and M. V. K. Sukhdeo. **2012**. The roles of mosquito and bird communities on the prevalence of West Nile virus in urban wetland and residential habitats. Urban Ecosyst. 15: 531.

Johnson, B. J., and M. V. K. Sukhdeo. **2013**. Drought-induced amplification of local and regional West Nile virus infection rates in New Jersey. J. Med. Entomol. 50: 195–204.

Julian, K. G., M. Eidson, A. M. Kipp, E. Weiss, L. R. Petersen, J. R. Miller, S. R. Hinten, and A. A. Marfin. **2004**. Early season crow mortality as a sentinel for West Nile virus disease in humans, northeastern United States. Vector-Borne Zoonotic Dis. 2: 145–155.

Kading, R. C., L. W. Cohnstaedt, K. Fall, and G. L. Hamer. **2020**. Emergence of arboviruses in the United States: The boom or bust of funding, innovation, and capacity. Trop. Med. Infect. Dis. 5.

Kaiser, J. A., and A. D. T. Barrett. **2019**. Twenty years of progress toward West Nile virus vaccine development. Viruses. 11: 823.

Karki, S., W. M. Brown, J. Uelmen, M. O. Ruiz, and R. L. Smith. **2020**. The drivers of West Nile virus human illness in the Chicago, Illinois, USA area: Fine scale dynamic effects of weather, mosquito infection, social, and biological conditions. PLoS One. 15: e0227160.

Karki, S., G. L. Hamer, T. K. Anderson, T. L. Goldberg, U. D. Kitron, B. L. Krebs, E. D. Walker, and M. O. Ruiz. **2016**. Effect of trapping methods, weather, and landscape

on estimates of the *Culex* vector mosquito abundance. Environ. Health Insights. 10: 93–103.

Karki, S., N. E. Westcott, E. J. Muturi, W. M. Brown, and M. O. Ruiz. **2017**. Assessing human risk of illness with West Nile virus mosquito surveillance data to improve public health preparedness. Zoonoses Public Health. 00: 1–8.

Kent, R., L. Juliusson, M. Weissmann, S. Evans, and N. Komar. **2009**. Seasonal blood-feeding behavior of *Culex tarsalis* (Diptera: Culicidae) in Weld County, Colorado, 2007. J. Med. Entomol. 46: 380–390.

Keyel, A. C., O. E. Timm, P. Bryon Backenson, C. Prussing, S. Quinones, K. A. McDonough, M. Vuille, J. E. Conn, P. M. Armstrong, T. G. Andreadis, and L. D. Kramer. **2019**. Seasonal temperatures and hydrological conditions improve the prediction of West Nile virus infection rates in *Culex* mosquitoes and human case counts in New York and Connecticut. PLoS One. 14: e0217854.

Kilpatrick, A. M., P. Daszak, M. J. Jones, P. P. Marra, and L. D. Kramer. **2006**. Host heterogeneity dominates West Nile virus transmission. Proc R Soc B. 273: 2327–2333.

Kilpatrick, A. M., L. D. Kramer, M. J. Jones, P. P. Marra, and P. Daszak. **2006**. West Nile virus epidemics in North America are driven by shifts in mosquito feeding behavior. PLoS Biol. 4: 606–610.

Kilpatrick, A. M., M. A. Meola, R. M. Moudy, and L. D. Kramer. **2008**. Temperature, viral genetics, and the transmission of West Nile virus by *Culex pipiens* mosquitoes. PLOS Pathog. 4: e1000092.

Kilpatrick, A. M., and W. J. Pape. **2013**. Predicting human West Nile virus infections with mosquito surveillance data. Am. J. Epidemiol. 178: 829–835.

Komar, N., S. Langevin, S. Hinten, N. Nemeth, E. Edwards, D. Hettler, B. Davis, R. Bowen, and M. Bunning. **2003**. Experimental infection of North American birds with the New York 1999 strain of West Nile virus. Emerg. Infect. Dis. 9: 311–322.

Kothera, L., J. P. Mutebi, J. L. Kenney, K. Saxton-Shaw, M. P. Ward, H. M. Savage, and G. Hamer. **2020**. Bloodmeal, host selection, and genetic admixture analyses of *Culex pipiens* complex (Diptera: Culicidae) mosquitoes in Chicago, IL. J. Med. Entomol. 57: 78–87.

Kothera, L., B. Nelms, H. M. Savage, and W. K. Reisen. **2012**. Complexity of the *Culex pipiens* complex in California. Proc. Pap. Conf. Mosq. Vector Control Assoc. Calif. 80: 1–3.

Kothera, L., E. M. Zimmerman, C. M. Richards, and H. M. Savage. **2009**. Microsatellite characterization of subspecies and their hybrids in *Culex pipiens* complex (Diptera: Culicidae) mosquitoes along a north-south transect in the central United States. J. Med. Entomol. 46: 236–248.

Kovach, T. J., and A. M. Kilpatrick. **2018**. Increased human incidence of West Nile virus disease near rice felds in California but not in southern United States. Am. J. Trop. Med. Hyg. 99: 222–228.

Kramer, L. D., and K. A. Bernard. **2001**. West Nile virus infection in birds and mammals. Ann. N. Y. Acad. Sci. 951: 84–93.

Kramer, L. D., A. T. Ciota, and A. Marm Kilpatrick. **2019**. Introduction, spread, and

establishment of West Nile virus in the Americas. J. Med. Entomol. 56: 1448–1455.

Kramer, L. D., L. M. Styer, and G. D. Ebel. **2008**. A global perspective on the epidemiology of West Nile virus. Annu. Rev. Entomol. 53: 61–81.

Kwan, J. L., S. Kluh, M. B. Madon, D. V. Nguyen, C. M. Barker, and W. K. Reisen. **2010**. Sentinel chicken seroconversions track tangential transmission of West Nile virus to humans in the greater Los Angeles area of California. Am. J. Trop. Med. Hyg. 83: 1137–1145.

Kwan, J. L., S. Kluh, M. B. Madon, and W. K. Reisen. **2010**. West Nile virus emergence and persistence in Los Angeles, California, 2003-2008. Am. J. Trop. Med. Hyg. 83: 400–412.

Kwan, J. L., S. Kluh, and W. K. Reisen. **2012**. Antecedent avian immunity limits tangential transmission of West Nile virus to humans. PLoS One. 7: e34127.

Kwan, J. L., B. K. Park, T. E. Carpenter, V. Ngo, R. Civen, and W. K. Reisen. **2012**. Comparison of enzootic risk measures for predicting West Nile disease, Los Angeles, California, USA, 2004-2010. Emerg. Infect. Dis. 18: 1298–1306.

Lampman, R. L., N. M. Krasavin, M. P. Ward, T. A. Beveroth, E. W. Lankau, B. W. Alto, E. Muturi, and R. J. Novak. **2013**. West Nile virus infection rates and avian serology in east-central Illinois. J. Am. Mosq. Control Assoc. 29: 108–122.

Lanciotti, R. S., J. T. Roehrig, V. Deubel, J. Smith, M. Parker, K. Steele, B. Crise, K. E. Volpe, M. B. Crabtree, J. H. Scherret, R. A. Hall, J. S. MacKenzie, C. B. Cropp, B. Panigrahy, E. Ostlund, B. Schmitt, M. Malkinson, C. Banet, J. Weissman, N. Komar, H. M. Savage, W. Stone, T. McNamara, and D. J. Gubler. **1999**. Origin of the West Nile virus responsible for an outbreak of encephalitis in the Northeastern United States. Science (80-.). 286: 2333–2337.

Levine, R. S., D. L. Hedeen, M. W. Hedeen, G. L. Hamer, D. G. Mead, and U. D. Kitron. **2017**. Avian species diversity and transmission of West Nile virus in Atlanta, Georgia. Parasites and Vectors. 10: 1–12.

Lindsey, N. P., M. Fischer, D. Neitzel, E. Schiffman, M. L. Salas, C. A. Glaser, T. Sylvester, M. Kretschmer, A. Bunko, and J. E. Staples. **2016**. Hospital-based enhanced surveillance for West Nile virus neuroinvasive disease. Epidemiol. Infect. 144: 3170–3175.

Lindsey, N. P., J. E. Staples, J. A. Lehman, and M. Fischer. **2010**. Surveillance for human West Nile virus disease - United States, 1999-2008. Surveill. Summ. 59: 1–17.

Liu, A., V. Lee, D. Galusha, M. D. Slade, M. Diuk-Wasser, T. Andreadis, M. Scotch, and P. M. Rabinowitz. **2009**. Risk factors for human infection with West Nile Virus in Connecticut: a multi-year analysis. Int. J. Health Geogr. 8.

Lord, C. C., and J. F. Day. **2004**. Simulation studies of St. Louis encephalitis and West Nile viruses: The impact of bird mortality. Vector-Borne Zoonotic Dis. 1: 317–329.

Macedo, P. A., J. J. Schleier, M. Reed, K. Kelley, G. W. Goodman, D. A. Brown, and R. K. D. Peterson. **2010**. Evaluation of efficacy and human health risk of aerial ultra-low volume applications of pyrethrins and piperonyl butoxide for adult mosquito management in response to West Nile virus activity in Sacramento County, California. J. Am. Mosq. Control Assoc. 26: 57–66.

Maharaj, P. D., A. M. Bosco-Lauth, S. A. Langevin, M. Anishchenko, R. A. Bowen, W. K. Reisen, and A. C. Brault. **2018**. West Nile and St. Louis encephalitis viral genetic determinants of avian host competence. PLoS Negl. Trop. Dis. 12: e0006302.

Martinez, D., K. O. Murray, M. Reyna, R. R. Arafat, R. Gorena, U. A. Shah, and M. Debboun. **2017**. West Nile virus outbreak in Houston and Harris County, Texas, USA, 2014. Emerg. Infect. Dis. 23: 1376.

Mattingly, P. F., L. E. Rozeboom, K. L. Knight, H. Laven, F. H. Drummond, S. R. Christophers, and P. G. Shute. **1951**. The *Culex pipiens* complex. Trans. R. Entomol. Soc. London. 102: 382.

McDonald, E., S. W. Martin, K. Landry, C. V. Gould, J. Lehman, M. Fischer, and N. P. Lindsey. **2019**. West Nile virus and other domestic nationally notifiable arboviral diseases — United States, 2018. Morb. Mortal. Wkly. Rep. 68: 673–678.

McDonald, E., S. Mathis, S. W. Martin, J. E. Staples, M. Fischer, and N. P. Lindsey. **2021**. Surveillance for West Nile virus disease - United States, 2009–2018. Am. J. Transplant. 21: 1959–1974.

McLean, R. G., S. R. Ubico, D. E. Docherty, W. R. Hansen, L. Sileo, and T. S. McNamara. **2001**. West Nile virus transmission and ecology in birds. Ann. N. Y. Acad. Sci. 951: 54–57.

Mclver, S. B. 1968. Host preferences and discrimination by the mosquitoes *Aedes aegypti* and *Culex tarsalis* (Diptera: Culicidiae). J. Med. Entomol. 5: 422–428.

Metzger, M., C. Myers, S. Kluh, J. Wekesa, R. Hu, and V. Kramer. **2008**. An assessment of mosquito production and nonchemical control measures in structural stormwater best management practices in southern California. J. Am. Mosq. Control Assoc. 24: 70–81.

Meuti, M. E., C. A. Short, and D. L. Denlinger. **2015**. Mom matters: Diapause characteristics of *Culex pipiens-Culex quinquefasciatus* (Diptera: Culicidae) hybrid mosquitoes. J. Med. Entomol. 52: 131–137.

Molaei, G., T. G. Andreadis, P. M. Armstrong, J. F. Anderson, and C. R. Vossbrinck. **2006**. Host feeding patterns of *Culex* mosquitoes and West Nile virus transmission, northeastern United States. Emerg. Infect. Dis. 12: 468–474.

Molaei, G., R. F. Cummings, T. Su, P. M. Armstrong, G. A. Williams, M. L. Cheng, J. P. Webb, and T. G. Andreadis. **2010**. Vector-host interactions governing epidemiology of West Nile virus in southern California. Am. J. Trop. Med. Hyg. 83: 1269–1282.

Montgomery, M. J., T. Thiemann, P. Macedo, D. A. Brown, and T. W. Scott. **2011**. Blood-feeding patterns of the *Culex pipiens* complex in Sacramento and Yolo Counties, California. J. Med. Entomol. 48: 398–404.

Mosquito & Vector Control Association of California. **2021**. History of Mosquito Control in California. (https://www.mvcac.org/about/history/).

Mostashari, F., M. L. Bunning, P. T. Kitsutani, D. A. Singer, D. Nash, M. J. Cooper, N. Katz, K. A. Liljebjelke, B. J. Biggerstaff, A. D. Fine, M. C. Layton, S. M. Mullin, A. J. Johnson, D. A. Martin, E. B. Hayes, and G. L. Campbell. **2001**. Epidemic West Nile encephalitis, New York, 1999: Results of a household-based seroepidemiological survey. Lancet. 358: 261–264.

Mostashari, F., M. Kulldorff, J. J. Hartman, J. R. Miller, and V. Kulasekera. **2003**. Dead bird clusters as an early warning system for West Nile virus activity. Emerg. Infect. Dis. 9: 641.

Murphy, T. D., J. Grandpre, S. L. Novick, S. A. Seys, R. W. Harris, and K. Musgrave. **2005**. West Nile virus infection among health-fair participants, Wyoming 2003: Assessment of symptoms and risk factors. Vector-Borne Zoonotic Dis. 5: 246–251.

Murray, K. O., M. N. Garcia, M. H. Rahbar, D. Martinez, S. A. Khuwaja, R. R. Arafat, and S. Rossmann. **2014**. Survival analysis, long-term outcomes, and percentage of recovery up to 8 years post-infection among the Houston West Nile virus cohort. PLoS One. 9: e102953.

Murray, K. O., E. Mertens, and P. Desprès. **2010**. West Nile virus and its emergence in the United States of America. Vet. Res. 41.

Murray, K., C. Walker, E. Herrington, J. A. Lewis, J. McCormick, D. W. C. Beasley, R. B. Tesh, and S. Fisher-Hoch. **2010**. Persistent infection with West Nile virus years after initial infection. J. Infect. Dis. 201: 2–4.

Nasci, R. S., and J.-P. Mutebi. **2019**. Reducing West Nile virus risk through vector management. J. Med. Entomol. 56: 1516–1521.

Nash, D., F. Mostashari, A. Fine, J. Miller, D. O'Leary, K. O. Murray, A. Huang, A. Rosenberg, A. Greenberg, M. Sherman, S. Wong, and M. Layton. **2001**. The outbreak of West Nile virus infection in the New York City area in 1999. N. Engl. J. Med. 344: 1807–1814.

Nelms, B. M., L. Kothera, T. Thiemann, P. A. Macedo, H. M. Savage, and W. K. Reisen. **2013**. Phenotypic variation among *Culex pipiens* complex (Diptera: Culicidae) populations from the Sacramento Valley, California: Horizontal and vertical transmission of West Nile virus, diapause potential, autogeny, and host selection. Am. J. Trop. Med. Hyg. 89: 1168–1178.

Nelms, B. M., P. A. Macedo, L. Kothera, H. M. Savage, and W. K. Reisen. **2013**. Overwintering biology of *Culex* (Diptera: Culicidae) mosquitoes in the Sacramento Valley of California. J. Med. Entomol. 50: 790.

Ng, T., D. Hathaway, N. Jennings, D. Champ, Y. W. Chiang, and H. J. Chu. **2003**. Equine vaccine for West Nile virus. Dev. Biol. (Basel). 114: 221–7.

Nielsen, C. F., M. V. Armijos, S. Wheeler, T. E. Carpenter, W. M. Boyce, K. Kelley, D. Brown, T. W. Scott, and W. K. Reisen. **2008**. Risk factors associated with human infection during the 2006 West Nile virus outbreak in Davis, a residential community in northern California. A. J. Trop. Med. Hyg. 78: 53–62.

Patel, H., B. Sander, and M. P. Nelder. **2015**. Long-term sequelae of West Nile virus-related illness: a systematic review. Lancet Infect. Dis. 15: 951–959.

Paull, S. H., D. E. Horton, M. Ashfaq, D. Rastogi, L. D. Kramer, N. S. Diffenbaugh, and A. M. Kilpatrick. **2017**. Drought and immunity determine the intensity of West Nile virus epidemics and climate change impacts. Proc. R. Soc. B Biol. Sci. 284.

Petersen, L. R., P. J. Carson, B. J. Biggerstaff, B. Custer, S. M. Borchardt, and M. P. Busch. **2013**. Estimated cumulative incidence of West Nile virus infection in US adults, 1999–2010. Epidemiol. Infect. 141: 591–595.

Planitzer, C. B., J. Modrof, M. W. Yu, and T. R. Kreil. **2009**. West Nile virus infection in plasma of blood and plasma donors, United States. Emerg. Infect. Dis. 15: 1668–1670.

Poh, K. C., L. F. Chaves, M. Reyna-Nava, C. M. Roberts, C. Fredregill, R. Bueno, M. Debboun, and G. L. Hamer. **2019**. The influence of weather and weather variability on mosquito abundance and infection with West Nile virus in Harris County, Texas, USA. Sci. Total Environ. 675: 260–272.

Poh, K. C., M. C. I. Medeiros, and G. L. Hamer. **2020**. Landscape and demographic determinants of *Culex* infection with West Nile virus during the 2012 epidemic in Dallas County, TX. Spat. Spatiotemporal. Epidemiol. 33: 100336.

Pokhrel, V., N. A. DeLisi, R. G. Danka, T. W. Walker, J. A. Ottea, and K. B. Healy. **2018**. Effects of truck-mounted, ultra low volume mosquito adulticides on honey bees (*Apis mellifera*) in a suburban field setting. PLoS One. 13: e0193535.

Ramírez, A. L., A. F. Van Den Hurk, D. B. Meyer, and S. A. Ritchie. **2018**. Searching for the proverbial needle in a haystack: advances in mosquito-borne arbovirus surveillance. Parasit Vectors. 11: 320.

Reisen, W. K. 1995. Effect of temperature on *Culex tarsalis* (Diptera: Culicidae) from the Coachella and San Joaquin Valleys of California. J. Med. Entomol. 32: 636–645.

Reisen, W. K. 2012. The contrasting bionomics of *Culex* mosquitoes in western North America. J. Am. Mosq. Control Assoc. 28: 82–91.

Reisen, W. K. 2013. Ecology of West Nile virus in North America. Viruses. 5: 2079–2105.

Reisen, W. K., B. D. Carroll, R. Takahashi, Y. Fang, S. Garcia, V. M. Martinez, and R. O. B. Quiring. **2009**. Repeated West Nile Virus epidemic transmission in Kern County, California, 2004-2007. J. Med. Entomol. 46: 139–157.

Reisen, W. K., D. Cayan, M. Tyree, C. M. Barker, B. Eldridge, and M. Dettinger. **2008**. Impact of climate variation on mosquito abundance in California. J. Vector Ecol. 33: 89–98.

Reisen, W. K., R. E. Chiles, V. M. Martinez, Y. Fang, and E. N. Green. **2003**. Experimental infection of California birds with western equine encephalomyelitis and St. Louis encephalitis viruses. J. Med. Entomol. 40: 968–982.

Reisen, W. K., Y. Fang, and V. M. Martinez. **2006**. Effects of temperature on the transmission of West Nile virus by *Culex tarsalis* (Diptera: Culicidae). J. Med. Entomol. 43: 309–317.

Reisen, W. K., J. L. Hardy, and H. D. Lothrop. **1995**. Landscape ecology of arboviruses in southern California: Patterns in the epizootic dissemination of western equine encephalomyelitis and St. Louis encephalitis viruses in Coachella Valley, 1991–1992. J. Med. Entomol. 32: 267–275.

Reisen, W. K., J. L. Hardy, S. B. Presser, M. M. Milby, R. P. Meyer, S. L. Durso, M. J. Wargo, and E. Gordon. **1992**. Mosquito and arbovirus ecology in southeastern California, 1986–1990. J. Med. Entomol. 29: 512–524.

Reisen, W. K., H. D. Lothrop, and J. L. Hardy. **1995**. Bionomics of *Culex tarsalis* (Diptera: Culicidae) in relation to arbovirus transmission in southeastern California. J. Med. Entomol. 32: 316–327.

Reisen, W. K., H. D. Lothrop, S. S. Wheeler, M. Kennsington, A. Gutierrez, Y. Fang, S. Garcia, and B. Lothrop. **2008**. Persistent West Nile virus transmission and the apparent displacement St. Louis encephalitis virus in Southeastern California, 2003-2006. J. Med. Entomol. 45: 494–508.

Reisen, W. K., R. P. Meyer, J. Shields, and C. Arbolante Shields. **1989**. Population ecology of preimaginal *Culex tarsalis* (Diptera: Culicidae) in Kern County, California. J. Med. Entomol. 26: 10–22.

Reisen, W. K., M. M. Milby, and R. P. Meyer. **1992**. Population dynamics of adult *Culex* mosquitoes (Diptera: Culicidae) along the Kern River, Kern County, California, in 1990. J. Med. Entomol. 29: 531–543.

Reisen, W. K., M. M. Milby, S. B. Presser, and J. L. Hardy. **1992**. Ecology of mosquitoes and St. Louis encephalitis virus in the Los Angeles Basin of California, 1987-1990. J. Med. Entomol. 29: 582–598.

Reisen, W. K., K. Padgett, Y. Fang, L. Woods, L. Foss, J. Anderson, and V. Kramer. **2013**. Chronic infections of West Nile virus detected in California dead birds. Vector-Borne Zoonotic Dis. 13: 401–405.

Reisen, W. K., and W. C. Reeves. **1990**. Bionomics and ecology of *Culex tarsalis* and other potential mosquito vector species., pp. 254–329. *In* Epidemiol. Control Mosquito-Borne Arboviruses California, 1943-1987. California Mosquito and Vector Control Association, Sacramento, CA.

Reisen, W., H. Lothrop, R. Chiles, M. Madon, C. Cossen, L. Woods, S. Husted, V. Kramer, and J. Edman. **2004**. West Nile virus in California. Emerg. Infect. Dis. 10: 1369–1378.

Reisen, W., P. Smith, and H. Lothrop. **1995**. Short-term reproductive diapause by *Culex tarsalis* (Diptera: Culicidae) in the Coachella Valley of California. J. Med. Entomol. 32: 654–662.

Richards, S. L., C. N. Mores, C. C. Lord, and W. J. Tabachnick. **2008**. Impact of extrinsic incubation temperature and virus exposure on vector competence of *Culex pipiens quinquefasciatus* Say (Diptera: Culicidae) for West Nile virus. Vector-Borne Zoonotic Dis. 7: 629–636.

Ripoche, M., C. Campagna, A. Ludwig, N. H. Ogden, and P. A. Leighton. **2019**. Short-term forecasting of daily abundance of West Nile virus vectors *Culex pipiens-restuans* (Diptera: Culicidae) and *Aedes vexans* based on weather conditions in southern Québec (Canada). J. Med. Entomol. 56: 859–872.

Rochlin, I., A. Faraji, K. Healy, and T. G. Andreadis. **2019**. West Nile virus mosquito vectors in North America. J. Med. Entomol. 56: 1475–1490.

Roehrig, J. T. 2013. West Nile virus in the United States - A historical perspective. Viruses. 5: 3088–3108.

Ronca, S. E., K. O. Murray, and M. S. Nolan. **2019**. Cumulative incidence of West Nile Virus infection, continental United States, 1999–2016. Emerg. Infect. Dis. 25: 325–327.

Ronca, S. E., J. C. Ruff, and K. O. Murray. **2021**. A 20-year historical review of West Nile virus since its initial emergence in North America: Has West Nile virus become a neglected tropical disease? PLoS Negl. Trop. Dis. 15: e0009190.

Rudolph, K. E., J. Lessler, R. M. Moloney, B. Kmush, and D. A. T. Cummings. **2014**. Incubation periods of mosquito-borne viral infections: a systematic review. Am. J. Trop. Med. Hyg.

Rueda, L. M., K. J. Patel, R. C. Axtell, and R. E. Stinner. **1990**. Temperature-dependent development and survival rates of *Culex quinquefasciatus* and *Aedes aegypti* (Diptera: Culicidae). J. Med. Entomol. 27: 892–898.

Ruiz, M. O., L. F. Chaves, G. L. Hamer, T. Sun, W. M. Brown, E. D. Walker, L. Haramis, T. L. Goldberg, and U. D. Kitron. **2010**. Local impact of temperature and precipitation on West Nile virus infection in *Culex* species mosquitoes in northeast Illinois, USA. Parasites and Vectors. 3.

Sardelis, M. R., M. J. Turell, D. J. Dohm, and M. L. O'Guinn. **2001**. Vector competence of selected North American *Culex* and *Coquillettidia* mosquitoes for West Nile virus. Emerg. Infect. Dis. 7: 1018–1022.

Sardelis, M. R., M. J. Turell, M. L. O'Guinn, R. G. Andre, and D. R. Roberts. **2002**. Vector competence of three North American strains of *Aedes albopictus* for West Nile virus. J. Am. Mosq. Control Assoc. 18: 284–289.

Savage, H. M., and L. Kothera. **2012**. The *Culex pipiens* complex in the Mississippi River basin: Identification, distribution, and bloodmeal hosts. J. Am. Mosq. Control Assoc. 28: 93–99.

Schurich, J. A., S. Kumar, L. Eisen, and C. G. Moore. **2014**. Modeling *Culex tarsalis* abundance on the Northern Colorado Front Range using a landscape-level approach. J. Am. Mosq. Control Assoc. 30: 7–20.

Sejvar, J. J. 2003. West Nile virus: an historical overview. Ochsner J. 5: 6–10.

Sejvar, J. J. 2007. The long-term outcomes of human West Nile virus infection. Clin. Infect. Dis. 44: 1617–1624.

Sejvar, J. J., A. T. Curns, L. Welburg, J. F. Jones, L. M. Lundgren, L. Capuron, J. Pape, W. C. Reeves, and G. L. Campbel. **2008**. Neurocognitive and functional outcomes in persons recovering from West Nile virus illness. J. Neuropsychol. 2: 477–499.

Sejvar, J. J., and A. A. Marfin. **2006**. Manifestations of West Nile neuroinvasive disease. Rev. Med. Virol. 16: 209–224.

Shaman, J., J. F. Day, and M. Stieglitz. **2005**. Drought-induced amplification and epidemic transmission of West Nile virus in Southern Florida. J. Med. Entomol. 42: 134–141.

Shapiro, L. L. M., S. A. Whitehead, and M. B. Thomas. **2017**. Quantifying the effects of temperature on mosquito and parasite traits that determine the transmission potential of human malaria. PLoS Biol. 15: e2003489.

Silk, B. J., J. R. Astles, J. Hidalgo, R. Humes, L. A. Waller, J. W. Buehler, and R. L. Berkelman. **2010**. Differential West Nile fever ascertainment in the United States: A multilevel analysis. Am. J. Trop. Med. Hyg. 83: 795–802.

Smithburn, K. C., T. P. Hughes, A. W. Burke, and J. H. Paul. **1940**. A neurotropic virus isolated from the blood of a native of Uganda. Am. J. Trop. Med. Hyg. s1-20: 471–492.

Snyder, R. E., G. S. Cooksey, V. Kramer, S. Jain, and D. J. Vugia. **2020**. West Nile

virus–associated hospitalizations, California, 2004–2017. Clin. Infect. Dis.

Snyder, R. E., T. Feiszli, L. Foss, S. Messenger, Y. Fang, C. M. Barker, W. K. Reisen, D. J. Vugia, K. A. Padgett, and V. L. Kramer. **2020**. West Nile virus in California, 2003–2018: A persistent threat. PLoS Negl. Trop. Dis. 14: e0008841.

Staples, J. E., M. B. Shankar, J. J. Sejvar, M. I. Meltzer, and M. Fischer. **2014**. Initial and long-term costs of patients hospitalized with West Nile virus disease. Am. J. Trop. Med. Hyg. 90: 402–409.

Stead, F. M., and R. F. Peters. **1953**. The 1952 outbreak of encephalitis in California; vector control aspects. Calif. Med. 79: 91–93.

Sudia, W. D., R. W. Emmons, V. F. Newhouse, and R. F. Peters. **1971**. Arbovirus-vector studies in the Central Valley of California, 1969. Mosq. News. 31: 160–168.

Swetnam, D. M., J. B. Stuart, K. Young, P. D. Maharaj, Y. Fang, S. Garcia, C. M. Barker, K. Smith, M. S. Godsey, H. M. Savage, V. Barton, B. G. Bolling, N. Duggal, A. C. Brault, and L. L. Coffey. **2020**. Movement of St. Louis encephalitis virus in the Western United States, 2014- 2018. PLoS Negl. Trop. Dis. 14: e0008343.

Talbot, B., M. Caron-Lévesque, M. Ardis, R. Kryuchkov, and M. A. Kulkarni. **2019**. Linking bird and mosquito data to assess spatiotemporal West Nile virus risk in humans. Ecohealth. 16: 70–81.

Tempelis, C. H., W. C. Reeves, R. E. Bellamy, and M. F. Lofy. **1965**. A three-year study of the feeding habits of *Culex tarsalis* in Kern County, California. Am. J. Trop. Med. Hyg. 14: 170–177.

Thiemann, T. C., D. A. Lemenager, S. Kluh, B. D. Carroll, H. D. Lothrop, and W. K. Reisen. **2012**. Spatial variation in host feeding patterns of *Culex tarsalis* and the *Culex pipiens* complex (Diptera: Culicidae) in California. J. Med. Entomol. 49: 903–916.

Thiemann, T. C., S. S. Wheeler, C. M. Barker, and W. K. Reisen. **2011**. Mosquito host selection varies seasonally with host availability and mosquito density. PLoS Negl Trop Dis. 5.

Tiawsirisup, S., J. R. Kinley, B. J. Tucker, R. B. Evans, W. A. Rowley, and K. B. Platt. **2008**. Vector Competence of *Aedes vexans* (Diptera: Culicidae) for West Nile Virus and Potential as an Enzootic Vector. J. Med. Entomol. 45: 452–457.

Tjaden, N. B., S. M. Thomas, D. Fischer, and C. Beierkuhnlein. **2013**. Extrinsic incubation period of dengue: Knowledge, backlog, and applications of temperature dependence. PLoS Negl. Trop. Dis. 7: e2207.

Trawinski, P. R., and D. S. Mackay. **2010**. Identification of environmental covariates of West Nile virus vector mosquito population abundance. Vector-Borne Zoonotic Dis. 10: 515–526.

Turell, M. J. 2012. Members of the *Culex pipiens* complex as vectors of viruses. J. Am. Mosq. Control Assoc. 28: 123–126.

Turell, M. J., M. L. O'Guinn, D. J. Dohm, and J. W. Jones. **2001**. Vector competence of North American mosquitoes (Diptera: Culicidae) for West Nile virus. J. Med. Entomol. 38: 130–134.

Turell, M. J., M. R. Sardelis, D. J. Dohm, and M. L. O'Guinn. **2001**. Potential North

American vectors of West Nile virus. Ann. N. Y. Acad. Sci. 951: 317–324.

Urbanelli, S., F. Silvestrini, W. K. Reisen, E. De Vito, and L. Bullini. **1997**. Californian hybrid zone between *Culex pipiens pipiens* and *Cx. p. quinquefasciatus* revisited (Diptera: Culicidae). J. Med. Entomol. 34: 116–127.

Vaidyanathan, R., and T. W. Scott. **2007**. Geographic variation in vector competence for West Nile virus in the *Culex pipiens* (Diptera: Culicidae) complex in California. Vector-Borne Zoonotic Dis. 7: 193–198.

Vanichanan, J., L. Salazar, S. H. Wootton, E. Aguilera, M. N. Garcia, K. O. Murray, and R. Hasbun. **2016**. Use of testing for West Nile virus and other arboviruses. Emerg. Infect. Dis. 22: 1587–1593.

Walton, W. E., N. S. Tietze, and M. S. Mulla. **1990**. Ecology of *Culex tarsalis* (Diptera: Culicidae): Factors influencing larval abundance in mesocosms in southern California. J. Med. Entomol. 27: 57–67.

Wang, G., R. B. Minnis, J. L. Belant, and C. L. Wax. **2010**. Dry weather induces outbreaks of human West Nile virus infections. BMC Infect. Dis. 10.

Wang, J., N. H. Ogden, and H. Zhu. **2011**. The impact of weather conditions on *Culex pipiens* and *Culex restuans* (Diptera: Culicidae) abundance: A case study in Peel Region. J. Med. Entomol. 48: 468–475.

Weatherhead, J. E., V. E. Miller, M. N. Garcia, R. Hasbun, L. Salazar, M. M. Dimachkie, and K. O. Murray. **2015**. Long-term neurological outcomes in West Nile virus-infected patients: An observational study. Am. J. Trop. Med. Hyg. 92: 1006–1012.

Wheeler, S. S., C. M. Barker, Y. Fang, M. V. Armijos, B. D. Carroll, S. Husted, W. O. Johnson, and W. K. Reisen. **2009**. Differential Impact of West Nile Virus on California Birds. Condor. 111: 1–20.

Wheeler, S. S., S. A. Langevin, A. C. Brault, L. Woods, B. D. Carroll, and W. K. Reisen. **2012**. Detection of persistent West Nile virus RNA in experimentally and naturally infected avian hosts. Am. J. Trop. Med. Hyg. 87: 559–564.

White, G. S., K. Symmes, P. Sun, Y. Fang, S. Garcia, C. Steiner, K. Smith, W. K. Reisen, and L. L. Coffey. **2016**. Reemergence of St. Louis encephalitis virus, California, 2015. Emerg. Infect. Dis. 22: 2185--2188.

Winokur, O. C., B. J. Main, J. Nicholson, and C. M. Barker. **2020**. Impact of temperature on the extrinsic incubation period of Zika virus in *Aedes aegypti*. PLoS Negl. Trop. Dis. 14: e0008047.

Zeller, H. G., and I. Schuffenecker. **2004**. West Nile virus: an overview of its spread in Europe and the Mediterranean Basin in contrast to its spread in the Americas. Eur J Clin Microbiol Infect Dis. 23: 147–156.

Zou, S., G. A. Foster, R. Y. Dodd, L. R. Petersen, and S. L. Stramer. **2010**. West Nile fever characteristics among viremic persons identified through blood donor screening. J. Infect. Dis. 202: 1354–1361.

Chapter 1: Data-based entomological thresholds for spatially targeted adult mosquito control to reduce risk for West Nile virus disease

Pascale C. Stiles[1], Christopher M. Barker[1]

[1]Davis Arbovirus Research and Training Lab, Department of Pathology, Microbiology, and Immunology, University of California, Davis, CA, 95616

Abstract

West Nile virus (WNV; family *Flaviviridae*) is a zoonotic arbovirus that is maintained in transmission cycles between avian hosts and mosquito vectors of the genus *Culex*, making the risk of spillover transmission to humans difficult to predict. Human infections are associated with increases in the abundance of infected female mosquitoes, which is estimated as the product of nightly mosquito trap counts and WNV infection prevalence, known as the vector index (VI). Vector control agencies conduct surveillance of mosquito populations to monitor for increases in this metric and enact organized insecticide measures when action thresholds are reached. However, action thresholds are determined by each agency based on their local context and experience, and objective methods for defining action thresholds have not been established. In this study, we analyzed mosquito surveillance and reported human disease data from six representative vector control districts representing different ecological regions of California and aggregated these data weekly at four spatial scales: district, census county division, city, and zip code. We used receiver operating characteristic (ROC) curves to evaluate the ability of observed weekly VIs to predict whether the following three weeks would exceed the average WNV disease incidence for that three-week period in a variety of settings. Additionally, we related weekly VI observations to human WNV disease incidence in the following three weeks for each of the four spatial scales through hierarchical generalized linear models and compared model performance across spatial scales. We found the VI to be positively associated with the cumulative incidence of human WNV disease in the following three weeks. Best empirical VI thresholds for predicting high-risk periods varied by mosquito control agency and the primary vector mosquito species and trap type from which the VI was derived. Following a comparison of spatial scales, city-level data aggregation represented a scale coarse enough to include adequate surveillance data for accurate predictions yet fine enough to be actionable for targeting mosquito control. The results of this study will help guide decisions about antecedent thresholds for enacting vector control aimed at reducing local WNV transmission risk.

1.1 Introduction

West Nile virus (WNV; family *Flaviviridae*) is a zoonotic encephalitic arbovirus that can infect mammals, including humans, and is the most common cause of arboviral disease in humans in the United States (McDonald et al. 2019). It amplifies in an avian-mosquito cycle with incidental spillover to mammalian hosts, which typically do not produce high enough viremias to infect mosquitoes (McLean et al. 2001, Hayes et al. 2005, Ciota 2017). The primary vectors for WNV are mosquitoes within the genus *Culex,* with transmission in the western United States dominated by *Cx. tarsalis* and the *Cx. pipiens* complex (Goddard et al. 2002, Rochlin et al. 2019). California experiences annual seasonal transmission of WNV and has recorded 7,258 symptomatic human WNV infections and 320 deaths since its introduction into the state in 2003 (Snyder et al. 2020, California Department of Public Health 2021). Although most WNV infections remain asymptomatic, approximately 20% of infections lead to a febrile illness and a small fraction (< 1%) of infections will develop into severe West Nile neuroinvasive disease (WNND), which has a fatality rate of approximately ten percent (Lindsey et al. 2010, Petersen et al. 2013). The risk for developing WNND increases in older individuals and individuals with weakened immune systems (Nash et al. 2001, Lindsey et al. 2010, Murray et al. 2013). There is no specific treatment for WNV infection and although an equine vaccine is licensed to protect equids, no such vaccine has been approved for humans (Beasley 2011, Kaiser and Barrett 2019). This means that disease prevention relies primarily on a combination of personal protective actions against mosquito bites (i.e., wearing insect repellent) and organized mosquito control enacted by local vector control agencies to reduce infected mosquitoes during periods of increased transmission risk (Gubler et al. 2000, California Department of Public Health et al. 2020).

Vector control agencies throughout California conduct surveillance of sentinel chickens, dead birds, and mosquitoes to monitor risk of WNV spillover to humans. Detections of WNV infections in birds trigger intensified surveillance and control efforts, but in most areas,

entomological data indicating increasing mosquito abundance and infection prevalence serve as the primary basis for initiating adult mosquito control (California Department of Public Health et al. 2020). Previous outbreak studies have shown that increased risk for human WNV disease is related to increased abundance of mosquitoes in the genus *Culex* (Bolling et al. 2009, Colborn et al. 2013, Kilpatrick and Pape 2013) and increased mosquito infection prevalence (Liu et al. 2009, Kwan et al. 2010, Giordano et al. 2017, Karki et al. 2017, 2020, Dunphy et al. 2019), both of which are measured routinely through mosquito trapping and arboviral testing. The vector index (VI) is the product of mosquito abundance and WNV infection prevalence and measures the relative abundance of infected female mosquitoes (Gujral et al. 2007). Despite its use as an entomological indicator of human infection risk to guide vector control programs, there is little published information about its ability to predict increases in human WNV incidence accurately, and there is no established action threshold to identify times and places for initiating mosquito control. A number of studies have found the VI to be predictive of human WNV disease incidence several weeks later in both epidemic and endemic transmission settings (Bolling et al. 2009, Jones et al. 2011, Kwan et al. 2012, Chung et al. 2013, Colborn et al. 2013, Kilpatrick and Pape 2013, Fauver et al. 2016, Uelmen et al. 2021). Studies by Kwan et al. (2012) and Kilpatrick and Pape (2013) evaluated the accuracy of these predictions, finding high predictive value for the cost of entomological surveillance alone (Kwan et al. 2012, Kilpatrick and Pape 2013), although Uelmen et al. (2021) suggested that the VI was not more accurate than abundance or infection prevalence alone. Fauver et al. (2016) addressed the implications for integrated vector management, suggesting that a universal action threshold would be inappropriate given the heterogeneous nature of the VI.

We were interested in whether we could identify data-based VI thresholds for different geographic regions when the risk of human WNV disease begins to increase and the geographic scale that is most informative for predicting this rising incidence. To that end, this study aimed to characterize the relationship between the VI and reported human disease incidence, to

estimate objective mosquito control action thresholds, and to determine whether such thresholds were generalizable across agencies and geographic regions with different vector species. The models developed in this study will improve prediction of when and where human disease would be expected to occur. This method of comparing models across geographic scales while controlling for demographic features will be informative for indicating the most appropriate spatial scale for enacting adult mosquito control. Overall, the results of this study will improve the evidence basis for antecedent vector control actions to reduce the risk of human WNV disease.

1.2 Methods

1.2.1 Ethics statement

This study was approved as minimal risk by the Institutional Review Board (IRB) of the University of California, Davis (FWA: 00004557, IORG: 0000251; Project ID 916060-1) and by the California Committee for the Protection of Human Subjects (FWA: 00000681; Project ID 17-02-2895).

1.2.2 Study area

The study area consisted of six mosquito and vector control districts (MVCDs) across California encompassing the counties of Los Angeles, Orange, Placer, Sacramento, Stanislaus, and Yolo (Figure 1.1). These six counties span diverse ecological regions, from the mixed-urban agricultural landscape of the Central Valley (Placer, Sacramento, Stanislaus, Yolo) to highly urbanized areas of Southern California (Los Angeles, Orange) and comprise approximately 39% of California's population, or more than 15.3 million people (US Census Bureau 2012). The Central Valley and Southern California also have contributed approximately 95% of WNV disease case reports in the state (California Department of Public Health 2021). The MVCDs included in the study vary in their vector control practices in response to high WNV transmission risk, ranging from a mix of aerial and ground-based insecticide treatments in

Sacramento, Yolo, and Stanislaus Counties to exclusively ground-based treatments in Los Angeles and Orange Counties.

1.2.3 Data

All entomological data relating to the surveillance of adult *Culex tarsalis* and the *Cx. pipiens* complex (*Cx. pipiens, Cx. quinquefasciatus* and their intergrades), including geolocated trap sites, trap type, mosquito abundance records, and arbovirus testing results, were obtained from collaborating MVCDs (see acknowledgements) for the years 2006-2016 via the VectorSurv Gateway (VectorSurv 2021). We restricted these data to observations from CO_2-baited (Newhouse et al. 1966) and gravid traps (Cummings 1992), which specifically target adult female mosquitoes in the genus *Culex*. Arbovirus testing was conducted either by the collaborating MVCD or by the Davis Arbovirus Research and Training (DART) Laboratory and consisted of testing batches (pools) of up to 50 mosquitoes of the same species for the presence of arboviral RNA by RT-PCR (Brault et al. 2015). The minimum infection prevalence then was calculated per 1,000 mosquitoes using bias-corrected maximum likelihood estimation in the binGroup R package version 2.2-1 (Hepworth and Biggerstaff 2017, Zhang et al. 2018). Mosquito abundance and arbovirus prevalence estimates that result from these traps may differ due to their attraction of different demographic segments of the adult female mosquito population. CO_2-baited traps utilize dry ice to emit carbon dioxide to attract host-seeking mosquitoes and generally attract large numbers of nulliparous females (Newhouse et al. 1966), whereas gravid traps utilize organic infusions to attract gravid ovipositing mosquitoes, which are generally older, have ingested and digested at least one blood meal, and therefore yield greater estimates of infection prevalence (Reiter 1987, Cummings 1992). Gravid traps tend to be ineffective at collecting *Cx. tarsalis*, as this species tends to lay eggs in open, irrigated areas with clean water sources (Bailey et al. 1965, Reisen et al. 1992).

Reported human case data, including onset date and patient addresses, were obtained from the California Department of Public Health for the same years (2006-2016) following IRB

approval for the use of potentially identifiable data. Because WNV disease is a notifiable disease, this registry encompassed all reported symptomatic cases of WNND and West Nile fever (WNF) during the time period, which were not differentiated for the purposes of this study. Finally, spatial census data were obtained from the United States Census Bureau Tiger/LINE database for county, census county division, city, and zip code tabulation by area boundaries and population information (US Census Bureau 2012). Cities with populations over 300,000 were subdivided further into neighborhoods based on administrative units defined by the respective city governments to better represent mosquito control-relevant spatial units. From the 2010 census, the cities in the study area that fell into this category were Los Angeles, Sacramento, Anaheim, and Santa Ana. Population density was calculated as the number of persons per square mile within each spatial scale.

We applied a spatial overlay to the geolocated mosquito trap sites and human WNV disease case addresses to determine the relevant jurisdictional boundary for each of the four spatial scales. Mosquito trap counts and mosquito pool testing results were aggregated for all traps within a spatial boundary in each week and year, and numbers of human cases were tabulated by week and year within a spatial boundary. All data were matched in time and space. Observations were considered at the weekly level to examine the effect of the VI on WNV disease incidence. The VI for a given week was calculated separately by species and trap type, excluding any observations of *Cx. tarsalis* in gravid traps, by multiplying the observed abundance per trap-night by the concurrent maximum likelihood estimate of infection rate per 1,000 female mosquitoes (Gujral et al. 2007). WNV disease incidence per million was calculated by dividing the number of cases recorded during each week in a location by that location's population (in millions) as recorded in the 2010 census (US Census Bureau 2012).

Data were restricted to 14 weeks from the beginning of July to the end of September to capture the peak periods of WNV activity for each of the years 2006-2016. Weeks with no record of any mosquito surveillance were not included. Additionally, we excluded surveillance

observations that were collected by other agencies outside the collaborating MVCDs' defined operating boundaries.

1.2.4 Statistical analyses

The outcome variable to be predicted by statistical models was defined as the number of human cases, based on date of symptom onset, occurring within each 3-week period following a single week's entomological surveillance. The lag from observed entomological data and future cases in the following three weeks accounted for expected lags due to viral transmission dynamics, such the extrinsic incubation period in mosquitoes and delays from infection to the onset of symptoms in human cases and allowed us to evaluate the near-future predictive value of the VI. Initial model selection focused on city-level data as a spatial scale that was small enough to provide targets for vector control decisions and large enough to reduce stochastic variation in the VI-WNV disease relationship. The goal was to determine a VI threshold to define a cutoff point at which the entomological data could identify higher-than-average WNV risk.

We used receiver operating characteristic (ROC) curve analyses to determine the best VI threshold for predicting whether incidence in the following three weeks exceeded the spatial unit's overall average incidence for that same three-week period (hereafter: typical incidence). Observations with VI values of 0 were excluded because adult mosquito control decisions would not be triggered by perceived epidemic risk in the absence of detected mosquitoes or virus activity. The best threshold was the VI that maximizes the sum of sensitivity and specificity when compared to whether or not typical incidence was actually exceeded (Fawcett 2006).

Finally, we fitted a negative binomial regression model of the number of WNV disease cases, controlling for species and trap type, population density, and the random effects of district on baseline WNV disease incidence and the relationship between the VI and WNV disease incidence. For the model, we included all VI observations, including values of 0, that were below the 95th percentile of observed positive VI values to reduce the undue effect of high outliers due to sparse surveillance sampling. This model was fitted to all spatial scales to

demonstrate how spatial scale affects the predictive ability of the VI through ROC curve analyses. All statistical analyses were carried out in R version 4.0.3 (R Core Team 2020) using the pROC package version 1.17.0.1 (Robin et al. 2011) and lme4 package version 1.1-27 (Bates et al. 2015).

1.3 Results

Overall, 1,666 cases of WNV disease were reported in humans within the study area and time period. Total case numbers were greatest in highly urbanized Greater LA County VCD and Orange County MVCD, representing 70% of all cases, whereas incidence was highest in the more rural Yolo County within the Sacramento-Yolo MVCD, which had a cumulative incidence of 64.6 cases per 100,000 people (Table 1.1). Across the study area, there was temporal and geographic variability in entomological WNV detections as seen in Figure 1.2a. In many years, high VIs in Southern California were not associated with high VIs in the Central Valley. Similarly, there were clear seasonal and geographic trends to mean WNV disease incidence throughout the study period, with incidence peaking slightly earlier in the Central Valley districts than in the Southern California districts (Figure 1.2b). Individually, greater VI was associated with increased WNV disease case incidence for all data combined (Figure 1.3a) and after stratification by district, although the magnitude of the association varied by district (Figure 1.3b) and by mosquito species and trap type (Figure 1.3c).

In general, mean infection prevalence was lower for *Cx. tarsalis* than for the *Cx. pipiens* complex in CO_2-baited traps, with an average difference in means of 2.06 per 1,000 females (Table 1.2). *Cx. tarsalis* was captured only rarely in gravid traps, leading to extremely low abundance estimates and unstable infection prevalence estimates, therefore data from *Cx. tarsalis* in gravid traps were excluded from analyses. The mean VI for *Cx. tarsalis* in CO_2-baited traps tended to be higher relative to the mean VI for the *Cx. pipiens* complex in the rural Central Valley districts compared to the urbanized Southern California districts where *Cx. tarsalis* is less widespread. Relative usage of the trap types varied among districts, with Placer MVCD and

Turlock MAD using CO_2-baited traps almost exclusively whereas other districts routinely used both types (Table 1.2). The low number of collections with gravid traps in Placer MVCD and Turlock MAD were excluded from further analysis.

Universal ROC analyses including all city-week observations with non-zero VIs indicated that the optimal overall VI thresholds for discriminating between high and low risk for WNV disease incidence during the subsequent three-week period ranged from 498 to 1,043, depending on the species and trap type for which the VI was estimated (Table 1.3). However, stratified analysis by district revealed variability among districts in optimal local VI thresholds (Table 1.3). In the Central Valley districts, thresholds were very similar across species and trap types in Turlock MAD and Sacramento County, which both feature a mix of urbanized areas and irrigated agriculture. However, in Placer MVCD and Yolo County where rice fields are a highly productive source of *Cx. tarsalis*, much higher thresholds were observed for *Cx. tarsalis* in CO_2-baited traps than in the other districts. In the Southern California districts, which span much of the urbanized landscape in the greater Los Angeles area, thresholds across the three districts were similar to each other for the two species in CO_2-baited traps, although we were unable to estimate a threshold in San Gabriel Valley for *Cx. tarsalis* in CO_2-baited traps as there were no city-weeks with non-zero VI observations that were associated with a three-week period exceeding typical WNV disease incidence.

In general, VI thresholds tended to be higher when estimated from gravid traps than from either *Cx. tarsalis* or the *Cx. pipiens* complex in CO_2-baited traps. Estimates from CO_2-baited traps were similar for both species in all districts except Placer MVCD and Yolo County due to large numbers of *Cx. tarsalis* associated with rice cultivation increasing the observed non-zero VIs in these districts. The discriminatory ability of the VI was driven by the distribution of non-zero VI observations for each species-trap type combination, thus higher thresholds were identified for city-weeks with greater observed VIs during the study period (Figure S1.1). For 294 city-weeks where both a CO_2-baited trap and a gravid trap were used to

collect *Cx. pipiens*, the VI estimates from gravid traps were consistently greater than the CO_2-baited trap counterparts (Figure S1.2).

The lowest VI threshold was 132 for *Cx. tarsalis* in CO_2-baited traps based on 470 city-weeks with non-zero VI observations in Sacramento County, whereas the highest was 1,046 for the *Cx. pipiens* complex in gravid traps based on 777 city-weeks with non-zero VI observations in Greater LA County VCD (Table 1.3). These thresholds were exceeded in 10.73% and 13.80% of all city-weeks during the study period, respectively (Table S1.1). The greatest threshold exceedance frequency was for the *Cx. pipiens* complex in San Gabriel Valley MVCD, where an estimated VI threshold of 582 was exceeded in 17.66% of 402 city-week observations (Table 1.3, Table S1.1). The VI thresholds identified here tended to have higher sensitivity for detecting above-normal WNV disease incidence in the next three weeks when VI estimates were based on the predominant WNV vector species in each district (Table S1.2).

The positive predictive value (PPV) was highest for the district-level model and decreased at finer spatial scales that had increased stochastic variability (Table 1.4). The PPV ranged from 40% at the coarsest district aggregation level to 13% at the finest zip code aggregation level. Sensitivity increased as aggregate area size decreased, with the exception of zip code, ranging from 63% at the district level to 73% at the city level. Specificity did not follow a singular trend across scales. The highest area under the ROC curve (AUC) was observed for the census county division model at 74%, but a nearly identical AUC of 73% was observed with the city-level data (Table 1.4, Figure 1.4).

The final city-level model showed that the VI was a statistically significant predictor of human WNV disease incidence. After controlling for the combined effects of species and trap type and the random effect of district, there was a significant increase in the incidence of human WNV disease cases as a function of the VI. On average, each 500-unit increase in the VI was associated with a 78% (95% CI: 54-105%) increase in WNV disease incidence during the next three weeks, with little variation among districts (Table S1.3). Observations from the *Cx. pipiens*

complex in gravid traps and from *Cx. tarsalis* in CO_2-baited traps were significantly associated with lower baseline human WNV disease incidence in the next three weeks compared to *Cx. pipiens* complex in CO_2-baited traps after controlling for the VI and variation in baseline WNV disease incidence among districts (Table S1.3). Population density interacted negatively with the VI such that increases in both VI and population density were associated with decreased incidence. There was wide variation in baseline incidence among districts, ranging from 40% lower in Sacramento County to 139% higher in Yolo County, than the average 2.39 cases per million people (95% CI: 1.65-3.45 cases per million). The predicted WNV disease incidence for a range of VI estimates in a city of approximately 35,000 people reflected the baseline differences in incidence between the districts (Figure 1.5). All else held equal, the greatest numbers of cases would be expected for this city in Yolo County while predictions for the remaining districts were clustered together.

1.4 Discussion

This study characterized the relationship between entomological surveillance and human WNV disease incidence through statistical models and evaluated the generalizability of this relationship across different vector control districts with different ecological settings and vector species. Our findings corroborated studies showing that entomological surveillance outcomes, specifically the VI, were positively associated with human WNV disease incidence (Winters et al. 2008, Jones et al. 2011, Kwan et al. 2012, Kilpatrick and Pape 2013, Fauver et al. 2016, Uelmen et al. 2021). We extended previous findings by characterizing the generalizability of the relationship and identifying a threshold for predicting periods of higher-than-average human WNV disease incidence for enacting adult vector control. Initial analyses between VI and human WNV disease incidence showed a positive relationship, lending support to the presence of a VI threshold for predicting high-risk periods.

The average relationship between the VI and WNV disease incidence was driven strongly by the districts with large populations and more data that met this study's inclusion criteria.

Further, VI thresholds for exceedance of typical incidence were driven by the density of VI observations that were greater than 0 in each category of mosquito species and trap type. For the *Cx. pipiens* complex, the threshold for VIs estimated from CO_2-baited traps was lower than VIs estimated from gravid traps. Because VIs from gravid traps were typically greater than from CO_2-baited traps, the distribution of VIs considered for classifying WNV risk also was shifted towards higher values. Similarly, VI thresholds from *Cx. tarsalis* tended to be higher than for the *Cx. pipiens* complex in CO_2-baited traps in districts where *Cx. tarsalis* was the more abundant WNV vector species. Although *Cx. tarsalis* is not commonly associated with urban areas, the thresholds for this species in Southern California were similar to those observed in the Central Valley districts characterized by rice fields, an important larval habitat for *Cx. tarsalis* which is associated with high abundance estimates (Pitcairn et al. 1994, Wekesa et al. 1996). However, these thresholds in Southern California were based on a small number of city-weeks with non-zero VIs, indicating a more focal distribution of *Cx. tarsalis* around limited irrigated agriculture and wetlands compared to its more widespread distribution in the rural areas of the Central Valley.

The final model showed that the incidence of human WNV disease in the three weeks following a VI observation increased significantly as the VI increased. This increase in risk was not significantly different among districts after controlling for trap type and species. Interestingly, *Cx. tarsalis* collected in CO_2-baited traps and the *Cx. pipiens* complex in gravid traps were associated with lower WNV disease incidence than was the *Cx. pipiens* complex in CO_2-baited traps. Gravid traps tend to collect older, ovipositing mosquitoes, which are more likely to be infected with WNV than mosquitoes collected from CO_2-baited traps, thus yielding higher VI estimates (Cummings 1992). Collections of *Cx. tarsalis* also tend to yield higher VI estimates in rural areas than the *Cx. pipiens* complex as it is found in large numbers around irrigated agriculture (Reisen 2012). Therefore, higher VI observations in these two surveillance

situations were related to periods with no WNV disease incidence, which is intermittent at the city level of data aggregation, contributing to the negative association seen in this model.

We were unable to control for the effect of vector control measures currently in place in our models. Vector control agencies typically respond to high VIs through adulticiding measures, which may reduce the subsequent risk of WNV transmission to humans through a reduction of the infected vector population (Elnaiem et al. 2008). The Central Valley districts tend to respond to entomological observations through broad-scale aerial insecticide applications, whereas the urban Southern California districts strictly use ground-based adult mosquito control. Large-scale aerial measures are effective at immediately reducing both mosquito abundance and mosquito infection prevalence, leading to an ultimate reduction in human cases (Carney et al. 2008, Elnaiem et al. 2008, Holcomb et al. 2021). However, mosquito numbers tend to rebound quickly during the summer months due to adult emergence from large aquatic habitats, which are not directly impacted by adulticidal applications or through immigration from neighboring, unsprayed areas, making repeated applications necessary (Mitchell et al. 1970, Holcomb et al. 2021). In contrast, ground-based methods are also effective at reducing mosquito numbers, but only when the insecticide physically reaches the mosquitoes. An abundance of urban landscaping that creates refugia for mosquitoes could make these control methods less effective than expected (Lothrop et al. 2002, Bonds 2012). We attempted to account for differences in control methods by allowing the relationship between VI and human WNV disease to vary by district. However, the timing, location, or type of vector control applied during the study period may have impacted entomological observations within the same district, and this model was unable to take temporal variation in control responses into account. Future studies that account for the type and duration of vector control measures on both mosquito abundance and infection prevalence would likely see a stronger association between the VI and WNV disease incidence.

Although there was little variability in the relationship between VI and WNV disease among districts, there was a significant association between the combined effect of population density and the VI on WNV disease incidence, which decreased in the most densely populated cities as VI increased. This holds with findings that human WNV disease in the western United States is associated with increased proportions of agricultural land, particularly irrigated agriculture (Eisen et al. 2010, Bowden et al. 2011, Kovach and Kilpatrick 2018). This is because the primary vector in rural areas is *Cx. tarsalis* rather than the *Cx. pipiens* complex, which is the primary vector in the highly urbanized cities in southern California, although the *Cx. pipiens* complex are also found around urban centers within the Central Valley. These areas more closely resemble eastern and midwestern US metropolitan areas where transmission is driven by mosquitoes of the *Cx. pipiens* complex, which are more adapted to urban infrastructure (Trawinski and Mackay 2010, Deichmeister and Telang 2011, Landau and van Leeuwen 2012, Reisen 2012). Although the entomological observations included in this study were reasonably balanced between Southern California and Central Valley districts, the majority of observations were derived from traps placed in more densely populated and urbanized cities in these two regions, which may be under-accounting for the enzootic *Cx. tarsalis*-agriculture transmission cycle that contributes to the highest WNV incidence in the country in the Great Plains and other heavily agriculturalized counties, where lower population density increases the stochastic variability of WNV disease incidence despite low case numbers (Centers for Disease Control and Prevention et al. 2020).

The predictive value of our model differs drastically across different spatial scales. At the coarsest district scale, high-risk periods were predicted with greater accuracy because larger areas are more representative of actual disease risk. However, at finer scales, whether disease occurs in a particular spatial area is highly variable, thus lowering the predictive accuracy. The model using city-level data correctly predicted high-risk periods in the next three weeks 19% of the time. The zip code level model performed worse than the city-level model, in large part

because zip code areas tended to be smaller than cities. Despite the low PPV, the sum of sensitivity and specificity, a metric that maximizes correct positive and negative classifications, and the area under the ROC curve were nearly identical to those found for the larger census county division aggregation. The observed sensitivity of 73% for the model using city-level data means that nearly three-quarters of high-risk periods were correctly identified using antecedent VI estimates. In the case of disease prevention, high sensitivity is preferred to high specificity, and sensitivity was equal to or higher than specificity in all the models we examined. Other studies assessing the accuracy of the VI in predicting human WNV disease in Los Angeles and Colorado found higher areas under the curve, sensitivities, specificities, and PPVs than we observed, but typically utilized coarser spatial and temporal scales and used a presence/absence outcome rather than exceedance of typical incidence (Kwan et al. 2012, Kilpatrick and Pape 2013). However, Kilpatrick and Pape (2013) also evaluated the ability of the VI to predict the detection of at least four cases at the county level in a 3-week moving window similar to our lagged period, and also found a high PPV. However, these studies did not consider the spatial heterogeneity of the VI within large areas nor the fact that vector control operates at finer scales than its entire jurisdiction. A recent study in Chicago found that the VI was highly predictive of the presence/absence of human WNV cases at a 1 km spatial scale, which is smaller than the units used in our study, but mosquito abundance or infection prevalence were better predictors than the VI at coarser scales (Uelmen et al. 2021). Based on our findings, we maintain that the city level, with large cities divided by their administrative boundaries, is the most actionable scale in terms of balancing the scope of vector control with the probability of human WNV disease cases and the accuracy of predictions of high-risk periods.

A limitation to our study that contributes to better model prediction at larger spatial scales is that fine geographic heterogeneity in both the VI and WNV disease incidence was smoothed over larger areas. At finer spatial scales, there was a higher rate of dropping observations due to the lack of spatial matching, and we did not account for instances where

entomological surveillance occurred in one city and cases occurred in a neighboring city, particularly in dense urban areas where humans and mosquitoes can easily move across city boundaries. Another limitation was data quality, particularly human data. Human case data are matched to the patient's residential address, which is not necessarily the site of infection, and we were unable to include cases that were not reported with an address in the analysis. Additionally, human case data relies on passive surveillance of WNV disease, and WNF cases are often underdiagnosed or possibly misdiagnosed if serological testing is not conducted (Gyure 2009, Silk et al. 2010). Having a more robust accounting of symptomatic infections would increase the quantity of entomological surveillance observations that are spatially and temporally matched to human outcome data and improve overall model estimation. We also did not include demographic variables with known associations with WNV disease because we focused on factors that resulted from surveillance observations.

Overall, our study has demonstrated that the VI can predict human WNV disease with relative accuracy during the next three weeks at a range of spatial scales relevant to vector control. Increases in entomological indices as approximated with the VI were associated with increases in human WNV disease incidence, even after adjusting for operational differences among districts. Furthermore, our study also demonstrated that a universal VI threshold for making vector control decisions is inappropriate across a state as geographically diverse as California. Different regions have different vector species, which in turn contributed to varying the relationships between VI and human WNV disease. Vector control districts across the state that use the VI as an indicator of human WNV disease risk should consider the combination of individual district-level surveillance and control practices and population characteristics within a defined boundary for the VI to have predictive meaning and decision-making relevance.

1.5 Acknowledgements

The authors acknowledge the following collaborating agencies for funding support: Orange County Mosquito and Vector Control District, Greater Los Angeles County Vector

Control District, San Gabriel Valley Mosquito and Vector Control District, Sacramento-Yolo Mosquito and Vector Control District, Placer Mosquito and Vector Control district, and Turlock Mosquito Abatement District. CMB also acknowledges support from the Pacific Southwest Regional Center of Excellence for Vector-Borne Diseases funded by the U.S. Centers for Disease Control and Prevention (Cooperative Agreement U01CK000516). The mosquito surveillance data that were analyzed in this study were collected by the agencies who funded the study as part of their routine operations, but the funders had no role in study design, data analysis, decision to publish, or preparation of the manuscript.

We thank Robert Cummings of Orange County Mosquito and Vector Control District for his work to coordinate funding for this project and William Reisen and Woutrina Smith of the University of California, Davis for providing feedback on manuscript drafts.

1.6 Tables and figures

Table 1.1. Summary statistics for WNV disease cases and demographic characteristics by vector control district. Statistics are calculated using data from all cities and towns within each district, regardless of entomological surveillance observations.

	N** (%)	Cumulative number of WNV disease cases (%)	Cumulative incidence of WNV disease per 100,000	Total district population (median city size)	Median population density (persons/mi^2)
Greater LA County VCD	109 (35)	700 (42)	15.3	4,583,288 (29,712)	8,170.6
Orange County MVCD	60 (19)	505 (30)	14.6	3,448,069 (49,062)	5,561.0
Placer MVCD	23 (7)	38 (2)	12.2	310,795 (1,963)	609.1
Sacramento County*	39 (12)	128 (8)	9.1	1,401,823 (31,184.5)	3,000.4
San Gabriel Valley MVCD	49 (16)	188 (11)	9.7	1,932,308 (30,912)	7,792.9
Turlock MAD	22 (7)	34 (2)	8.8	387,115 (3,689.5)	3,106.5
Yolo County*	13 (4)	73 (5)	64.6	112,898 (1,542)	675.5

*Sacramento and Yolo Counties are part of Sacramento-Yolo MVCD.

**All incorporated cities and census-designated places

Table 1.2. Summary of entomological surveillance data by district using data aggregated by city.

	Trap type	N** (%)	Mean *Cx. tarsalis* abundance per trap-night	Mean *Cx. pipiens** abundance per trap-night	Mean *Cx. tarsalis* infection prevalence†	Mean *Cx. pipiens** infection prevalence†	Mean *Cx. tarsalis* vector index†	Mean *Cx. pipiens** vector index†
Greater LA County VCD	CO_2	49 (17.1)	4.9	25.7	6.3	6.5	36.5	160.1
	Gravid	2,407 (82.9)	< 1	57.6	NA	8.4	NA	427.1
Orange County MVCD	CO_2	1,135 (30.5)	5.3	7.1	1.5	7.4	14.6	88.3
	Gravid	2,592 (69.5)	< 1	36.3	NA	9.1	NA	366.6
Placer MVCD	CO_2	1,248 (97.3)	28.8	71.4	2.5	3.4	129.7	35.3
	Gravid	34 (2.7)	< 1	8.5	NA	0.5	NA	12.1
Sacramento County‡	CO_2	5,642 (68.6)	12.9	8.9	6.7	6.0	58.2	31.1
	Gravid	2,580 (31.4)	< 1	10.4	NA	10.8	NA	87.6
San Gabriel Valley MVCD	CO_2	223 (35.2)	1.9	3.5	4.1	9.2	22.7	27.9
	Gravid	410 (64.8)	< 1	39.7	NA	8.7	NA	328.5
Turlock MAD	CO_2	731 (98.5)	12.5	37.0	2.8	4.3	45.5	135.0
	Gravid	11 (1.5)	< 1	1.3	NA	0.0	NA	0.0
Yolo County‡	CO_2	1,762 (70.7)	58.3	6.7	3.0	4.6	157.3	16.5
	Gravid	730 (29.3)	< 1	7.2	NA	7.4	NA	53.5

**Cx. pipiens* complex: *Cx. pipiens, Cx. quinquefasciatus* and intergrades.

**Number of city-weeks with entomological surveillance.

†per 1,000 mosquitoes.

‡Sacramento and Yolo Counties are part of Sacramento-Yolo MVCD.

Table 1.3. Vector index thresholds for classifying high risk of WNV disease at city scale in each district for each of the two major trap types targeting *Culex* spp. mosquitoes.

Region	District	VI thresholds – *Cx. tarsalis* (N*)	VI thresholds – *Cx. pipiens* complex (N*)	
		CO_2-baited traps	CO_2-baited traps	Gravid traps
All districts		498 (806)	574 (715)	1,043 (2,139)
Southern California	Greater LA County VCD	413 (8)	550 (76)	1,046 (777)
	Orange County MVCD	383 (14)	237 (65)	759 (702)
	San Gabriel Valley MVCD	NA	552 (17)	582 (107)
Central Valley	Turlock MAD	152 (22)	174 (102)	NA
	Sacramento County**	132 (470)	160 (370)	485 (475)
	Yolo County**	487 (178)	121 (47)	440 (78)
	Placer MVCD	498 (108)	181 (38)	NA

*Number of city-weeks with a VI above 0.

**Sacramento and Yolo Counties are part of Sacramento-Yolo MVCD.

Table 1.4. Comparing negative binomial model performance among spatial scales.

Models contain a population offset and the random effects of district while controlling for the vector index, the combination of species and trap type, and population density.

Spatial scale	Positive predictive value	Sensitivity	Specificity	Area under the curve
District	0.40	0.64	0.47	0.54
Census County Division	0.34	0.58	0.78	0.74
City	0.17	0.80	0.54	0.73
Zip Code	0.13	0.67	0.61	0.70

Table S1.1. Number of city-weeks with entomological surveillance during the study period and percentage of city-weeks for which the observed VI exceeded the threshold for higher-than-average human WNV risk in each district.

District	*Cx. tarsalis*		*Cx. pipiens* complex			
	CO_2 traps	Gravid traps	CO_2 traps		Gravid traps	
	N	%	N	%	N	%
All districts	5,443	6.28	5,763	7.63	8,612	6.78
Greater LA County VCD	104	4.81	391	11.00	2,347	13.80
Orange County MVCD	500	1.40	631	6.50	2,514	13.09
Placer MVCD	687	7.42	556	4.32	34	NA**
Sacramento County*	2,843	10.73	2,793	6.59	2,576	6.17
San Gabriel Valley MVCD	70	5.71	153	1.31	402	17.66
Turlock MAD	290	4.83	437	17.39	11	NA**
Yolo County*	949	7.59	802	3.99	728	3.57

*Sacramento and Yolo Counties are part of Sacramento-Yolo MVCD.

**None of these city-weeks observed a VI greater than 0, so these observations were not included in the empirical ROC analysis to estimate a VI threshold.

Table S1.2. Empirical ROC results for using the VI to classify higher-than-average risk of human WNV disease by district.

District	*Cx. tarsalis*			*Cx. pipiens* complex					
	CO_2 traps			CO_2 traps			Gravid traps		
	Sensitivity	Specificity	Positive predictive value	Sensitivity	Specificity	Positive predictive value	Sensitivity	Specificity	Positive predictive value
All districts	0.80	0.34	0.20	0.28	0.84	0.35	0.48	0.62	0.31
Greater LA County VCD	1.00	0.50	0.40	0.77	0.46	0.23	0.53	0.52	0.26
Orange County MVCD	0.57	0.57	0.57	0.88	0.60	0.78	0.71	0.49	0.43
Placer MVCD	0.81	0.59	0.32	0.55	0.74	0.46	NA	NA	NA
Sacramento County*	0.48	0.68	0.18	0.64	0.52	0.19	0.75	0.36	0.18
San Gabriel Valley MVCD	NA	NA	NA	0.33	1.00	1.00	0.47	0.78	0.29
Turlock MAD	0.75	0.78	0.43	0.37	0.83	0.43	NA	NA	NA
Yolo County*	0.70	0.52	0.33	0.56	0.81	0.60	0.78	0.43	0.42

*Sacramento and Yolo Counties are part of Sacramento-Yolo MVCD.

Table S1.3. Results from the hierarchical negative binomial regression model using the city-level data aggregation.

	Variable	Rate ratio (95% CI)	*P*-value
Fixed effects	Intercept*	2.39 (1.65,3.45)	< 0.0001
	VI (per 500-unit change)	1.78 (1.54, 2.05)	< 0.0001
	Population density (per 1,000 persons/mi^2)	1.06 (1.04, 1.08)	< 0.0001
	Cx. pipiens complex in gravid traps	0.71 (0.63, 0.80)	< 0.0001
	Cx. tarsalis in CO_2 traps	0.90 (0.79, 1.02)	0.0967
	VI-population density interaction	0.99 (0.98, 1.00)	0.0632
Random effects	Greater LA County VCD	0.74	0.94
	Orange County MVCD	1.24	1.05
	Placer MVCD	1.05	1.01
	Sacramento County**	0.60	0.89
	San Gabriel Valley MVCD	0.62	0.90
	Turlock MAD	1.20	1.04
	Yolo County**	2.39	1.21

*The rate ratio for the intercept is the baseline rate of WNV disease.

**Sacramento and Yolo Counties are part of Sacramento-Yolo MVCD.

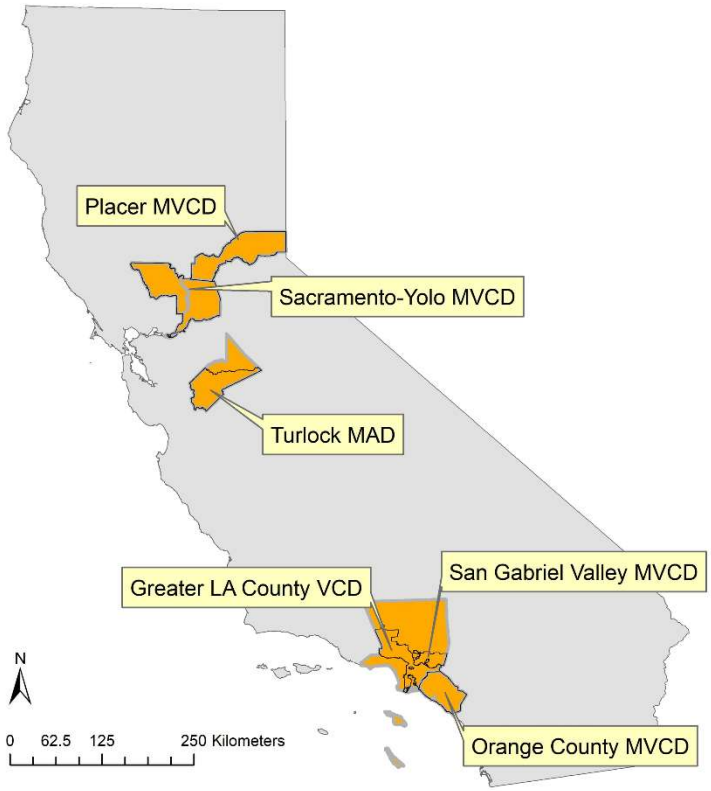

Figure 1.1. Map of the study area in California. Mosquito and vector control districts range from encompassing a single county, multiple counties, or partial counties. Counties are represented by orange polygons with gray outlines while districts are represented by black outlines. State and county boundaries were obtained from the 2010 TIGER/Line shapefiles prepared by the United States Census Bureau (US Census Bureau 2012) and mosquito and vector control district boundary shapefiles were obtained from the Mosquito and Vector Control Association of California (Mosquito & Vector Control Association of California 2017).

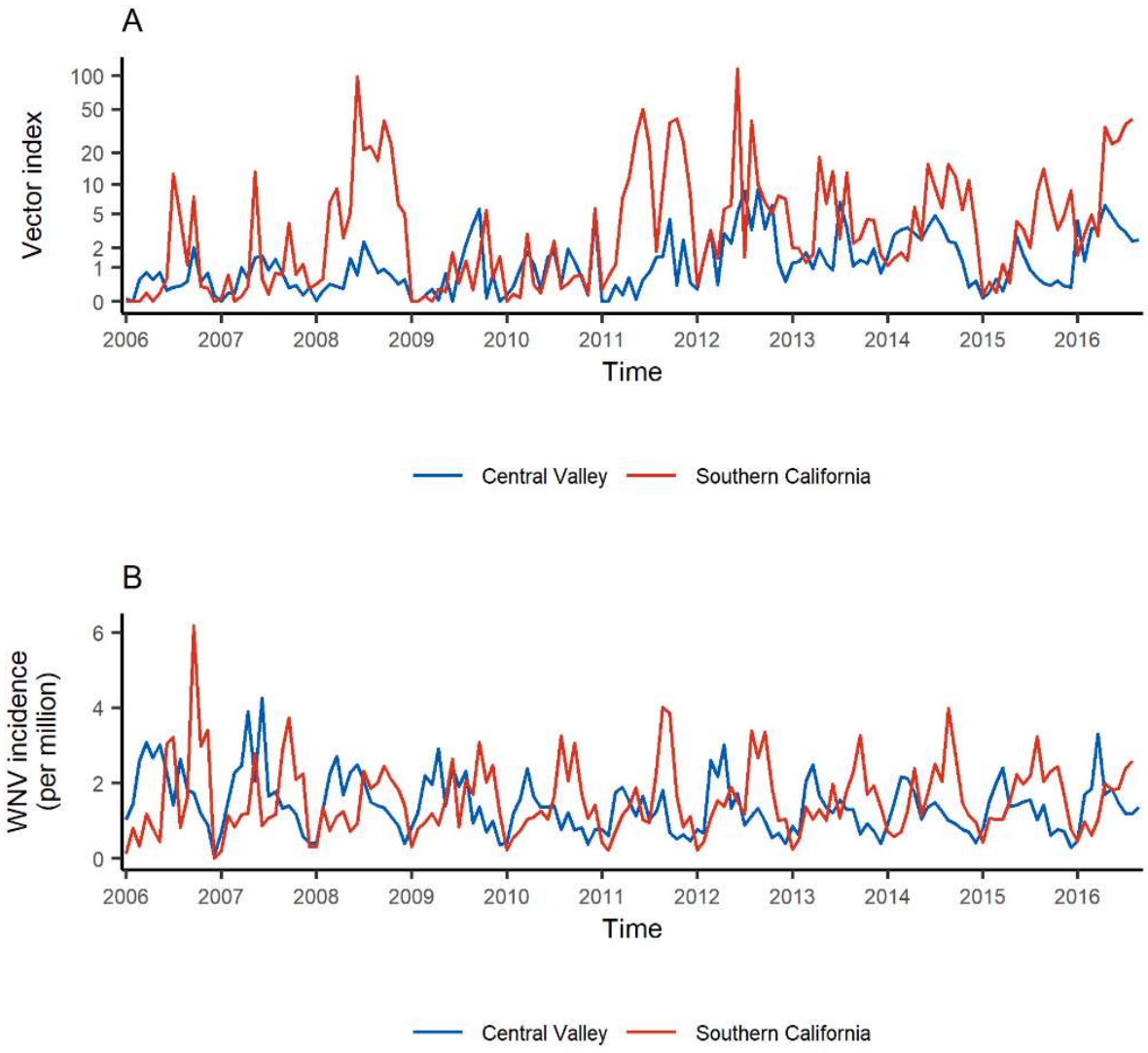

Figure 1.2. Weekly geometric mean city-scale vector index (A) and human WNV disease incidence during the subsequent three weeks (B) for districts in the Central Valley (blue) and Southern California (red). The VI was calculated as the product of mosquito abundance and WNV infection prevalence per 1,000 mosquitoes, and geometric means are shown for both VI and WNV disease incidence to reduce the influence of outliers. The y-axis of the VI panel is on the log scale to better reveal patterns over time.

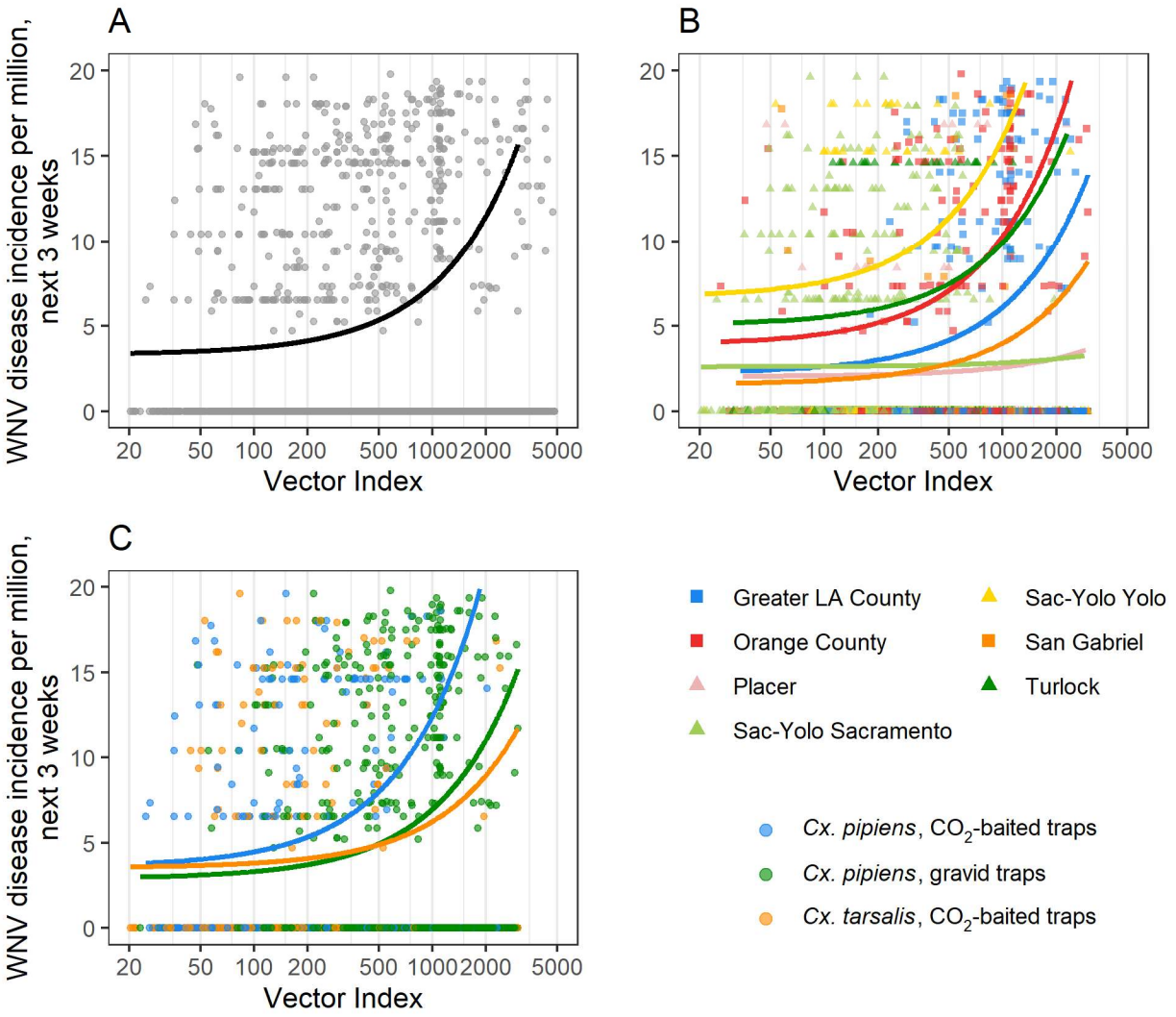

Figure 1.3. The unadjusted relationship between the vector index and WNV disease incidence in the subsequent three weeks. Panel A shows the overall relationship. Panel B shows the relationship stratified by district. Panel C shows the relationship stratified by trap type and mosquito species of the VI observation. The curves show the fitted values from linear models of lagged incidence by VI.

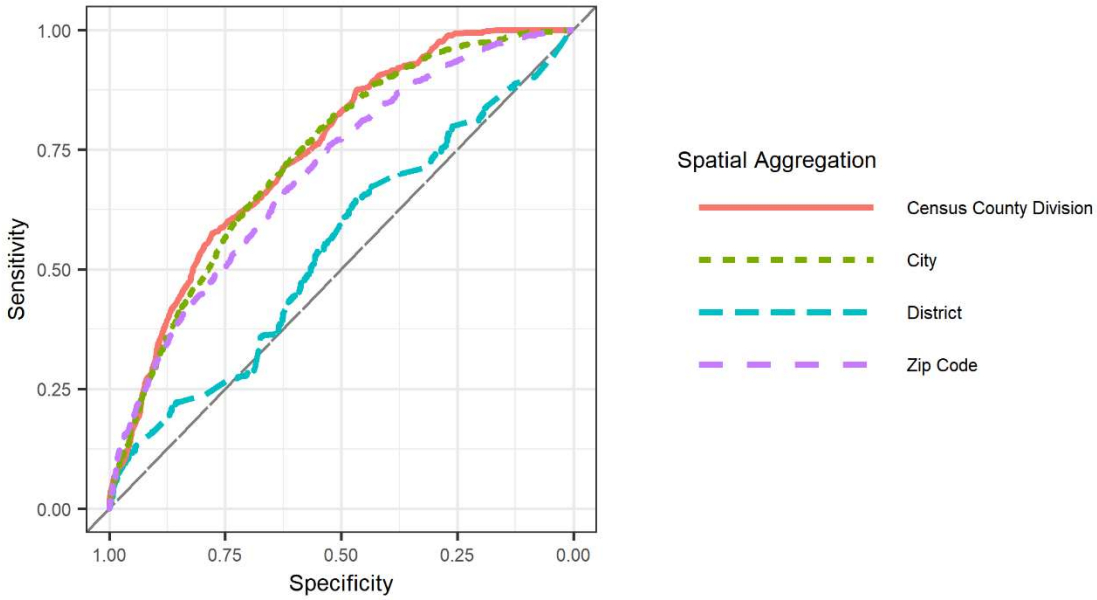

Figure 1.4. Receiver operating characteristic curves for models fitted to different spatial aggregations of observed entomological and epidemiological data. Curves closer to the upper-left corner indicate the greatest sensitivity and specificity.

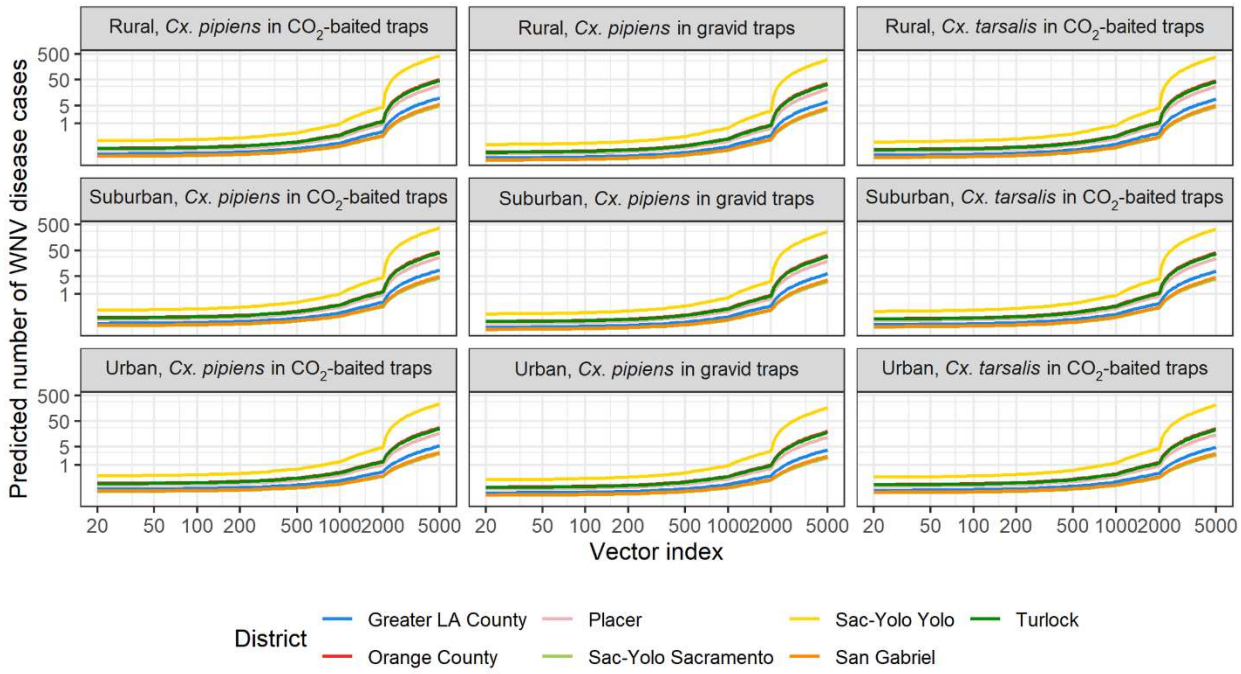

Figure 1.5. The number of human WNV disease cases predicted to occur in the three weeks following a range of observed vector indices in a city of 35,000 people in each district for a range of entomological and demographic scenarios. Rural was defined as having a population density of ≤ 500 persons/mi², suburban had 501-2,500 persons/mi², and urban had 2,501-10,000 persons/mi².

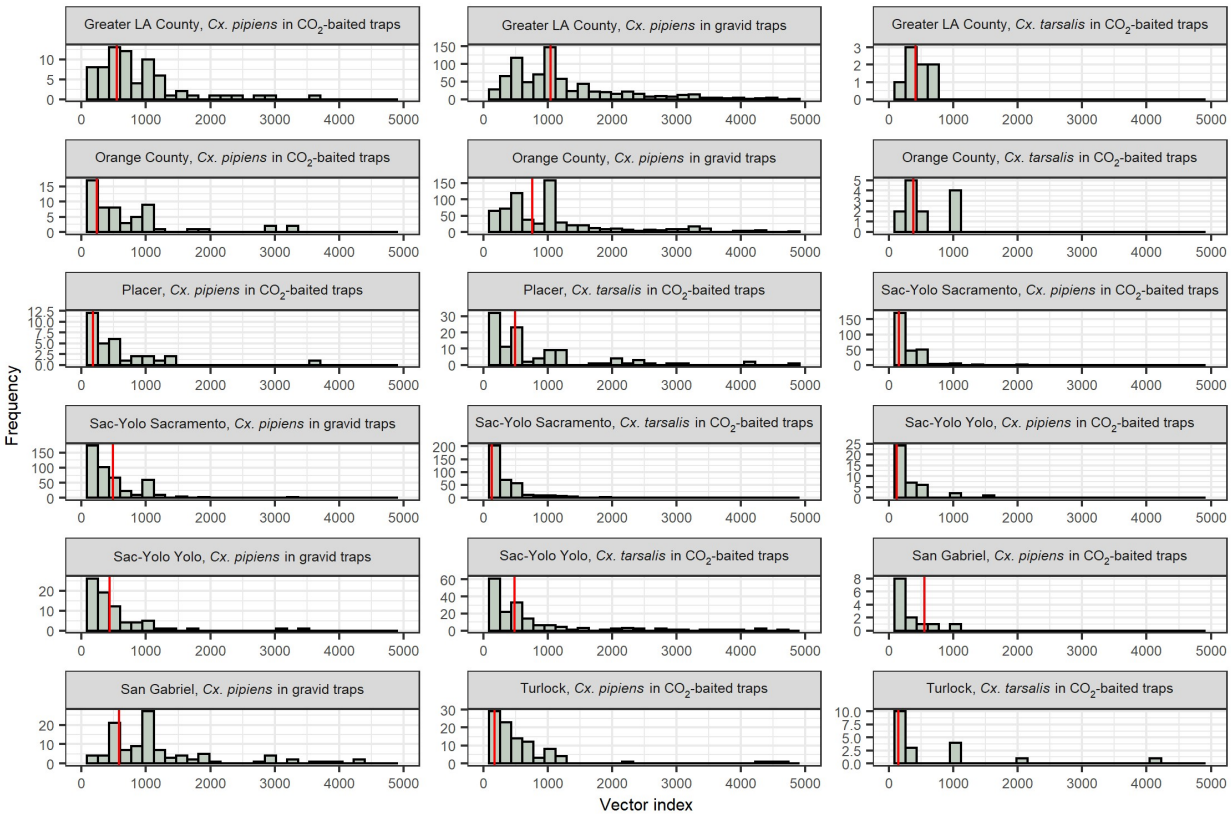

Figure S1.1. Density of VI observations for city-weeks where the VI exceeded 0 from different combinations of species and trap types in cities among the districts under consideration. The x-axis has been limited to an upper bound of 5,000 for visualization. The vertical red line indicates the VI threshold that maximizes sensitivity and specificity for the prediction of the next three weeks observing higher than average WNV disease incidence.

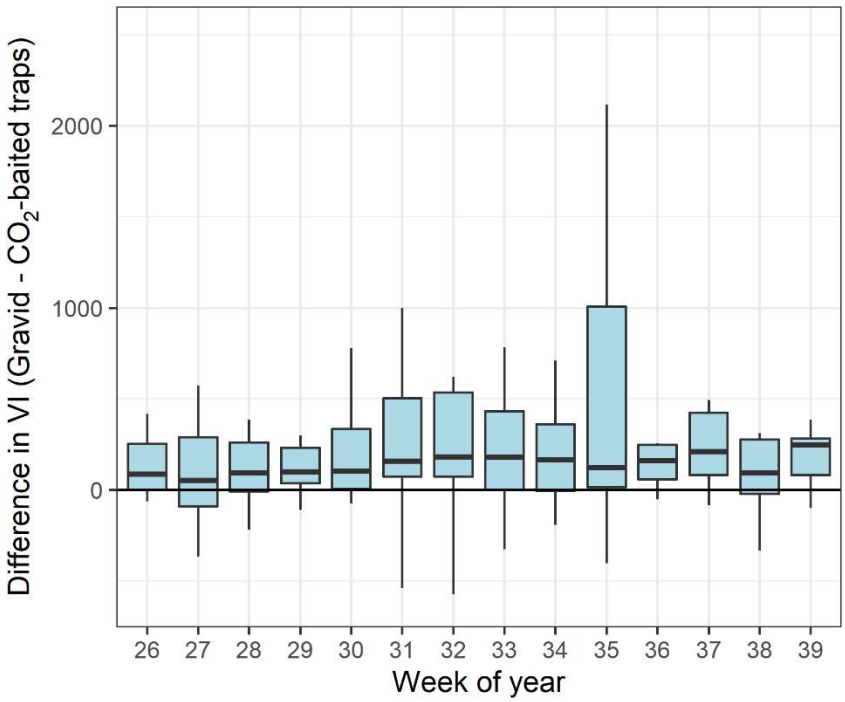

Figure S1.2. The difference in vector indices between paired CO_2-baited and gravid traps. Paired traps are traps run during the same week in the same city. VI observations from gravid traps are higher, on average, than from CO_2-baited traps.

1.7 References

Bailey, S. F., D. A. Eliason, and B. L. Hoffmann. **1965**. Flight and dispersal of the mosquito *Culex tarsalis* Coquillett in the Sacramento Valley of California. Hilgardia. 37: 73–113.

Bates, D., M. Maechler, B. Bolker, and S. Walker. **2015**. Fitting linear mixed-effects models using lme4. J. Stat. Softw. 67: 1–48.

Beasley, D. W. 2011. Vaccines and immunotherapeutics for the prevention and treatment of infections with West Nile virus. Immunotherapy. 3: 269–285.

Bolling, B. G., C. M. Barker, C. G. Moore, W. J. Pape, and L. Eisen. **2009**. Seasonal patterns for entomological measures of risk for exposure to *Culex* vectors and West Nile virus in relation to human disease cases in northeastern Colorado. J. Med. Entomol. 46: 1519–1531.

Bonds, J. A. S. 2012. Ultra-low-volume space sprays in mosquito control: a critical review. Med Vet Entomol. 26: 121–130.

Bowden, S. E., K. Magori, and J. M. Drake. **2011**. Regional differences in the association between land cover and West Nile virus disease incidence in humans in the United States. Am. J. Trop. Med. Hyg. 84: 234–238.

Brault, A. C., Y. Fang, and W. K. Reisen. **2015**. Multiplex qRT-PCR for the detection of

western equine encephalomyelitis, St. Louis encephalitis, and West Nile viral RNA in mosquito pools (Diptera: Culicidae). J. Med. Entomol. 52: 491–499.

California Department of Public Health. **2021**. Human Reports. (https://westnile.ca.gov/resources_reports.php?report_category_id=1).

California Department of Public Health, Mosquito & Vector Control Association of California, and University of California. **2020**. California Mosquito-Borne Virus Surveillance & Response Plan. Sacramento.

Carney, R. M., S. Husted, C. Jean, C. Glaser, and V. Kramer. **2008**. Efficacy of aerial spraying of mosquito adulticide in reducing incidence of West Nile virus, California, 2005. Emerg. Infect. Dis. 14: 747–754.

Centers for Disease Control and Prevention, National Center for Emerging and Zoonotic Infectious Diseases, and Division of Vector-Borne Diseases. **2020**. Final Cumulative Maps and Data. (https://www.cdc.gov/westnile/statsmaps/cumMapsData.html).

Chung, W. M., C. M. Buseman, S. N. Joyner, S. M. Hughes, T. B. Fomby, J. P. Luby, and R. W. Haley. **2013**. The 2012 West Nile encephalitis epidemic in Dallas, Texas. J. Am. Med. Assoc. 310: 297–307.

Ciota, A. T. 2017. West Nile virus and its vectors. Curr. Opin. Insect Sci. 22: 28–36.

Colborn, J. M., K. A. Smith, J. Townsend, D. Damian, R. S. Nasci, and J.-P. Mutebi. **2013**. West Nile virus outbreak in Phoenix, Arizona—2010: Entomological observations and epidemiological correlations. J. Am. Mosq. Control Assoc. 29: 123–132.

Cummings, R. F. 1992. The design and use of a modified Reiter gravid mosquito trap for mosquito-borne encephalitis surveillance in Los Angeles County, California. Proc. Pap. Conf. Mosq. Vector Control Assoc. Calif. 60: 170–176.

Deichmeister, J. M., and A. Telang. **2011**. Abundance of West Nile virus mosquito vectors in relation to climate and landscape variables. J. Vector Ecol. 36: 75–85.

Dunphy, B. M., K. B. Kovach, E. J. Gehrke, E. N. Field, W. A. Rowley, L. C. Bartholomay, and R. C. Smith. **2019**. Long-term surveillance defines spatial and temporal patterns implicating *Culex tarsalis* as the primary vector of West Nile virus. Sci. Rep. 9: 6637.

Eisen, L., C. M. Barker, C. G. Moore, W. J. Pape, A. M. Winters, and N. Cheronis. **2010**. Irrigated agriculture is an important risk factor for West Nile virus disease in the hyperendemic Larimer-Boulder-Weld area of North Central Colorado. J. Med. Entomol. 47: 939–951.

Elnaiem, D. A., K. Kelley, S. Wright, R. Laffey, G. Yoshimura, M. Reed, G. Goodman, T. Thiemann, L. Reimer, W. K. Reisen, D. Brown, and D. A. Elnaiem. **2008**. Impact of aerial spraying of pyrethrin insecticide on Culex pipiens and Culex tarsalis (Diptera: Culicidae) abundance and West Nile virus infection rates in an urban/suburban area of Sacramento County, California. J. Med. Entomol. 45: 751–757.

Fauver, J. R., L. Pecher, J. A. Schurich, B. G. Bolling, M. Calhoon, N. D. Grubaugh, K. L. Burkhalter, L. Eisen, B. G. Andre, R. S. Nasci, A. LeBailly, G. D. Ebel, and C. G. Moore. **2016**. Temporal and spatial variability of entomological risk indices for West Nile virus infection in northern Colorado: 2006-2013. J. Med. Entomol. 53: 425–434.

Fawcett, T. 2006. An introduction to ROC analysis. Pattern Recognit. Lett. 27: 861–874.

Giordano, B. V., S. Kaur, and F. F. Hunter. **2017**. West Nile virus in Ontario, Canada: A twelve-year analysis of human case prevalence, mosquito surveillance, and climate data. PLoS One. 12: e0183568.

Goddard, L. B., A. E. Roth, W. K. Reisen, and T. W. Scott. **2002**. Vector competence of California mosquitoes for West Nile virus. Emerg. Infect. Dis. 8: 1385–1391.

Gubler, D. J., G. L. Campbell, R. Nasci, N. Komar, L. Petersen, and J. T. Roehrig. **2000**. West Nile virus in the United States: Guidelines for detection, prevention, and control. Viral Immunol.

Gujral, I. B., E. C. Zielinski-Gutierrez, A. LeBailly, and R. Nasci. **2007**. Behavioral risks for West Nile virus disease, northern Colorado, 2003. Emerg. Infect. Dis. 13: 419–425.

Gyure, K. A. 2009. West Nile virus infections. J. Neuropathol. Exp. Neurol. 68: 1053–1060.

Hayes, E. B., N. Komar, R. S. Nasci, S. P. Montgomery, D. R. O'Leary, and G. L. Campbell. **2005**. Epidemiology and transmission dynamics of West Nile virus disease. Emerg. Infect. Dis. 11: 1167–1173.

Hepworth, G., and B. J. Biggerstaff. **2017**. Bias correction in estimating proportions by pooled testing. J. Agric. Biol. Environ. Stat. 22: 602–614.

Holcomb, K., R. Reiner, and C. Barker. **2021**. Spatio-temporal impacts of aerial insecticide applications on West Nile virus vectors. Parasit. Vectors. 14: 120.

Jones, R. C., K. N. Weaver, S. Smith, C. Blanco, C. Flores, K. Gibbs, D. Markowski, and J. P. Mutebi. **2011**. Use of the vector index and geographic information system to prospectively inform West Nile virus interventions. J. Am. Mosq. Control Assoc. 27: 315–319.

Kaiser, J. A., and A. D. T. Barrett. **2019**. Twenty years of progress toward West Nile virus vaccine development. Viruses. 11: 823.

Karki, S., W. M. Brown, J. Uelmen, M. O. Ruiz, and R. L. Smith. **2020**. The drivers of West Nile virus human illness in the Chicago, Illinois, USA area: Fine scale dynamic effects of weather, mosquito infection, social, and biological conditions. PLoS One. 15: e0227160.

Karki, S., N. E. Westcott, E. J. Muturi, W. M. Brown, and M. O. Ruiz. **2017**. Assessing human risk of illness with West Nile virus mosquito surveillance data to improve public health preparedness. Zoonoses Public Health. 00: 1–8.

Kilpatrick, A. M., and W. J. Pape. **2013**. Predicting human West Nile virus infections with mosquito surveillance data. Am. J. Epidemiol. 178: 829–835.

Kovach, T. J., and A. M. Kilpatrick. **2018**. Increased human incidence of West Nile virus disease near rice felds in California but not in southern United States. Am. J. Trop. Med. Hyg. 99: 222–228.

Kwan, J. L., S. Kluh, M. B. Madon, and W. K. Reisen. **2010**. West Nile virus emergence and persistence in Los Angeles, California, 2003-2008. Am. J. Trop. Med. Hyg. 83: 400–412.

Kwan, J. L., B. K. Park, T. E. Carpenter, V. Ngo, R. Civen, and W. K. Reisen. **2012**. Comparison of enzootic risk measures for predicting West Nile disease, Los Angeles, California, USA, 2004-2010. Emerg. Infect. Dis. 18: 1298–1306.

Landau, K. I., and W. J. D. van Leeuwen. **2012**. Fine scale spatial urban land cover factors associated with adult mosquito abundance and risk in Tucson, Arizona. J. Vector Ecol. 37: 407–418.

Lindsey, N. P., J. E. Staples, J. A. Lehman, and M. Fischer. **2010**. Surveillance for human West Nile virus disease - United States, 1999-2008. Surveill. Summ. 59: 1–17.

Liu, A., V. Lee, D. Galusha, M. D. Slade, M. Diuk-Wasser, T. Andreadis, M. Scotch, and P. M. Rabinowitz. **2009**. Risk factors for human infection with West Nile Virus in Connecticut: a multi-year analysis. Int. J. Health Geogr. 8.

Lothrop, H. D., B. Lothrop, and W. K. Reisen. **2002**. Nocturnal microhabitat distribution of adult *Culex tarsalis* (Diptera: Culicidae) impacts control effectiveness. J. Med. Entomol. 39: 574–582.

McDonald, E., S. W. Martin, K. Landry, C. V. Gould, J. Lehman, M. Fischer, and N. P. Lindsey. **2019**. West Nile virus and other domestic nationally notifiable arboviral diseases — United States, 2018. Morb. Mortal. Wkly. Rep. 68: 673–678.

McLean, R. G., S. R. Ubico, D. E. Docherty, W. R. Hansen, L. Sileo, and T. S. McNamara. **2001**. West Nile virus transmission and ecology in birds. Ann. N. Y. Acad. Sci. 951: 54–57.

Mitchell, C. J., J. W. Kilpatrick, R. O. Hayes, and H. W. Curry. **1970**. Effects of ultra-low volume applications of malathion in Hale County, Texas. J. Med. Entomol. 7: 85–91.

Mosquito & Vector Control Association of California. **2017**. MVCAC Webmap. (https://www.arcgis.com/home/webmap/viewer.html?webmap=604a0fe9f2b74e98a53b53d192b2ac67&extent=-131.4442,32.5803,-108.7025,41.6862).

Murray, K. O., D. Ruktanonchai, D. Hesalroad, E. Fonken, and M. S. Nolan. **2013**. West Nile virus, Texas, USA, 2012. Emerg. Infect. Dis. 19: 1836–1838.

Nash, D., F. Mostashari, A. Fine, J. Miller, D. O'Leary, K. O. Murray, A. Huang, A. Rosenberg, A. Greenberg, M. Sherman, S. Wong, and M. Layton. **2001**. The outbreak of West Nile virus infection in the New York City area in 1999. N. Engl. J. Med. 344: 1807–1814.

Newhouse, V. F., R. W. Chamberlain, J. G. Johnston, and W. D. Sudia. **1966**. Use of dry ice to increase mosquito catches of the CDC miniature light trap. Mosq. News. 30–35.

Petersen, L. R., A. C. Brault, and R. S. Nasci. **2013**. West Nile virus: review of the literature. J. Am. Med. Assoc. 310: 308–315.

Pitcairn, M. J., L. T. Wilson, R. K. Washino, and E. Rejmankova. **1994**. Spatial patterns of *Anopheles freeborni* and *Culex tarsalis* (Diptera: Culicidae) larvae in California rice fields. J. Med. Entomol. 31: 545–553.

R Core Team. **2020**. R: A language and environment for statistical computing.

Reisen, W. K. 2012. The contrasting bionomics of *Culex* mosquitoes in western North America. J. Am. Mosq. Control Assoc. 28: 82–91.

Reisen, W. K., M. M. Milby, and R. P. Meyer. **1992**. Population dynamics of adult *Culex* mosquitoes (Diptera: Culicidae) along the Kern River, Kern County, California, in 1990. J. Med. Entomol. 29: 531–543.

Reiter, P. 1987. A revised version of the CDC gravid mosquito trap. J. Am. Mosq. Control Assoc. 3: 325–327.

Robin, X., N. Turck, A. Hainard, N. Tiberti, F. Lisacek, J. C. Sanchez, and M. Muller. **2011**. pROC: an open-source package for R and S+ to analyze and compare ROC curves. BMC Bioinformatics. 12: 77.

Rochlin, I., A. Faraji, K. Healy, and T. G. Andreadis. **2019**. West Nile virus mosquito vectors in North America. J. Med. Entomol. 56: 1475–1490.

Silk, B. J., J. R. Astles, J. Hidalgo, R. Humes, L. A. Waller, J. W. Buehler, and R. L. Berkelman. **2010**. Differential West Nile fever ascertainment in the United States: A multilevel analysis. Am. J. Trop. Med. Hyg. 83: 795–802.

Snyder, R. E., T. Feiszli, L. Foss, S. Messenger, Y. Fang, C. M. Barker, W. K. Reisen, D. J. Vugia, K. A. Padgett, and V. L. Kramer. **2020**. West Nile virus in California, 2003–2018: A persistent threat. PLoS Negl. Trop. Dis. 14: e0008841.

Trawinski, P. R., and D. S. Mackay. **2010**. Identification of environmental covariates of West Nile virus vector mosquito population abundance. Vector-Borne Zoonotic Dis. 10: 515–526.

Uelmen, J. A., P. Irwin, W. M. Brown, S. Karki, M. O. Ruiz, B. Li, and R. L. Smith. **2021**. Dynamics of data availability in disease modeling: An example evaluating the trade-offs of ultra-fine-scale factors applied to human West Nile virus disease models in the Chicago area, USA. PLoS One. 16: e0251517.

US Census Bureau. **2012**. TIGER/Line® Shapefiles and TIGER/Line® Files. (https://www.census.gov/geo/maps-data/data/tiger-line.html).

VectorSurv. **2021**. Vectorborne Disease Surveillance System. (https://vectorsurv.org/).

Wekesa, J. W., B. Yuval, and R. K. Washino. **1996**. Spatial distribution of adult mosquitoes (Diptera: Culicidae) in habitats associated with the rice agroecosystem of Northern California. J. Med. Entomol. 33: 344–350.

Winters, A. M., B. G. Bolling, B. J. Beaty, C. D. Blair, R. J. Eisen, A. M. Meyer, W. J. Pape, C. G. Moore, and L. Eisen. **2008**. Combining mosquito vector and human disease data for improved assessment of spatial West Nile virus disease risk. Am. J. Trop. Med. Hyg. 78: 654–665.

Zhang, B., C. Bilder, B. Biggerstaff, F. Schaarschmidt, and B. Hitt. **2018**. binGroup: evaluation and experimental design for binomial group testing. R package version 2.2-1.

Chapter 2. Effects of short-term weather on the timing and magnitude of West Nile virus vector host-seeking activity

Pascale C. Stiles[1], Gurmanpreet Kaur[1], Mary Sorensen[2], Mario Boisvert[2], Jake Hartle[2], Marcia Reed[3], Sarah Wheeler[3], Christopher M. Barker[1]

[1]Davis Arbovirus Research and Training Lab, Department of Pathology, Microbiology, and Immunology, University of California, Davis, CA, 95616

[2]Placer Mosquito and Vector Control District, Roseville, CA, 95678

[3]Sacramento-Yolo Mosquito and Vector Control District, Elk Grove, CA, 95624

Abstract

West Nile virus (WNV) is an arbovirus that circulates in the environment between mosquito vectors and avian reservoir hosts and can infect mammals through the bite of infected mosquitoes. The risk of WNV infection in humans is monitored partly through estimates of vector abundance, but these estimates are not adjusted for the effects of short-term variation in weather, despite demonstrated associations with trap counts. Our study aims to evaluate the interactions of daily weather variability and mosquito host-seeking activity in a WNV-endemic region of California. We collected *Culex tarsalis* mosquitoes from ten traps fitted with infrared sensors to detect mosquitoes entering the traps at 15-minute intervals, temperature at 15-minute intervals, and wind speed at 1-minute intervals during the months of July and August 2019. From these collections, we estimated four key outcomes for *Cx. tarsalis* host-seeking activity: the number of *Cx. tarsalis* per night, the time of host-seeking onset, the duration of host-seeking, and the hour with the highest *Cx. tarsalis* count. We related each of these outcomes to antecedent weather conditions through statistical models and found that each of the outcomes was highly sensitive to wind speed and temperature in the evening just before the onset of host-seeking activity. In all, windier evenings were associated with fewer mosquitoes being collected overnight, a later start to host-seeking activity, a longer duration of host-seeking, and a later hour of peak activity, whereas warmer evenings generally had the opposite impact, with the exception of its effect on the duration of evening activity. The results from this study will help guide mosquito control decisions through understanding weather-induced biases in mosquito trap counts and to optimize the timing of adult mosquito control operations to maximize their effect on vector populations.

2.1 Introduction

Mosquitoes of the genus *Culex* are a public health concern as vectors of multiple zoonotic arboviruses, including West Nile virus (WNV), Saint Louis encephalitis virus, and western equine encephalomyelitis virus (Sudia et al. 1971, Rochlin et al. 2019). WNV in particular is the leading cause of human arboviral disease in the United States (McDonald et al. 2019). WNV is maintained in the environment through an avian-mosquito cycle with occasional spillover to mammalian hosts (McLean et al. 2001). In California, the predominant vectors are *Cx. tarsalis* and the *Cx. pipiens* complex (*Cx. pipiens* and *Cx. quinquefasciatus*) (Goddard et al. 2002, Reisen et al. 2004, Rochlin et al. 2019). As there is no licensed vaccine against WNV for humans, disease prevention relies on a combination of personal protective measures and mosquito control by local vector control agencies (Gubler et al. 2000, California Department of Public Health et al. 2020). The decision to enact adult mosquito control to rapidly decrease vector populations when periods of epidemic risk are detected typically depends on two entomological surveillance endpoints which have been related to transmission of WNV: mosquito abundance (Bolling et al. 2009, Colborn et al. 2013, Kilpatrick and Pape 2013) and mosquito infection prevalence (Liu et al. 2009, Kwan et al. 2010, Giordano et al. 2017, Karki et al. 2017). To estimate these metrics, vector control agencies conduct routine surveillance trapping, typically using a combination of CO_2-baited and gravid traps to target the host-seeking and oviposition site seeking stages of the mosquito life cycle, respectively (Newhouse et al. 1966, Reiter 1987, Cummings 1992). However, a limitation of this approach is that estimates of mosquito abundance do not take nightly variability due to weather into account. Instead, trap counts are taken to represent the true state of vector abundance, which could over- or under-estimate the risk of WNV transmission to humans.

Most studies have investigated the effects of weather patterns on mosquito population dynamics. The effects of temperature on mosquitoes is well-documented, with many studies agreeing that warmer temperatures at a range of time lags are positively associated with

increased mosquito counts (Hribar et al. 2010, Chuang et al. 2011, Deichmeister and Telang 2011, Lebl et al. 2013, Montarsi et al. 2015, Karki et al. 2016, Groen et al. 2017, Moise et al. 2018, Ripoche et al. 2019), but the effect of wind speed is less studied and more variable (Hribar et al. 2010, Lebl et al. 2013, Karki et al. 2016, Endo and Eltahir 2018). Much less is known about the direct impact of weather variability on mosquito host seeking activity. Several studies found that increasing wind speeds overnight were associated with reductions in trap counts (Bailey et al. 1965, Bidlingmayer et al. 1995, Hoffmann and Miller 2003) while another found positive associations between temperature and mosquito trap counts but no effect of wind speed (Hribar 2017). In addition to the effect on total nightly trap counts, daily weather variability may have an impact on the timing of mosquito host-seeking activity within each night. Typically, *Culex* spp. mosquitoes are most active shortly after sunset, with a smaller morning peak of activity (Bailey et al. 1965, Reisen et al. 1997, Veronesi et al. 2012), but this timing is subject to seasonal, meteorological, and spatial variability (Bailey et al. 1965, Bidlingmayer 1985, Veronesi et al. 2012, Montarsi et al. 2015). To our knowledge, no study of *Culex* host-seeking behavior has examined the effect of antecedent daily weather variability on both total counts per trap night and the timing of host-seeking activity. Herein, we examined how daily weather, specifically temperature and wind speed, impacted the timing of *Cx. tarsalis* host-seeking activity and trap counts. This would serve to identify the best times for targeting mosquito control given the antecedent weather conditions and to understand how weather anomalies may cause bias in abundance estimates used in WNV risk assessment.

2.2 Methods

2.2.1 Study area

We collaborated with Placer Mosquito and Vector Control District (PMVCD) and Sacramento-Yolo Mosquito and Vector Control District (SYMVCD) to select ten continuously operating trap sites spanning a contiguous region of western Placer County, northwestern Sacramento County, and eastern Yolo County. These sites were chosen based on high historical

mosquito abundance estimates in order to maximize statistical power to detect any effects of weather on mosquito trap counts. The nearest sites were separated by a distance of 3.5 km, whereas the most distant sites were separated by a distance of 43.7 km (Figure 2.1). This region is characterized by a Mediterranean climate with hot, dry summers and is largely agricultural. All ten sites were located adjacent to irrigated agriculture, which predominantly consisted of rice fields, but also included corn, hay, almonds, and pastures for livestock grazing. Mosquito host-seeking activity typically occurs along ecotones (Lothrop et al. 2002), and therefore most trapping sites were located near brush or other vegetation with two located next to tree cover to maximize the capture rate of host-seeking females.

2.2.2 Mosquito collection

BG-Counter (BGC) traps are modified BG-Sentinel traps manufactured by Biogents that utilize a grid of infrared sensors to record counts of mosquito-sized objects entering the trap's collection bag and then transmit those counts at 15-minute intervals to an online server (Pruszynski 2016). They can be operated continuously as long as they are connected to a power source. The BGC traps used for this study were baited with compressed CO_2 released at 400 mL per minute to attract host-seeking mosquitoes. These were already in place at each of the ten sites by the start of the study period on July 3, 2019 and were operated continuously beyond the scope of the study period, which ended on September 6, 2019. The traps and 20-lb CO_2 cylinders were housed within locked cages made up of wire mesh coarse enough for mosquitoes to pass through unencumbered. In Placer MVCD, this mesh's openings were 3 by 1.5 cm while in Sacramento-Yolo MVCD, the openings were approximately 4 by 7.5 cm. Although the design of the cages differed slightly between the two MVCDs, all had the trap's entry point approximately 1 m above ground level (Figure 2.2). Because the automated counts of BGC traps are based only on size, we collected mosquitoes from each of the ten traps three times per week during July and two times per week during August and. All collections occurred before 11:00h. Note that all times referenced in this study were in the local time, Pacific Daylight Time (UTC-7). After every

trap collection event, mosquitoes were immobilized using triethylamine and trap catches were identified to species and counted within 24 hours of collection.

In addition to the BGC traps, we operated CO_2-baited traps one night per week ≤ 100 m from each BGC trap to assess any differences in species composition between the two trap types and to understand whether inferences made from BGC trap counts could be generalizable to trap types more commonly used for WNV surveillance. During July, these were John W. Hock Company CDC Miniature Light Traps (Model 512; Gainesville, FL; https://www.johnwhock.com/products/mosquito-sandfly-traps/cdc-miniature-light-trap/) baited using ≈2 pounds of dry ice pellets as the CO_2 source, while during August, the CDC Miniature Light Traps were fitted to a John W. Hock Company Collection Bottle Rotator (Model 1512; Gainesville, FL; https://www.johnwhock.com/products/programmable-collection/collection-bottle-rotator/) that could change collection cups up to 7 times during the trapping event, allowing us to compare the broad timing of mosquito activity between the BGC and CO_2-baited traps (Hock 2015). These rotator traps were set up for an overnight collection event before 18:00h and were collected alongside the respective BGC traps the following morning. The rotator plate was programmed to change collection cups at 20:00h, 21:00h, 22:00h, 00:00h, 02:00h, 04:00h, and 06:00h (Appendix 2.6.2, Table S2.2). We followed the same collection and counting procedure as for BGC trap collections. Any collection during which the BGC or CO_2-baited trap encountered a technical problem was discarded.

2.2.3 Weather recording

In addition to the infrared grid to detect objects entering the trap, BGC traps were fitted with environmental sensors that record temperature, relative humidity, ambient light, and precipitation and transmit 15-minute averages along with the counts of mosquito-sized objects (Pruszynski 2016). To monitor wind speed, we installed a HOBO USB Micro Station Data Logger (Model #H21-USB; Bourne, MA; https://www.onsetcomp.com/products/data-loggers/h21-usb/ with a Davis Wind Speed and Direction Smart Sensor (Model #S-WCF-M003;

Bourne, MA; https://www.onsetcomp.com/products/sensors/s-wcf-m003/) anemometer/wind vane attachment at each of the BGC trap enclosures before the start of the study period. These sensors recorded wind speed, maximum wind speed (gust speed), and wind direction at 1-minute intervals until the end of the study period. The anemometer and wind vane were approximately 2 m above ground level (Figure 2.2). Discontinuities in recorded air temperatures caused by direct sunlight on the BGC sensor housing during certain afternoon intervals were corrected using weather station data derived from the National Oceanic and Atmospheric Administration and the California Irrigation Management Information System (Snyder 1984, Menne et al. 2012) as described in Appendix 2.6.1.

2.2.4 Species composition comparison

For paired CO_2-baited (both traditional and rotator) and BGC trap collections, we estimated the proportions of each trap count that were comprised of the three predominant species in this area, *Cx. tarsalis*, *Cx. pipiens*, and *Anopheles freeborni*. These proportions were statistically compared using intraclass correlation coefficients (ICC) using the R package "irr", version 0.84.1, which test for agreement between paired observations (Gamer et al. 2019). A high ICC value would indicate that the species distribution did not differ between the two trap types.

2.2.5 Estimation of nightly mosquito activity

We began by comparing the ratio of manual mosquito counts to automated counts from the BGC traps, where a ratio of 1 indicates parity between the two counts. To ensure accurate mosquito counts and weather information, we excluded 28 collection events where the natural log of this ratio was ≥ 1 standard deviation above or below of the mean log ratio to capture variation around the mean ratio while excluding collections that would result in unreliable 15-minute count estimates. We used the log of the ratios because ratios are multiplicative quantities and to reduce the influence of outliers. Additionally, we excluded daily observations where the full 24-hour period was not recorded to ensure that we had full coverage of diurnal weather as

well as nocturnal mosquito activity. We then approximated 15-minute counts of *Cx. tarsalis* using the method described in Appendix 2.6.2. Hereafter, "mosquito activity" refers to *Cx. tarsalis* activity.

We divided each 24-hour day into three periods to delineate different landmarks during a host-seeking event. We used the R package "suncalc", version 0.5.0 (Thieurmel and Elmarhraoui 2019) to estimate the sun's elevation at 15-minute intervals and defined the daytime period as when the sun's elevation was greater than 10° above the horizon, typically from 07:00-18:00h. Mosquito counts during the daytime period were excluded from further analyses due to negligible trap counts. Night and morning were separated at 01:00h to differentiate between the two primary overnight peaks in activity. The total overnight trap count was the cumulative number of mosquitoes that entered the trap during the night and morning periods. Mosquito activity onset was defined as the first 15-minute interval during the nighttime period that recorded a trap count above 0. We then calculated the elapsed time in minutes from sunset to the time of activity onset (hereby referred to as time to onset) using daily sunset times estimated from the "suncalc" package to account for changes in the photoperiod across the study period. We also calculated the cumulative mosquito count and cumulative proportion of total count for the entire night and morning periods to estimate the timing at which landmark percentiles in mosquito collections occurred (Figure S2.3). We used these estimates to create a variable capturing the duration of the evening peak in activity, which we defined as the elapsed time in minutes from the time of activity onset to the time at which 50% of a given night's total count had entered the trap. Finally, we estimated the hour with the highest single count of *Cx. tarsalis* to evaluate the potential impact of a single 1-hour mosquito control event on the host-seeking population and assessed this outcome as the elapsed time, in minutes, since 12:00h. Ties were broken by taking the earlier time.

2.2.6 Statistical analyses

We evaluated the relationship with weather separately for four outcomes: 1) the total overnight trap count; 2) the time to activity onset; 3) the duration of evening activity; and 4) the hour with the highest total mosquito count. The onset, duration, and peak outcomes were modelled using linear regression whereas the total count outcome was modeled with negative binomial regression. For the three models of outcomes relating to the timing of mosquito activity throughout the night, we restricted the data to trap-nights when at least 50 mosquitoes were collected to avoid stochastic temporal variation associated with lower trap catches. Additionally, we further restricted the data used in the model for the nighttime peak in mosquito activity by excluding trap-nights where the peak occurred after midnight because we wanted to exclude broader host-seeking activity and focus on the primary period of *Cx. tarsalis* host-seeking. All models included site as a random effect to account for differences in mosquito populations at different locations.

Model selection was based on Bayesian Information Criterion (BIC) (Schwarz 1978). Wind speed, temperature, and relative humidity as observed on the hour from 12:00-20:00h initially were evaluated separately to determine the best-fitting time point for each factor before performing stepwise model selection by sequentially adding and removing variables at the best-fitting time points until the BIC was no longer reduced through the addition or removal of a variable. Other factors under consideration were the study day for all outcomes, time to activity onset for the duration, peak, and count outcomes, and duration of evening activity for the count outcome. All variables in the final models except study day were standardized by mean-centering and dividing by the standard deviation (SD). After establishing the best-fitting set of variables for each outcome, we compared the BIC for that model to models using weather measured at different time points to determine how much information may be lost by using weather observed at different times in the afternoon. Finally, we evaluated the change in model fit for each of the best-fitting models when using weather variables recorded at the Sacramento

Metropolitan Airport meteorological station (Station ID WBAN:93225; Latitude/Longitude 38.69556°/-121.58972°) (Menne et al. 2012) to assess whether the observed relationships could be generalizable to publicly available weather data from a fixed location. All statistical analyses were conducted in R version 4.0.3 using the "lme4" package, version 1.1-23 (Bates et al. 2015, R Core Team 2020).

2.3 Results

2.3.1 Mosquito collections

In all, there were 219 unique trapping intervals from the 10 BGC trap sites representing a total of 710 trap-nights between July 3 and September 6, 2019. Of these, 104 BGC collections were paired with either a CO_2-baited trap or a rotator trap. Eleven (5%) of these 219 BGC trapping events experienced a technical problem with the trap that invalidated the collection and were removed from further analysis. An additional 28 (13%) had a manual:automatic count ratio > 1 SD above or below the mean and were also excluded, along with 38 trap-nights that did not fulfill the criterion of 96 consecutive 15-minute periods in 24 hours, leaving 165 unique trapping events over 492 trap-nights for analysis. These BGC trap collections yielded 222,054 mosquitoes representing nine species (Table 2.1). Of these, 218 (< 0.1%) were males and were discarded. The most common species that in both trap types were *Cx. tarsalis* (69.0%), *Cx. pipiens* (16.9%), and *An. freeborni* (11.7%; Table 2.1), which differed in their geographic distribution (Figure 2.3). The BGC traps generally collected more mosquitoes than the CO_2-baited traps. The correlation for the proportion of *Cx. tarsalis* in total trap counts between the two trap types was 0.64 (Table 2.1). This gives evidence that conclusions made for *Cx. tarsalis* in BGC traps could be generalizable to the CO_2-baited traps more typically used for WNV surveillance. Overall, the timing of mosquito activity per hour was similar between the BGC and the rotator traps, although higher proportions of mosquitoes were collected during evening in rotator traps (Figure 2.4).

2.3.2 Weather

The mean daily minimum and maximum temperatures of trap-nights included in the statistical analyses were 16.37°C (SD 1.97°C) and 33.54°C (SD 2.03°C), respectively. There was a clear diel temperature pattern, with the coolest average temperature observed from 05:00-06:00h while highest average temperature was observed between 16:00-17:00h (Figure 2.5a). The average daily wind speed was 4.4 km/h (SD 2.5), with hourly averages ranging from 3.13 km/h between 06:00-07:00h to 5.21 km/h between 14:00-15:00h (Figure 2.5b). The corrected daily temperature profiles based on the observed air temperatures at nearby meteorological stations were similar to those observed at sites with external temperature sensors (Appendix 2.6.3).

2.3.3 Time of weather measurement for predicting host-seeking outcomes

Initial model selection for the best-fitting weather variables began with wind speed for all four models. However, each model had a different best-fitting time for measuring wind speed, which limited the times for temperature and relative humidity in the stepwise selection procedure. Wind speed and temperature were consistently found as important meteorological predictors of all four *Cx. tarsalis* host-seeking outcomes whereas relative humidity was not found to add any information once temperature was included in the models. When comparing the final model formulations fitted using wind speed and temperature every hour from 12:00h-20:00h, we found that the best-fitting time for predicting all four outcomes was consistently at 20:00h, although the difference in BIC within models was negligible, with a maximum 1.4% change between the lowest and highest BIC seen in the total overnight count model (Figure S2.4).

2.3.4 Model results

The nightly *Cx. tarsalis* count for trap-nights included in the model ranged from 1 to 7,501, with a median of 178.5 and SD of 479.67. There was strong spatial heterogeneity among sites (Figure 2.3a). The model fitted an average baseline count of 273 *Cx. tarsalis*, ranging from 151 to 1,011 depending on the site. Independently, each 3 km/h increase in wind speed above the

mean was associated with the total count being reduced by nearly 25% and each 2°C increase in temperature above the mean was associated a 51% increase in total count (Table 2.2). This model also adjusted for study day, the timing of activity onset, and the duration of evening activity. Later-than-average activity onset was associated with a reduction in total mosquito count, whereas longer-than-average duration was associated with more mosquitoes being collected.

The onset of host-seeking activity occurred most frequently during the hour from 20:00h to 21:00h on nights when at least 50 mosquitoes were collected, with a mean of 16.06 minutes after sunset (SD: 11.36 minutes). From the final model, the average onset of mosquito activity occurred approximately 20 minutes after sunset on any given day, although this ranged from 10.62 minutes to 27.00 minutes, depending on the site. Wind speed at 20:00h had a stronger impact than temperature, although the effect sizes for both were modest. Every 3 km/h increase in wind speed above the mean was associated with a 2-minute delay in the start of mosquito host-seeking activity, whereas each 2°C increase in temperature above the mean delayed onset by 1.5 minutes (Table 2.2). This model adjusted for study day, which was associated with activity onset occurring closer to sunset as the study period progressed.

The time of the collection of the median mosquito on a given night was more variable than the time of the first mosquito, primarily ranging from shortly after activity onset to more than three hours after activity onset (mean: 153.72 minutes; SD: 74.86 minutes). Evening mosquito activity was generally completed before 01:00h. The final model predicted that the median mosquito would arrive approximately 2.5 hours after the onset of mosquito activity, on average, again varying by site from just over one hour to over four hours. Each of the weather conditions included in the model independently had positive effects, where increases above the respective means were associated with lengthening the duration of evening activity (Table 2.2). Additionally, the combined effect of higher-than-average wind speed and temperature was associated with a moderation of the individual positive effects of these two factors. This model

also adjusted for study day and the timing of activity onset (the outcome of the previous model). Notably, later-than-average activity onset was associated with shortening the duration of evening activity (Table 2.2).

Culex tarsalis counts typically reached their maximum within one hour of sunset, between 21:00h and 22:00h. The observed mean time of the peak hour was 21:18h. The fitted model predicted the peak of activity to occur at 21:48h, on average, with variation between 21:08h and 23:00h depending on the site. This model was very similar to that of the onset of mosquito activity, where with each 3 km/h increase in wind speed or 2°C increase in temperature above their respective means delayed the time of the peak hour by more than 10 minutes, while each subsequent week of the study period was associated with the peak occurring 6 minutes earlier than during the previous week (Table 2.2). The time of activity onset relative to sunset did not have an effect on the timing of the peak in activity. The median number of *Cx. tarsalis* collected during the fitted peak hour was 86.93% of the number collected during the observed peak hour compared to 68.75% of the peak count during the hour beginning at 22:00h (Figure 2.6).

2.3.9 Generalizability of weather measurements

We compared model performance for each of the respective best-fitting models using wind speed and temperature records from the Sacramento Metropolitan Airport meteorological station and found that the change in fit for all four models was negligible compared to fitting the model with weather recorded at each individual site. The greatest loss in model fit was a 1.02% increase in BIC for the model predicting the duration of evening host-seeking activity (Table 2.3). The model predicting the total overnight mosquito count saw no change in BIC when using fixed point versus site-specific weather.

2.4 Discussion

Routine surveillance estimating mosquito abundance was highly sensitive to daily weather fluctuations. *Culex tarsalis* host-seeking endpoints are intertwined such that

accounting for weather fluctuations alone was insufficient for examining variability in the timing of host-seeking activity and the overnight trap counts used to estimate relative mosquito abundance as an indicator of arbovirus risk. Unlike prior studies that examined the effects of weather conditions at the time of the mosquito observation, we analyzed the effects of weather at a range of times during the afternoon leading to the collection event to aid vector control agencies in predicting the periods of highest adult female mosquito activity for enacting mosquito control. We observed that the onset of *Cx. tarsalis* host-seeking activity was highly correlated with sunset time and was most intense during the first half of the night. This is consistent with the findings of prior studies regarding *Cx. tarsalis* host-seeking behavior (Bailey et al. 1965, Reisen et al. 1997, Godsey et al. 2010). We found wind speed and temperature to be the most important factors affecting all the outcomes we observed, and the relationships were consistent regardless of the time in the afternoon used for the models. We also found that mosquito outcomes were related to each other, although we only considered antecedent outcomes as possible predictors for outcomes that occurred as the host-seeking night evolved. Although we cannot discount the possibility that overall lower counts may have impacted the detection of the first host-seeking mosquitoes, this was somewhat alleviated by excluding nights with fewer than 50 total mosquitoes from the host-seeking timing outcomes.

Generally, days with above-average winds resulted in fewer *Cx. tarsalis* collected during a trap-night, later onset and peak of *Cx. tarsalis* host-seeking activity, and a longer duration of the first half of host-seeking activity. The mechanism for the effects of wind speed on host-seeking activity was not clear. It has been suggested that host-seeking behavior of mosquitoes is greatly reduced at wind speeds beyond 3 km/h (Service 1980), so it is possible that the observed effect of wind speed on activity onset and peak was due to mosquitoes sheltering until more favorable conditions develop. We did observe slightly lower mean wind speeds at night, although nighttime wind speeds were more variable than during the day (Figure 2.4). The effect of increased wind speeds depressing trap catch has been documented previously (Bailey et al.

1965, Bidlingmayer 1985, Bidlingmayer et al. 1995, Hoffmann and Miller 2003, Gray et al. 2011) and could be the result of flight suppression as previously discussed or dispersal of the CO_2 lure resulting in fewer mosquitoes being attracted to the trap. One study suggested direct flight suppression as a possible mechanism (Bidlingmayer et al. 1995). However, another study posited that the CO_2 dispersal theory is more likely (Hoffmann and Miller 2003), although studies on the relationship between high winds, CO_2 plume dispersal, and mosquito attraction are limited (Lacey and Cardé 2011, Cummins et al. 2012). Regardless of the mechanism, *Cx. tarsalis* abundance estimates generated from traps that were in place on windier days would underestimate vector density as a metric of WNV risk. Conversely, collections taken on calmer days would be closer to true estimates of vector density in an area. Higher wind speeds also may limit the effectiveness of adult mosquito control by dispersing mosquito activity throughout the night and minimizing the host-seeking population that would be impacted by a single control event, which typically lasts for one hour.

Contrary to the observed effects of increasing wind speed, higher-than-average temperatures had the effect of increasing the overall number of *Cx. tarsalis* collected during a trap-night and accelerating the start and time of the peak hour of *Cx. tarsalis* host-seeking activity in the evening. However, temperature also had a positive association with the duration of the first half of an evening's host-seeking activity after adjusting for the time of activity onset. Other studies have also shown the positive effects of nightly temperature on overnight trap counts (Bidlingmayer 1985, Hribar 2017), which could at least partially be attributed to mosquitoes being less active at cooler temperatures (Bailey et al. 1965, Bidlingmayer 1985). Possibly some of the positive effect of temperature on trap counts resulted from the lagged effect of temperature on mosquito populations due to the increased rate of reproduction for mosquitoes at higher temperatures and temporal autocorrelation of temperature (Hribar et al. 2010, Chuang et al. 2011, Lebl et al. 2013, Ciota et al. 2014, Montarsi et al. 2015, Karki et al. 2016, Groen et al. 2017, Moise et al. 2018, Ripoche et al. 2019). The effect of temperature on the

timing of host-seeking activity by *Cx. tarsalis* is less well-established, although it could also be attributed to optimum temperature ranges for mosquito flight (Rudolfs 1925, Bidlingmayer 1974). Nevertheless, other studies examining the relationship between temperature and the timing of mosquito host-seeking have not clearly identified such associations (Bidlingmayer 1974, Reisen et al. 1997, Veronesi et al. 2012).

The ability to predict which hour during a night will represent the peak for *Cx. tarsalis* host-seeking activity is important for vector control agencies to target adult mosquito control measures in ways that impact the greatest proportion of the active vector population. Our study found that the peak hour of *Cx. tarsalis* activity was best predicted by the same set of variables influencing the start of host-seeking activity, namely late evening wind speed and temperature and study day, likely because of the timing of peak activity once host-seeking has begun. In our study, the peak hour typically began within three hours of activity onset. This range is in line with that identified for *Cx. tarsalis* in southern California and Colorado (Reisen et al. 1997, Godsey et al. 2010). Assuming vector control agencies have one hour in a given night to conduct a pesticide application, modifying mosquito control practices to commence at the start of the peak hour of mosquito activity predicted from the day's weather conditions would reach, on average, over 80% of the number of *Cx. tarsalis* females active during the actual peak hour. In comparison, only 66% of these mosquitoes would be impacted if consistently beginning operations at the fixed time of 22:00h. This does not necessarily mean that all host-seeking mosquitoes during this hour would be impacted by adulticide, nor that non-host-seeking mosquitoes would not be affected. However, targeting the peak hour would likely also have a greater reach on the non-host-seeking population as well and could have an overall impact of reducing the risk of WNV transmission by further decreasing the vector population, but this is beyond the scope of this study. It should be noted that there are other necessary meteorological conditions, such as temperature inversion, that need to be met in order for vector control operations to proceed, which we also did not evaluate. A caveat to this result is we did not

investigate potential differences in host-seeking activity between parous and nulliparous mosquitoes. Because parous mosquitoes are more likely to be infectious, targeting their peak hour of activity would likely have a greater impact on WNV risk reduction.

We observed very little loss of model performance by using weather conditions recorded from a fixed, publicly available source of meteorological data versus using site-specific weather conditions recorded earlier in the day. However, it is important to note that the Sacramento Metropolitan Airport meteorological station used as the source of our fixed-point weather data was surrounded by landscape similar to the trap sites, thus temperature or wind speed observations from this station may be more correlated to those at the trap sites than a more urban meteorological station, for example. This means it would not be necessary to deploy weather monitoring devices at routine surveillance sites in order to project the course of mosquito host-seeking activity throughout the night, but care should be taken to ensure that the weather estimates come from a reliable source within as close an environment to the locations of interest as possible. This also does not diminish the importance of understanding local meteorological phenomena such as temperature inversion for the successful deployment of adult mosquito control. Additionally, although model fit was progressively poorer when using time points farther from the start of mosquito activity, the change relative to fitting the models using weather at 20:00h remained very low, indicating that vector control agencies can determine in advance whether conditions would be suitable for reaching a high enough proportion of potential vectors and allocate resources accordingly.

A limitation to this study is the use of imperfect trapping methods for sampling mosquitoes. A recent study on the trapping efficiency of BG-Sentinel traps for collecting *Aedes aegypti* females found that 8% of trap encounters resulted in capture when using only CO_2 as an attractant (Amos et al. 2020). Similar levels of trapping efficiency were observed for both *Cx. tarsalis* and *Cx. quinquefasciatus* capture rates in CO_2-baited traps that are commonly used in arbovirus surveillance (Cooperband and Cardé 2006). This limitation should not result in

differential bias in our mosquito collections because we collected mosquitoes in line with standard surveillance practices for WNV vectors using CO_2 as an attractant, although one study of *Cx. tarsalis* in southern California found higher trapping efficiency when observed counts per trap-night were lowest (Reisen and Lothrop 1995). Regardless, it is important to acknowledge that these trap counts represent a small fraction of the host-seeking vector population in this area.

With this study, we have shown that the timing and magnitude of host-seeking activity by *Cx. tarsalis* in a rice-growing region of northern California is highly dependent on weather conditions prior to the start of mosquito activity. In all, a better understanding of how host-seeking mosquito vectors respond to daily fluctuations in weather conditions will help improve WNV risk estimation and targeting of mosquito control measures and ultimately reduce WNV transmission in this area.

2.5 Acknowledgements

The authors acknowledge Tom Moore of Placer Mosquito and Vector Control District and Kylie Letamendi and Elizabeth Stovall of Sacramento-Yolo Mosquito and Vector Control district for conducting routine trap maintenance throughout the study period. We also acknowledge Mirsha Torres of Placer MVCD for his assistance with mosquito collections and identification, as well as Karen Holcomb, Ania Kawiecki, and Matteo Marcantonio of the University of California, Davis for their assistance with trap set-up and mosquito collections. Finally, we thank the homeowners of Placer, Sacramento, and Yolo Counties who permitted us to collect from mosquito traps on their properties.

2.6 Appendix

2.6.1 BG-Counter temperature correction

The BG-Counter temperature sensors are directly on the trap beneath a plastic rain shade, so are susceptible to temperature fluctuations when subjected to direct sunlight at the hottest times of the day (Figure 2.2). Thus, we devised a correction to the 15-minute temperature observations

that better represents the true air temperature experienced at these sites. First, we gathered data from eight nearby meteorological stations monitored by the National Oceanic and Atmospheric Administration (NOAA) and the California Irrigation Management Information System (CIMIS) (Table S2.1) (Snyder 1984, Menne et al. 2012) and calculated the inverse-distance weighted mean hourly temperature using stations within 20 km of each site (R package "sp", version 1.4-5 (Pebesma and Bivand 2005, Bivand et al. 2013)) (Figure S2.1). We then took the average temperature during the nighttime hours of 21:00h-06:00h for each date and site separately and centered each 15-minute weighted average temperature observation on this mean. We chose these times because the temperature profiles in Appendix 2.6.3 (i.e., the daily temperature plots at each site) indicated little difference between weather station and BG-Counter temperature observations at those times. As the weather station temperature is hourly, values on the hour were repeated for each 15-minute period within the hour. Next, we calculated the median of the centered temperature for every 15-minute period using a moving window of the current week and one week before and after at each site. We used the median to reduce the potential effect of outliers. Finally, we added the nighttime mean temperature back to the median centered temperature to return to the original temperature scale.

2.6.2 Estimation of 15-minute Culex tarsalis counts

During the second month of mosquito collections, we placed a collection bottle rotator on a CO_2-baited trap 2 nights per week at each of the trap sites. These rotators were programmed to change collection bag at regular intervals throughout the night (Table S2.2), and the collections were speciated in the same manner as described in the paper. We estimated the proportion all mosquitoes collected during each rotator interval that were *Cx. tarsalis* (Figure S2.2). Using the start time of the rotator intervals, we determined the cup to which every hour of the day would have been associated in order to create a 24-hour profile of the proportion *Cx. tarsalis*, with a proportion of 0 applied during hours when the rotators were not in operation (i.e., 10:00h-18:00h). Finally, we fitted a generalized additive model of the proportion *Cx. tarsalis* against

hour of the day to create a smoothed 24-hour profile using the R package "mgcv", version 1.8-34 (Wood 2017). The smoothed hourly proportions were then multiplied to the 15-minute counts of mosquitoes that occurred during the same hour of the day to approximate the number of *Cx. tarsalis* every 15 minutes.

2.6.3 Temperature corrections

These daily time series show temperature at the sites that had two temperature recording devices. The black line is the observed temperature from the BGC trap, the red line is the observed temperature from the external temperature sensor, and the blue line is the corrected temperature following the procedure described in 2.5.1.

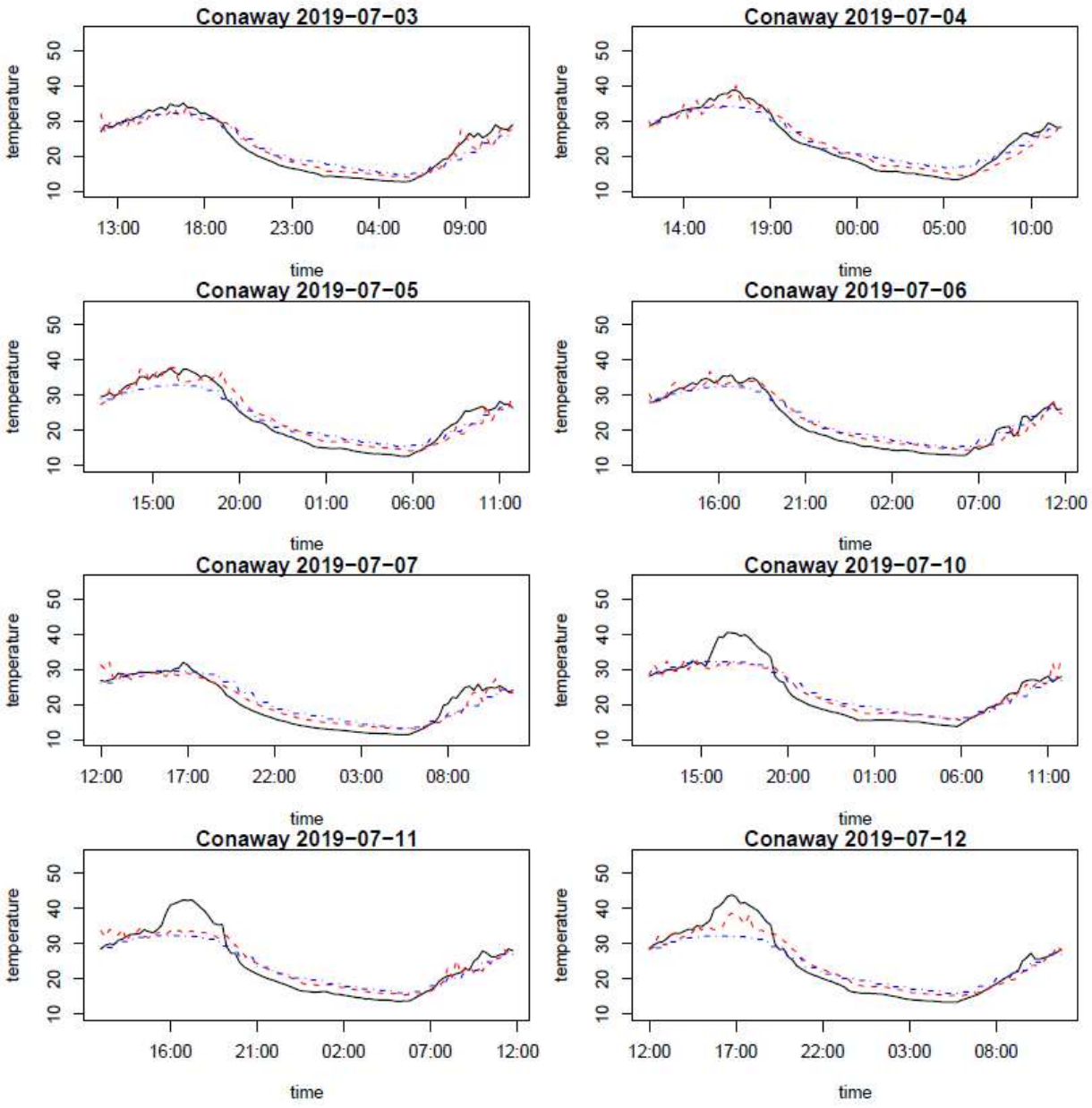
Conaway 2019-07-03
Conaway 2019-07-04
Conaway 2019-07-05
Conaway 2019-07-06
Conaway 2019-07-07
Conaway 2019-07-10
Conaway 2019-07-11
Conaway 2019-07-12
temperature
time
10
20
30
40
50
13:00
18:00
23:00
04:00
09:00
14:00
19:00
00:00
05:00
10:00
15:00
20:00
01:00
06:00
11:00
16:00
21:00
02:00
07:00
12:00
17:00
22:00
03:00
08:00

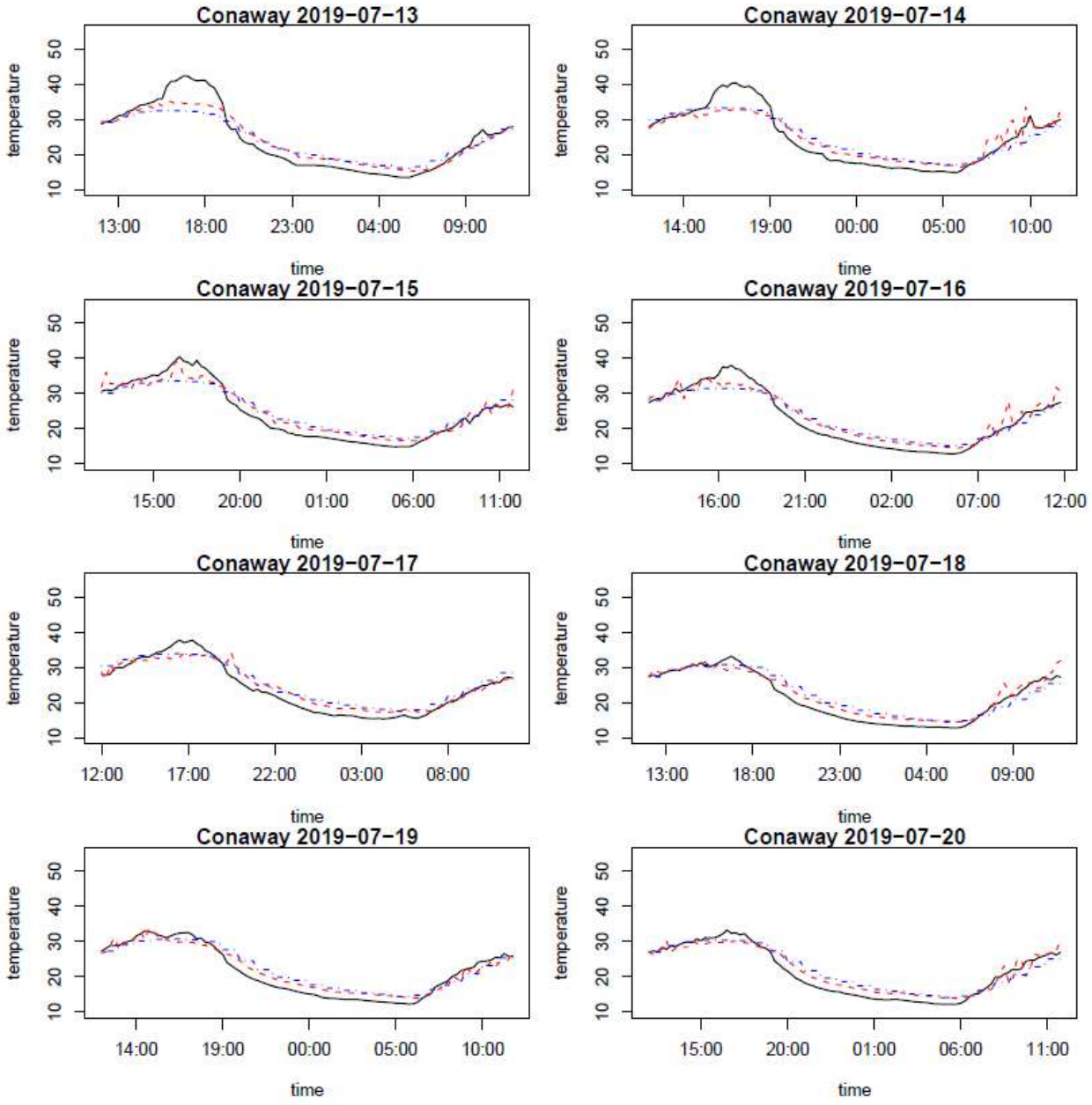
Conaway 2019-07-13
Conaway 2019-07-14
Conaway 2019-07-15
Conaway 2019-07-16
Conaway 2019-07-17
Conaway 2019-07-18
Conaway 2019-07-19
Conaway 2019-07-20
temperature
time

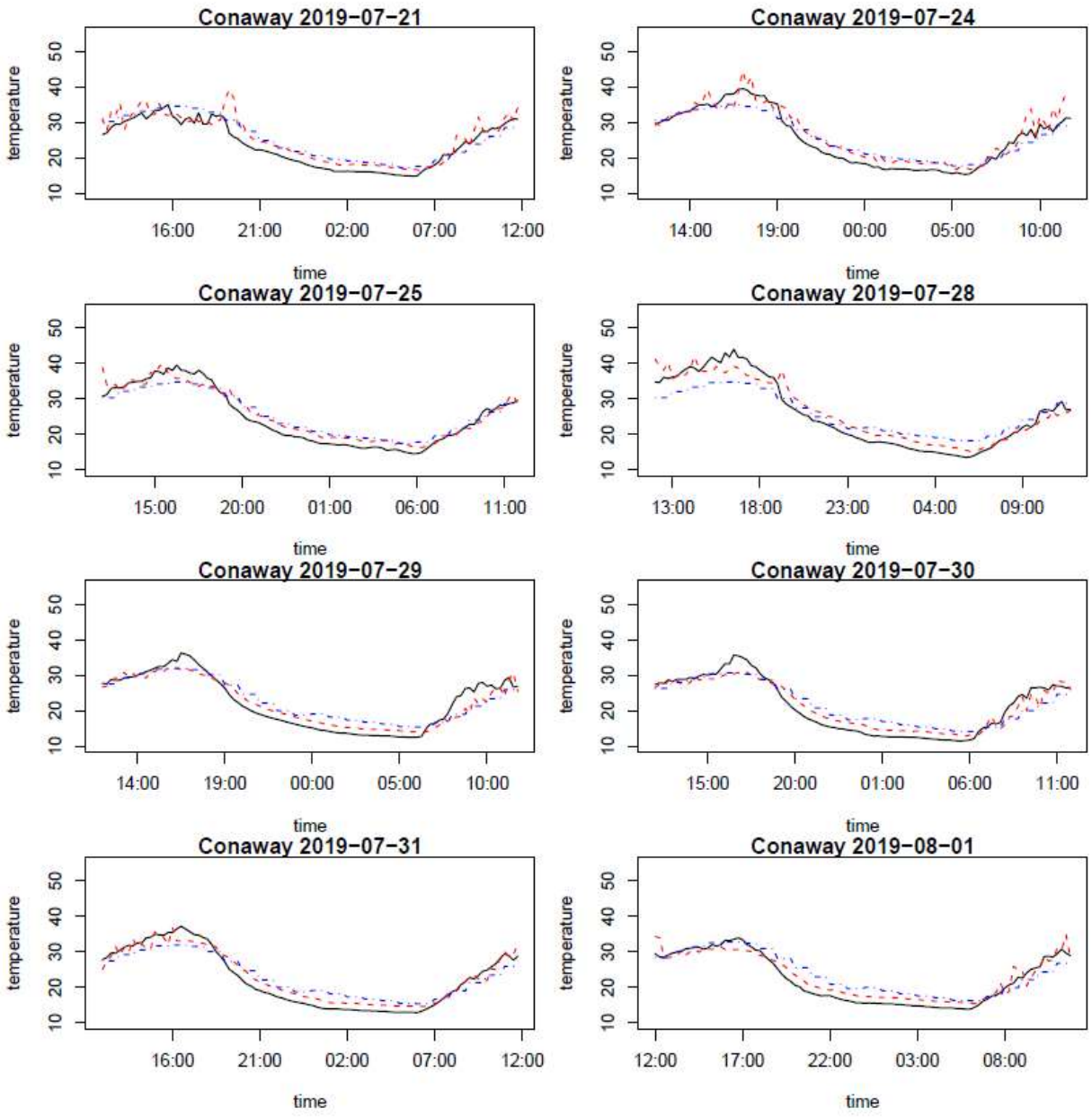
Conaway 2019-07-21
temperature
10 20 30 40 50
16:00 21:00 02:00 07:00 12:00
time
Conaway 2019-07-24
temperature
10 20 30 40 50
14:00 19:00 00:00 05:00 10:00
time
Conaway 2019-07-25
temperature
10 20 30 40 50
15:00 20:00 01:00 06:00 11:00
time
Conaway 2019-07-28
temperature
10 20 30 40 50
13:00 18:00 23:00 04:00 09:00
time
Conaway 2019-07-29
temperature
10 20 30 40 50
14:00 19:00 00:00 05:00 10:00
time
Conaway 2019-07-30
temperature
10 20 30 40 50
15:00 20:00 01:00 06:00 11:00
time
Conaway 2019-07-31
temperature
10 20 30 40 50
16:00 21:00 02:00 07:00 12:00
time
Conaway 2019-08-01
temperature
10 20 30 40 50
12:00 17:00 22:00 03:00 08:00
time

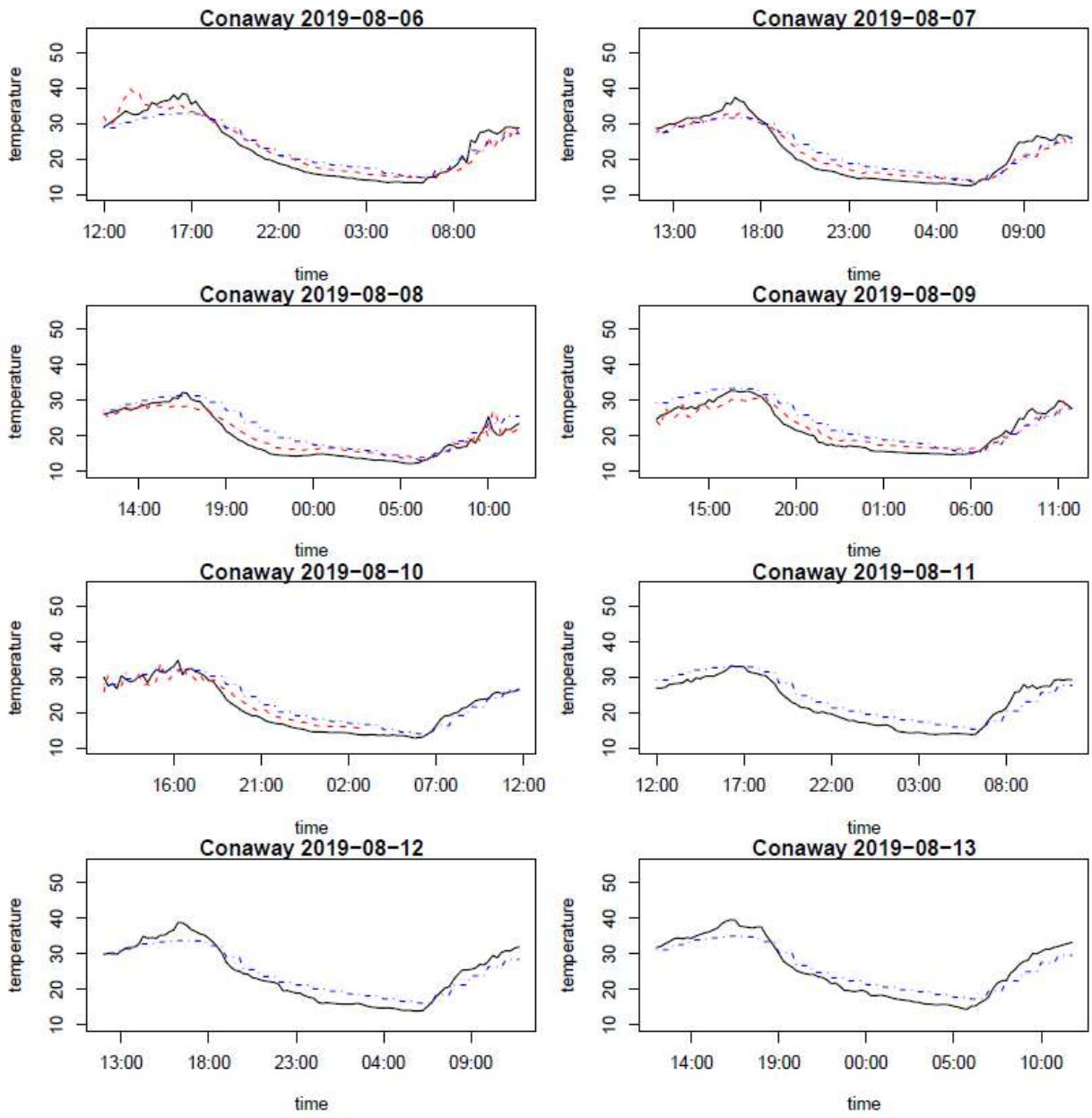
Conaway 2019-08-06
Conaway 2019-08-07
Conaway 2019-08-08
Conaway 2019-08-09
Conaway 2019-08-10
Conaway 2019-08-11
Conaway 2019-08-12
Conaway 2019-08-13
temperature
time
10
20
30
40
50
12:00
17:00
22:00
03:00
08:00
13:00
18:00
23:00
04:00
09:00
14:00
19:00
00:00
05:00
10:00
15:00
20:00
01:00
06:00
11:00
16:00
21:00
02:00
07:00
12:00

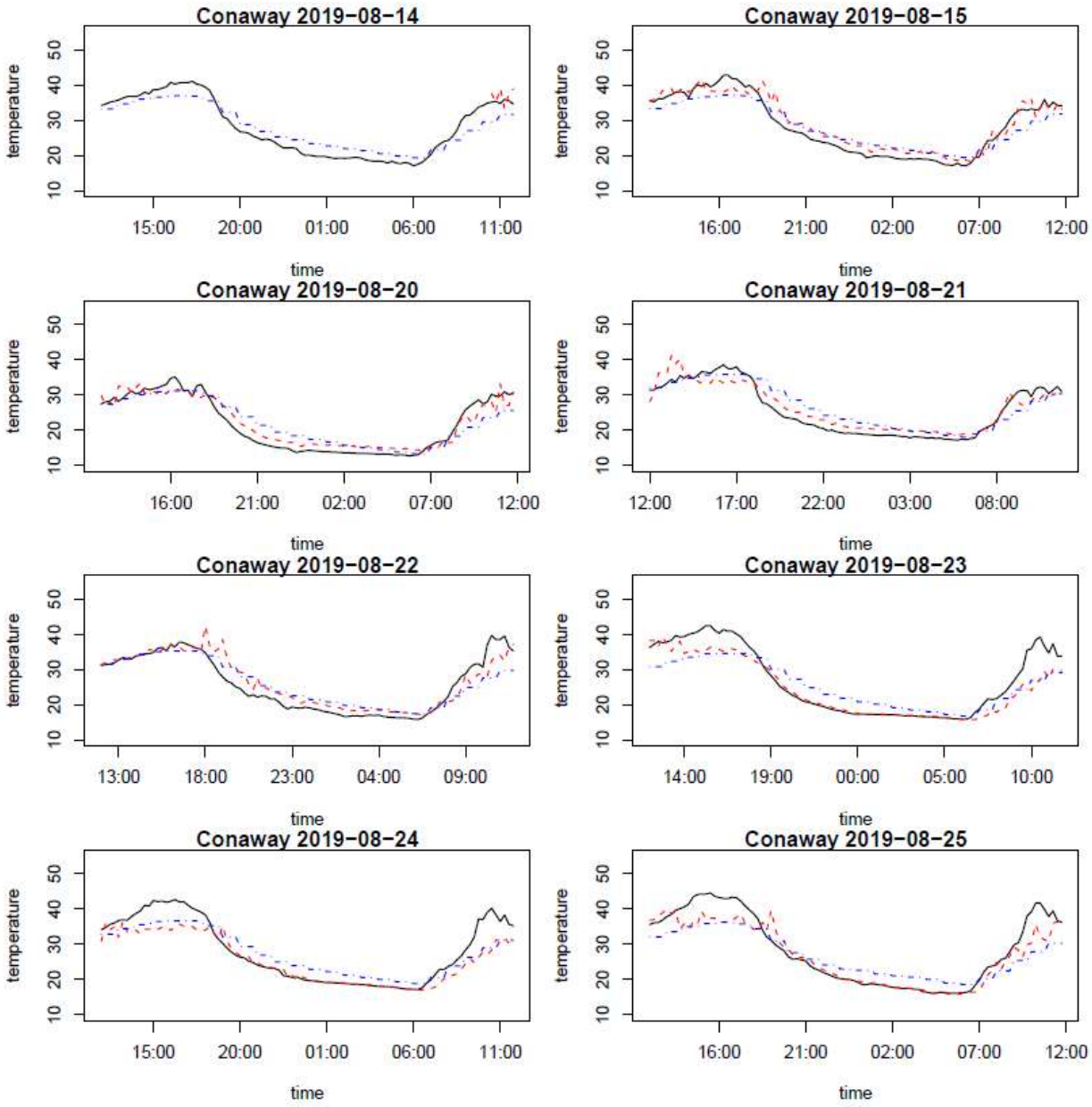
Conaway 2019-08-14
Conaway 2019-08-15
Conaway 2019-08-20
Conaway 2019-08-21
Conaway 2019-08-22
Conaway 2019-08-23
Conaway 2019-08-24
Conaway 2019-08-25
temperature
time

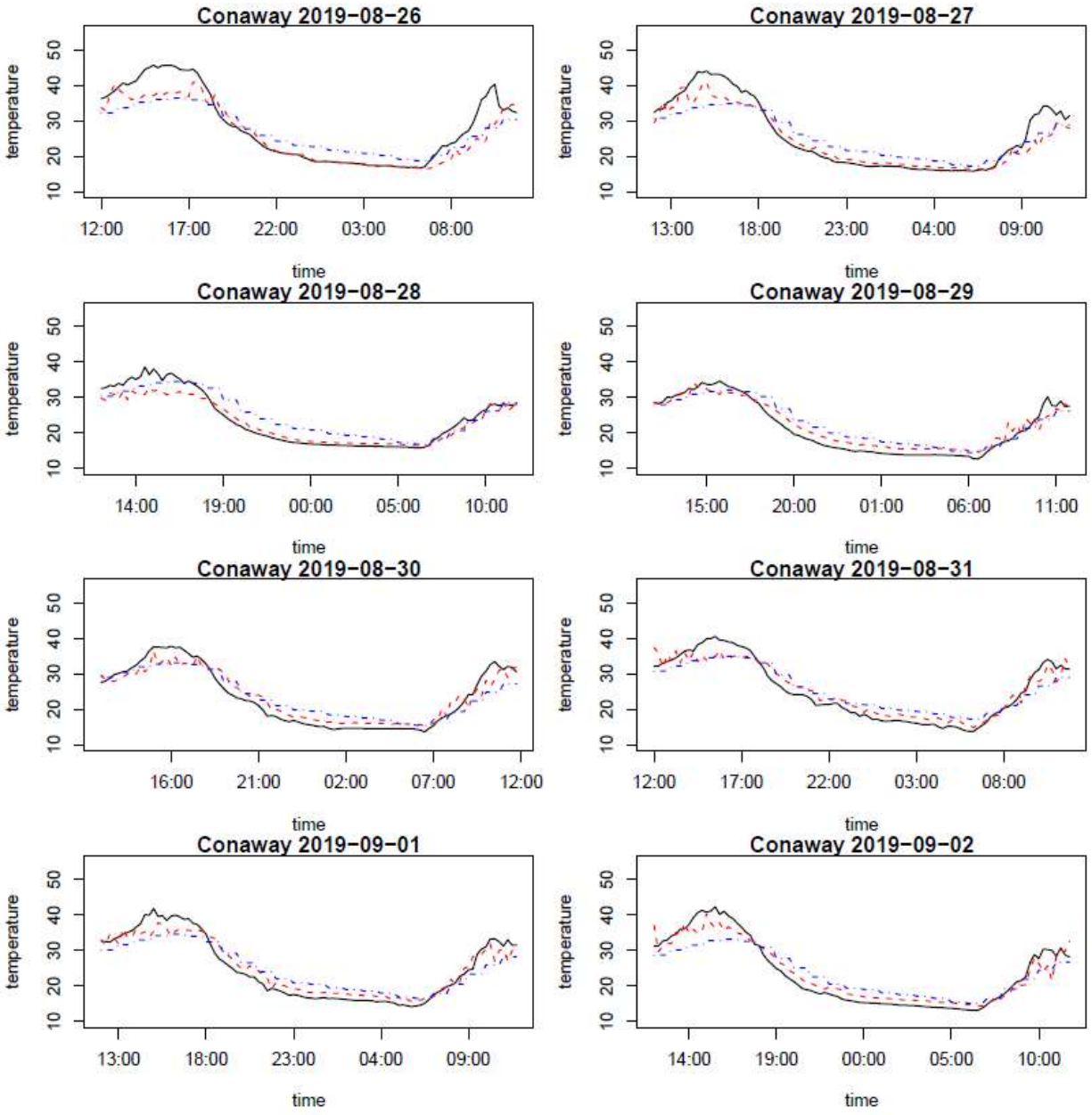
Conaway 2019-08-26
Conaway 2019-08-27
Conaway 2019-08-28
Conaway 2019-08-29
Conaway 2019-08-30
Conaway 2019-08-31
Conaway 2019-09-01
Conaway 2019-09-02
temperature
time

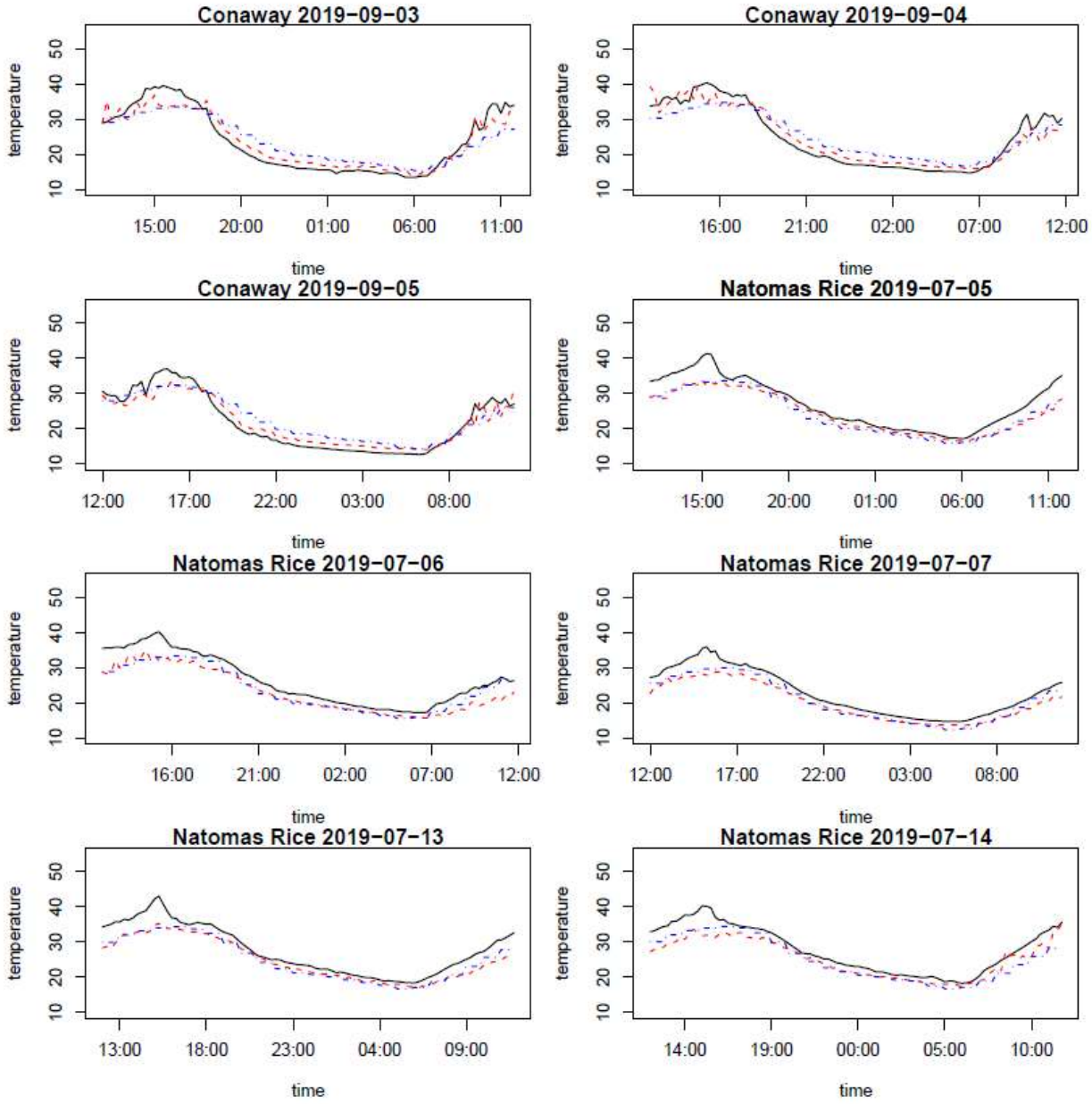
Conaway 2019-09-03
temperature
10 20 30 40 50
15:00 20:00 01:00 06:00 11:00
time
Conaway 2019-09-04
temperature
10 20 30 40 50
16:00 21:00 02:00 07:00 12:00
time
Conaway 2019-09-05
temperature
10 20 30 40 50
12:00 17:00 22:00 03:00 08:00
time
Natomas Rice 2019-07-05
temperature
10 20 30 40 50
15:00 20:00 01:00 06:00 11:00
time
Natomas Rice 2019-07-06
temperature
10 20 30 40 50
16:00 21:00 02:00 07:00 12:00
time
Natomas Rice 2019-07-07
temperature
10 20 30 40 50
12:00 17:00 22:00 03:00 08:00
time
Natomas Rice 2019-07-13
temperature
10 20 30 40 50
13:00 18:00 23:00 04:00 09:00
time
Natomas Rice 2019-07-14
temperature
10 20 30 40 50
14:00 19:00 00:00 05:00 10:00
time

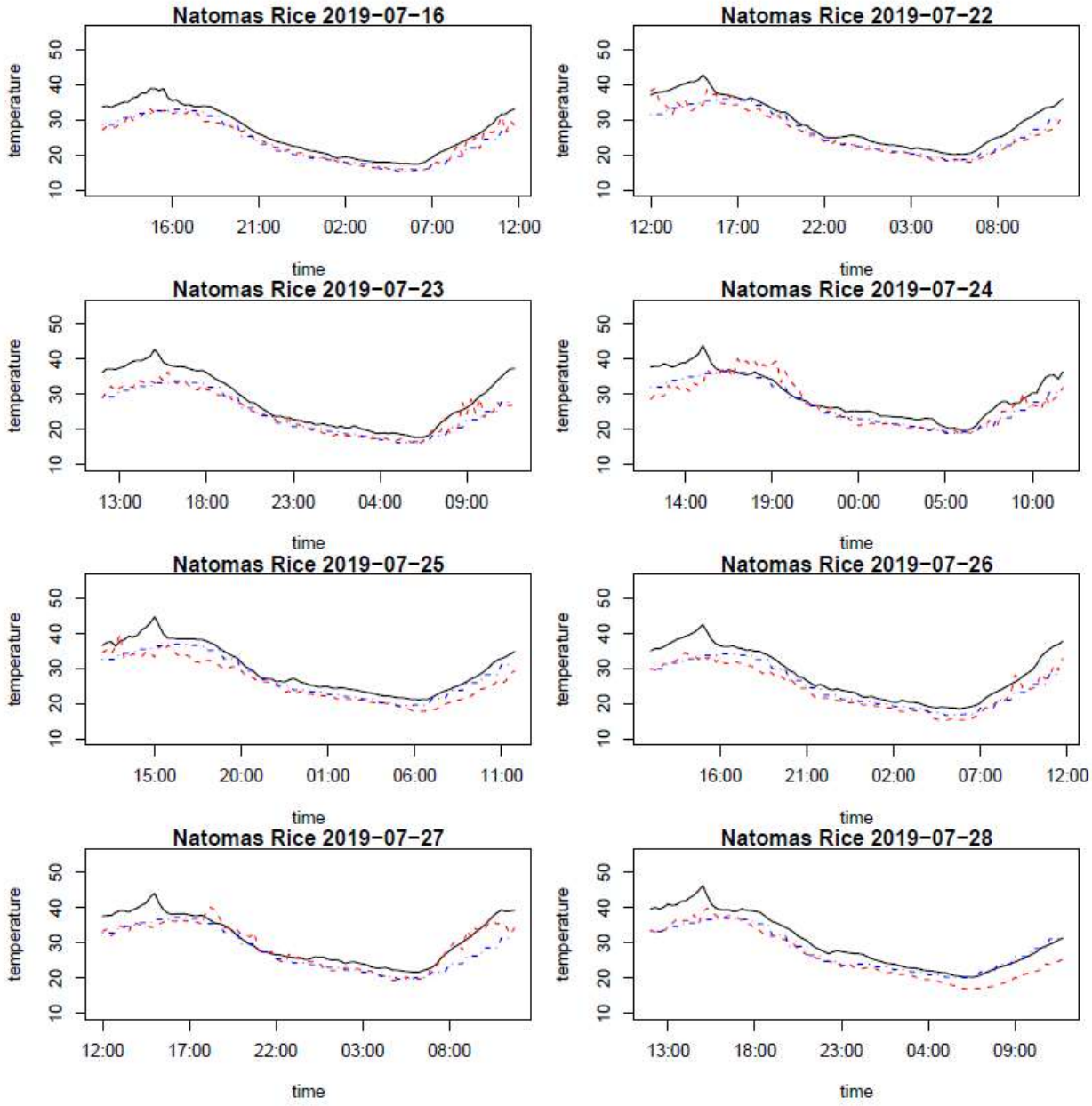
Natomas Rice 2019-07-16
temperature
10 20 30 40 50
16:00 21:00 02:00 07:00 12:00
time
Natomas Rice 2019-07-22
temperature
10 20 30 40 50
12:00 17:00 22:00 03:00 08:00
time
Natomas Rice 2019-07-23
temperature
10 20 30 40 50
13:00 18:00 23:00 04:00 09:00
time
Natomas Rice 2019-07-24
temperature
10 20 30 40 50
14:00 19:00 00:00 05:00 10:00
time
Natomas Rice 2019-07-25
temperature
10 20 30 40 50
15:00 20:00 01:00 06:00 11:00
time
Natomas Rice 2019-07-26
temperature
10 20 30 40 50
16:00 21:00 02:00 07:00 12:00
time
Natomas Rice 2019-07-27
temperature
10 20 30 40 50
12:00 17:00 22:00 03:00 08:00
time
Natomas Rice 2019-07-28
temperature
10 20 30 40 50
13:00 18:00 23:00 04:00 09:00
time

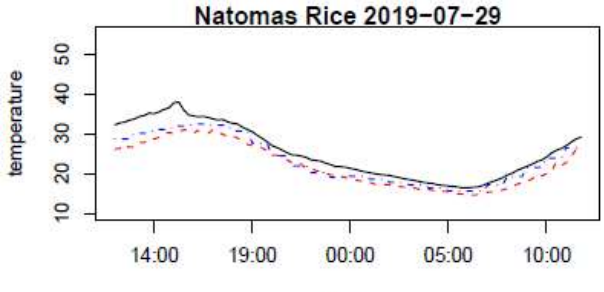
Natomas Rice 2019-07-29
temperature
10
20
30
40
50
14:00
19:00
00:00
05:00
10:00
time

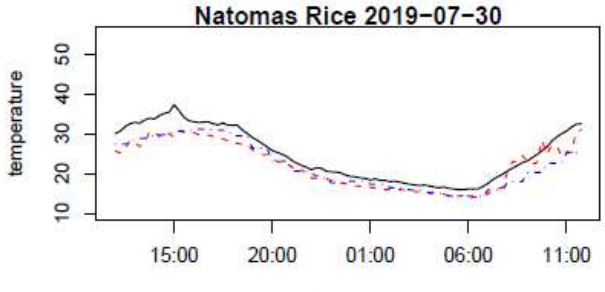
Natomas Rice 2019-07-30
temperature
10
20
30
40
50
15:00
20:00
01:00
06:00
11:00
time

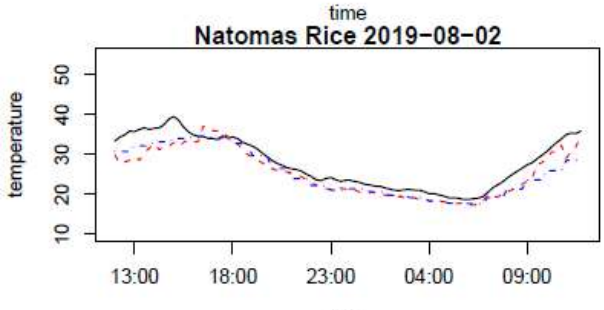
Natomas Rice 2019-08-02
temperature
10
20
30
40
50
13:00
18:00
23:00
04:00
09:00
time

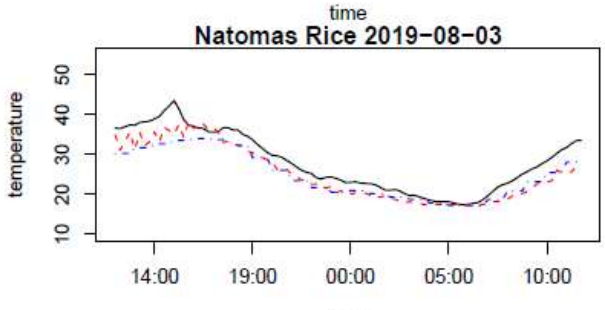
Natomas Rice 2019-08-03
temperature
10
20
30
40
50
14:00
19:00
00:00
05:00
10:00
time

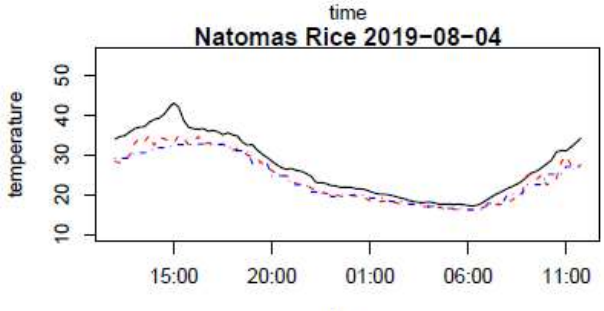
Natomas Rice 2019-08-04
temperature
10
20
30
40
50
15:00
20:00
01:00
06:00
11:00
time

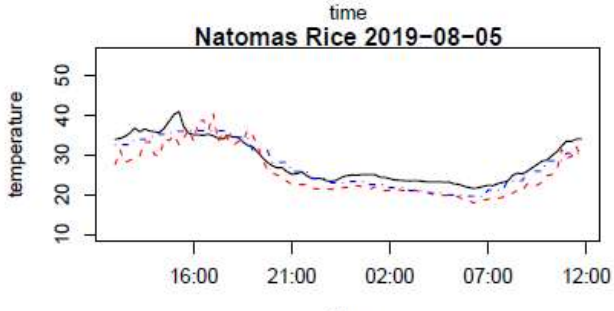
Natomas Rice 2019-08-05
temperature
10
20
30
40
50
16:00
21:00
02:00
07:00
12:00
time

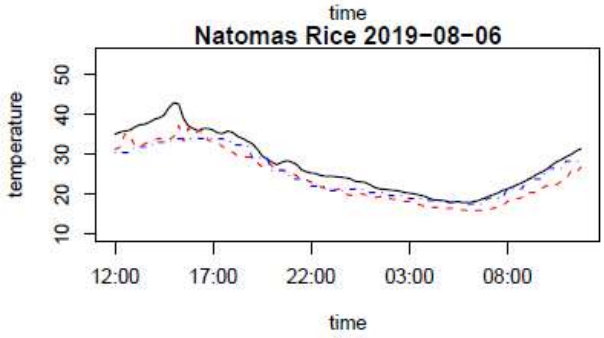
Natomas Rice 2019-08-06
temperature
10
20
30
40
50
12:00
17:00
22:00
03:00
08:00
time

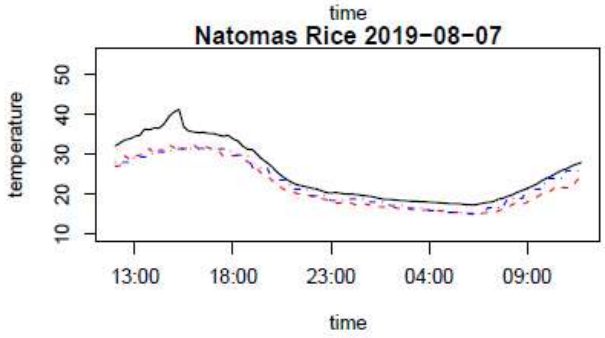
Natomas Rice 2019-08-07
temperature
10
20
30
40
50
13:00
18:00
23:00
04:00
09:00
time

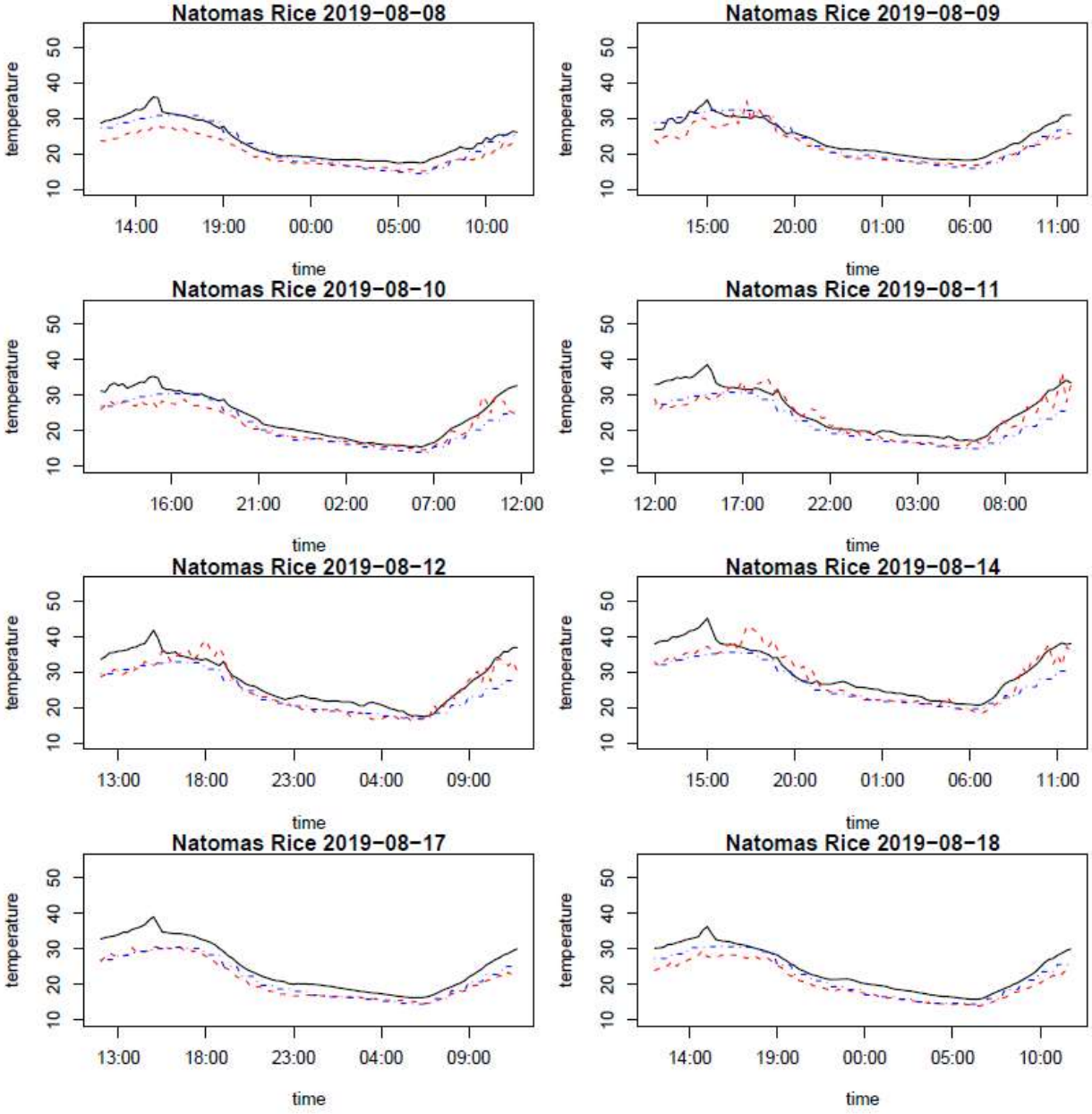
Natomas Rice 2019-08-08
Natomas Rice 2019-08-09
Natomas Rice 2019-08-10
Natomas Rice 2019-08-11
Natomas Rice 2019-08-12
Natomas Rice 2019-08-14
Natomas Rice 2019-08-17
Natomas Rice 2019-08-18
temperature
time

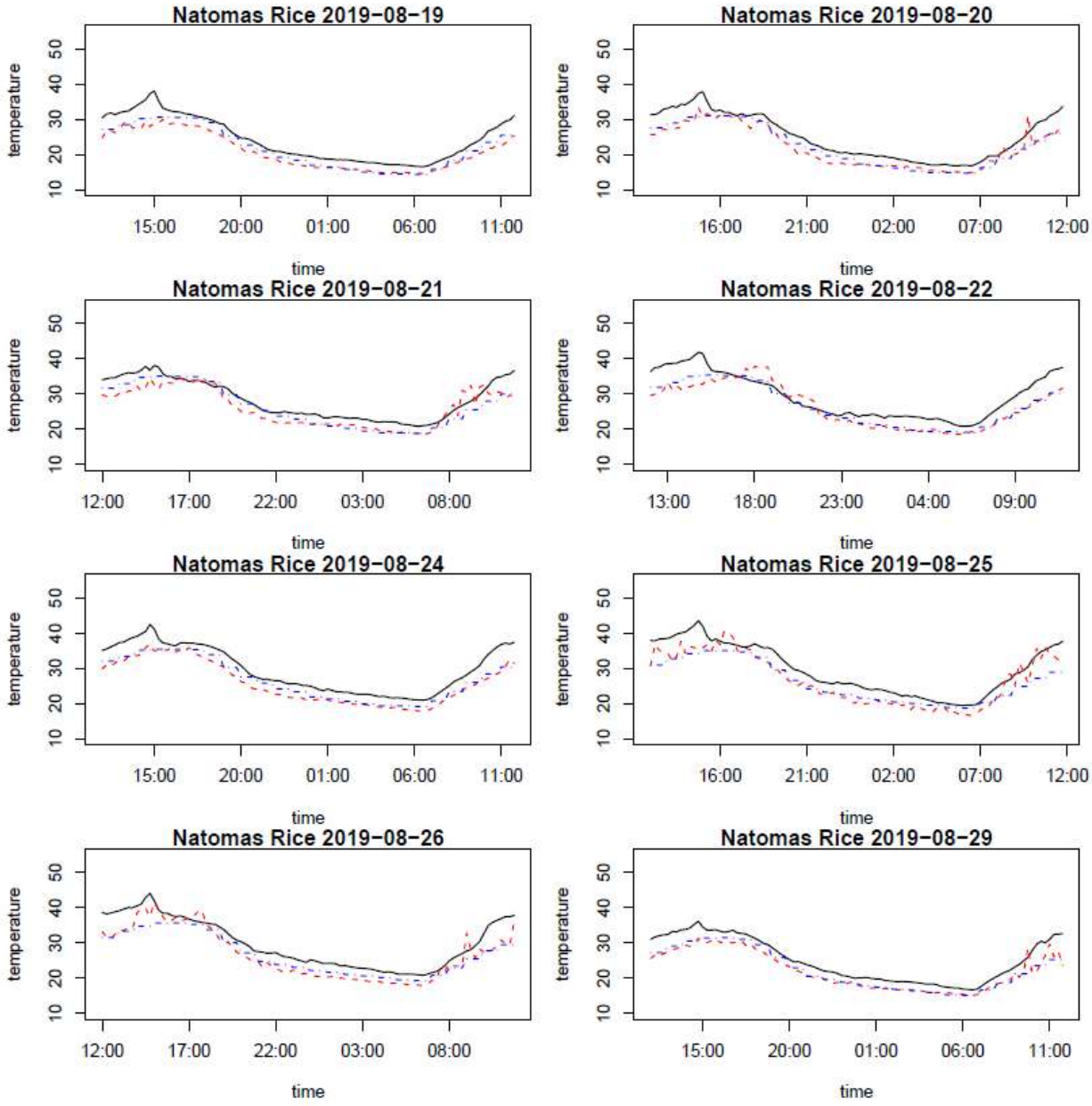
Natomas Rice 2019-08-19
Natomas Rice 2019-08-20
Natomas Rice 2019-08-21
Natomas Rice 2019-08-22
Natomas Rice 2019-08-24
Natomas Rice 2019-08-25
Natomas Rice 2019-08-26
Natomas Rice 2019-08-29
temperature
time
10
20
30
40
50
15:00
20:00
01:00
06:00
11:00
16:00
21:00
02:00
07:00
12:00
17:00
22:00
03:00
08:00
13:00
18:00
23:00
04:00
09:00

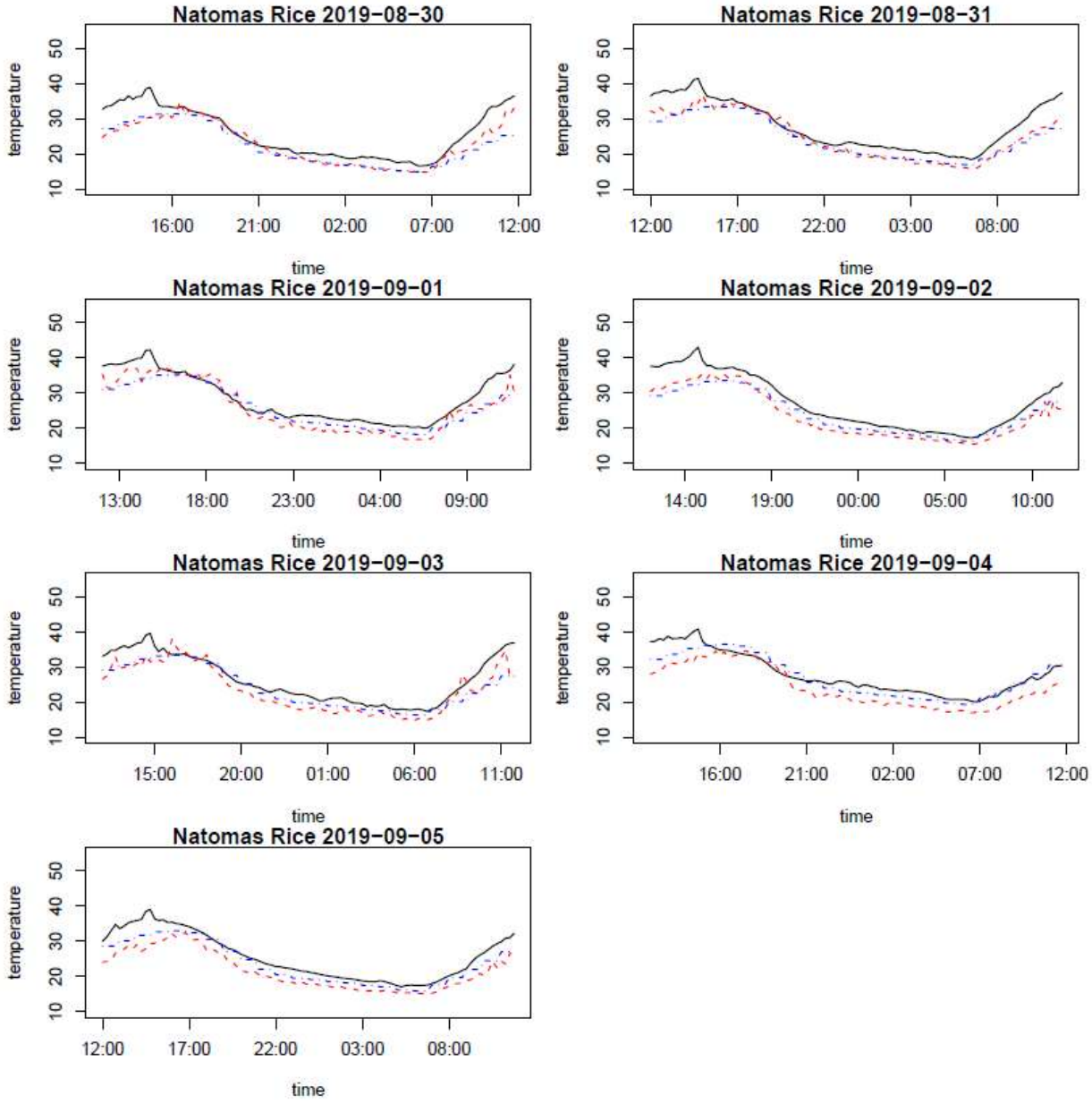
Natomas Rice 2019-08-30
temperature
10 20 30 40 50
16:00 21:00 02:00 07:00 12:00
time
Natomas Rice 2019-08-31
temperature
10 20 30 40 50
12:00 17:00 22:00 03:00 08:00
time
Natomas Rice 2019-09-01
temperature
10 20 30 40 50
13:00 18:00 23:00 04:00 09:00
time
Natomas Rice 2019-09-02
temperature
10 20 30 40 50
14:00 19:00 00:00 05:00 10:00
time
Natomas Rice 2019-09-03
temperature
10 20 30 40 50
15:00 20:00 01:00 06:00 11:00
time
Natomas Rice 2019-09-04
temperature
10 20 30 40 50
16:00 21:00 02:00 07:00 12:00
time
Natomas Rice 2019-09-05
temperature
10 20 30 40 50
12:00 17:00 22:00 03:00 08:00
time

2.7 Tables and figures

Table 2.1. Counts of female mosquitoes by species. The total number collected in BG-Counter and in CO_2-baited traps are presented. The Intraclass correlation coefficient (ICC) represents the degree of similarity between paired collections.

Species	Total collected in BG-Counter traps (%)	Total collected in CO_2-baited traps (%)	Total in all trap types (%)	ICC for the proportion of counts (95% CI)
Culex tarsalis	153,685 (69.3)	7,758 (64.2)	161,443 (69.0)	0.64 (0.48-0.76)
Culex pipiens	38,825 (17.5)	603 (5.0)	39,428 (16.9)	0.33 (0.11-0.52)
Anopheles freeborni	24,392 (11.0)	3,091 (25.6)	27,483 (11.7)	0.61 (0.45-0.74)
Culex stigmatasoma	2,695 (1.2)	127 (1.0)	2,822 (1.2)	
Aedes melanimon	856 (0.4)	337 (2.8)	1,193 (0.5)	
Aedes sierrensis	830 (0.4)	146 (1.2)	976 (0.4)	
Culex erythrothorax	533 (0.2)	27 (0.2)	560 (0.2)	
Anopheles franciscanus	12 (≈0)	0 (0)	12 (≈0)	
Culiseta incidens	8 (≈0)	0 (0)	8 (≈0)	
Total	221,836 (100)	12,089 (100)	233,925	

Table 2.2. Model results. Unadjusted and adjusted estimates for factors associated with each of the four outcomes. All variables were mean-centered where appropriate and scaled by the variable's standard deviation.

Model	Variable	Mean	Scaling factor	Unadjusted estimate (95% CI)	Adjusted estimate (95% CI)
Number of *Cx. tarsalis* collected overnight (count)† (N=490)	Wind speed* (km/h)	3.28 km/h	3.00 km/h	0.73 (0.68, 0.78)	0.76 (0.70, 0.82)
	Temperature* (°C)	25.93°C	1.99°C	1.28 (1.21, 1.36)	1.49 (1.32, 1.69)
	Study day		7 days	1.01 (0.98, 1.03)	0.97 (0.95, 0.99)
	Onset of host-seeking activity (min)	20.35 min	26.93 min	0.82 (0.76, 0.89)	0.85 (0.79, 0.91)
	Duration of evening activity (min)	153.83 min	78.88 min	1.26 (1.16, 1.37)	1.26 (1.18, 1.36)
	Temperature-day interaction			*NA*	0.96 (0.93, 0.98)
Onset of host-seeking activity, relative to sunset (min)‡ (N=427)	Wind speed* (km/h)	3.28 km/h	3.00 km/h	1.99 (0.82, 3.16)	2.24 (1.01, 3.48)
	Temperature* (°C)	25.93°C	1.99°C	1.01 (0.06, 1.95)	1.49 (0.52, 2.47)
	Study day		7 days	-0.80 (-1.15, -0.44)	-0.63 (-0.99, -0.27)
Duration of evening host-seeking activity (min)‡ (N=427)	Wind speed* (km/h)	3.28 km/h	3.00 km/h	13.72 (6.61, 20.83)	16.49 (8.92, 24.06)
	Temperature* (°C)	25.93°C	1.99°C	3.24 (-2.52, 8.99)	8.82 (2.99, 14.64)
	Onset of host-seeking activity (min)	16.06 min	11.36 min	-8.98 (-15.52, -2.43)	-13.75 (-20.08, -7.40)
	Wind-temperature interaction			*NA*	-12.02 (-17.28, -6.75)
Peak hour of *Cx. tarsalis* activity (elapsed time since 12:00) ‡ (N=381)	Wind speed (km/h)	3.28 km/h	3.00 km/h	10.23 (4.15, 16.31)	11.00 (5.02, 16.99)
	Temperature (°C)	25.93°C	1.99°C	9.09 (4.02, 14.16)	10.26 (5.32, 15.20)
	Study day		7 days	-7.03 (-8.83, -5.24)	-6.11 (-7.89, -4.33)

†Mixed effects negative binomial regression model with random intercept for site. Estimates presented as rate ratios. Significant effects are present when the 95% confidence interval excludes 1.00.

‡Mixed effects linear regression model with random intercept for site. Significant effects are present when the 95% confidence interval excludes 0.00.

*Weather variable measured at 20:00h.

Table 2.3. Generalizability of meteorological information. The Bayesian information criterion (BIC) was compared for models using weather measured at individual trap sites versus using weather from a publicly available source.

Model	BIC – site-specific weather data	BIC – publicly available, fixed-point weather data	Percent increase in BIC for publicly available weather data
Number of *Cx. tarsalis* collected overnight	5,379.4	5,380.6	0.02%
Onset of host-seeking activity, relative to sunset	3,188.9	3,193.1	0.13%
Duration of evening host-seeking activity	4,716.9	4,764.8	1.02%
Peak hour of *Cx. tarsalis* activity	4,042.5	4,059.5	0.42%

Table S2.1. Meteorological stations included in inverse distance-weighted mean temperature.

Station Name	Station ID	Source*	Latitude, Longitude
Bryte	155	CIMIS	38.59916°, -121.5404°
Davis	006	CIMIS	38.53569°, -121.7764°
Dixon	121	CIMIS	38.41556°, -121.7869°
Lincoln Regional Airport Karl Harder Field	WBAN:00205	NOAA	38.90900°, -121.3510°
Sacramento Metropolitan Airport	WBAN:93225	NOAA	38.69556°, -121.5897°
Verona	235	CIMIS	38.79794°, -121.6114°
Winters	139	CIMIS	38.50126°, -121.9785°
Woodland	226	CIMIS	38.67272°, -121.8117°

*NOAA: National Oceanic and Atmospheric Administration (Menne et al. 2012); CIMIS: California Irrigation Management Information System (Snyder 1984).

Table S2.2. Schedule of collection bottle rotators.

	Time interval
Cup 1	18:00-20:00
Cup 2	20:00-21:00
Cup 3	21:00-22:00
Cup 4	22:00-00:00
Cup 5	00:00-02:00
Cup 6	02:00-04:00
Cup 7	04:00-06:00
Cup 8	06:00-10:00

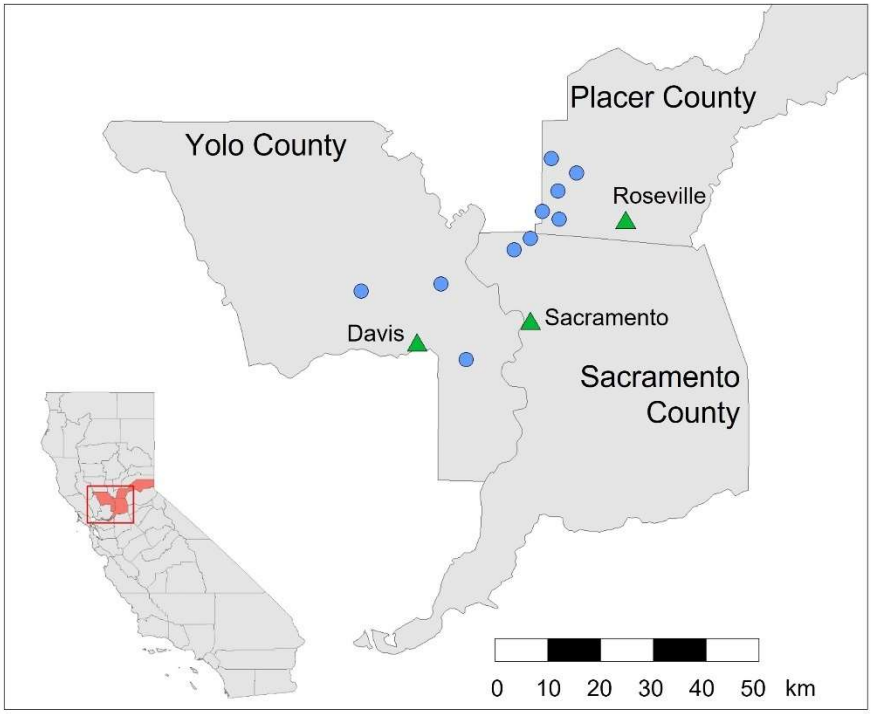

Figure 2.1. Map of the study area. Trap sites are represented by blue circles and major cities in each county are labelled and represented by green triangles. State and county boundaries were obtained from the Database of Global Administrative Areas (GADM 2018).

Figure 2.2. Examples of the BG-Counter trap configurations. Panel A shows the cage design in Sacramento-Yolo MVCD while Panel B shows the design in Placer MVCD. All traps were fitted with 1) a BGC trap, including the infrared sensor and temperature recording device.; 2) an anemometer and wind vane recording wind speed and direction every 1 minute; 3) a 20-lb CO_2 cylinder; 4) a solar panel; and 5) a 12V battery for powering the trap.

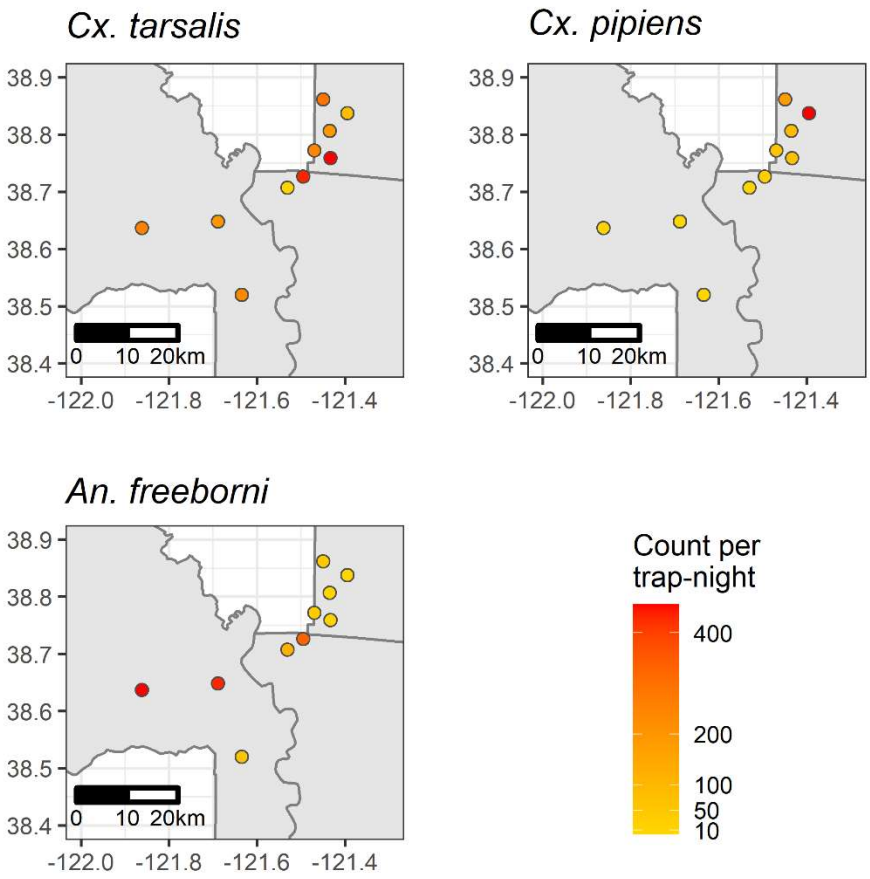

Figure 2.3. Spatial distribution of selected mosquito species. The mean count per trap-night of *Cx. tarsalis* is shown at the top-left, at each site of *Cx. tarsalis*, *Cx. pipiens* at the top-right, and *An. freeborni* at the lower-left. County boundaries were obtained from the Database of Global Administrative Areas (GADM 2018).

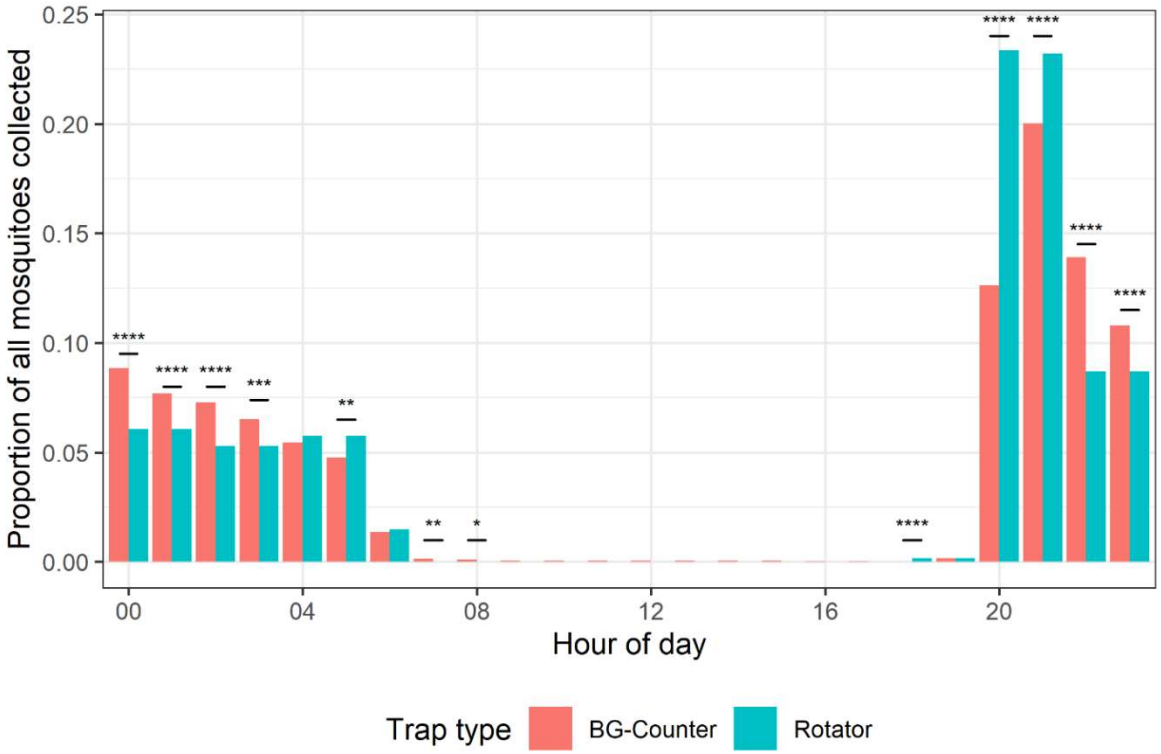

Figure 2.4. Hourly mosquito collections in BG-Counter and CO_2-baited traps with a collection bottle rotator (Rotator trap). Bars represent the proportion of all mosquitoes, regardless of species, collected during each hour of the day by the two trap types. Hourly proportions that had a significant Pearson's chi-square test statistic with a Bonferroni adjustment for multiple comparisons are denoted above the bars. The number of stars represents the level of significance: **** for $p < 0.0001$, *** for $p < 0.001$, ** for $p < 0.01$, and * for $p < 0.1$.

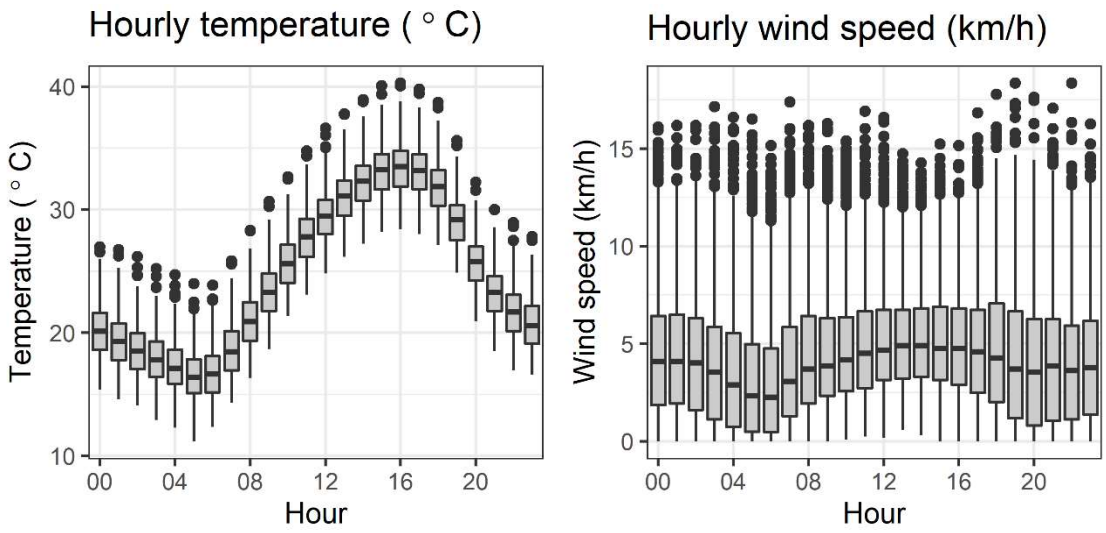

Figure 2.5. Observed hourly temperature and wind speed. Panel A shows temperature in Celsius and Panel B shows wind speed in kilometers per hour.

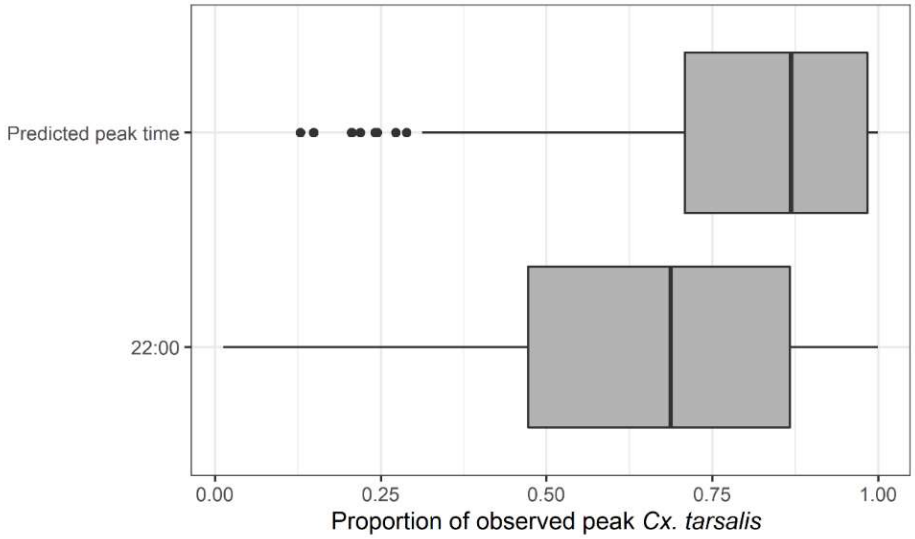

Figure 2.6. Proportion of night's maximum single-hour *Cx. tarsalis* count potentially impacted by two timings of mosquito control. The boxplots show the distribution of the proportion of the observed peak *Cx. tarsalis* count captured if predicting the peak hour from weather conditions (top) or using a fixed time to estimate the peak hour (bottom). The right side of the x-axis indicates better agreement with the actual peak hour of activity.

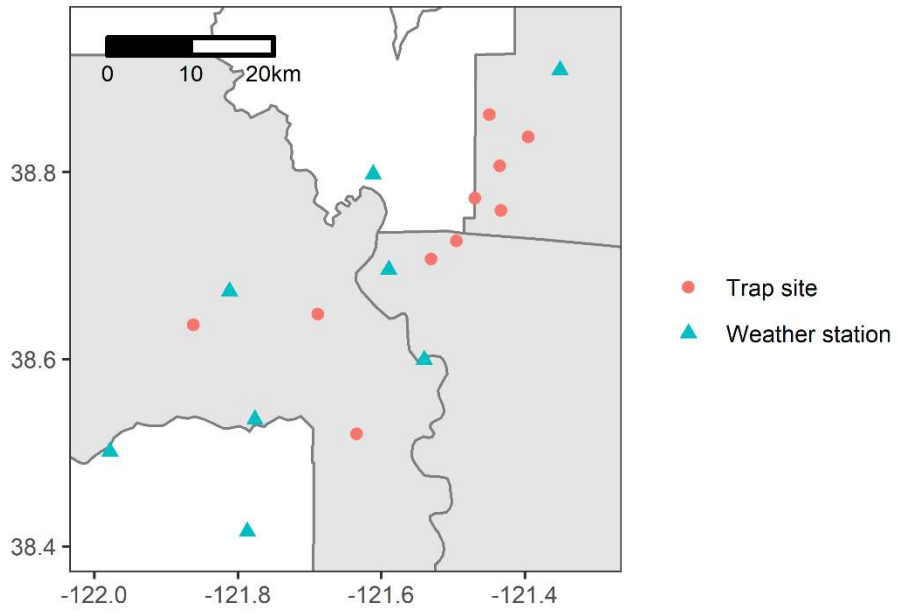

Figure S2.1. Map of meteorological stations included in inverse distance-weighted temperature. Red circles represent trap sites and blue triangles represent meteorological stations noted in Table S2.1. State and county boundaries were obtained from the Database of Global Administrative Areas (GADM 2018).

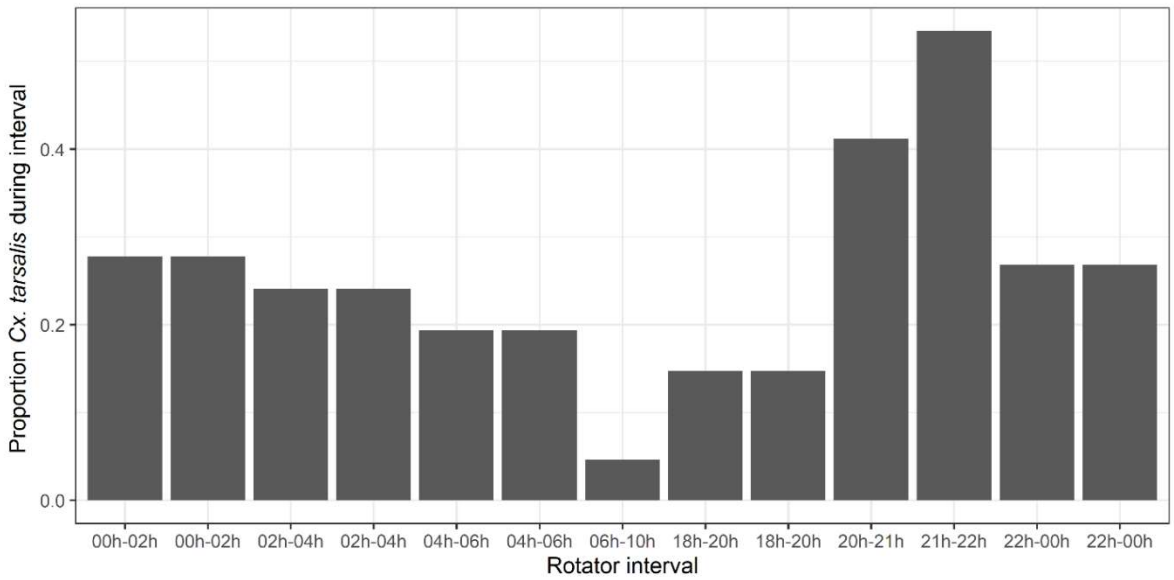

Figure S2.2. Proportion *Cx. tarsalis* during each rotator trap interval. Aggregated over all CO_2-baited rotator trap collections.

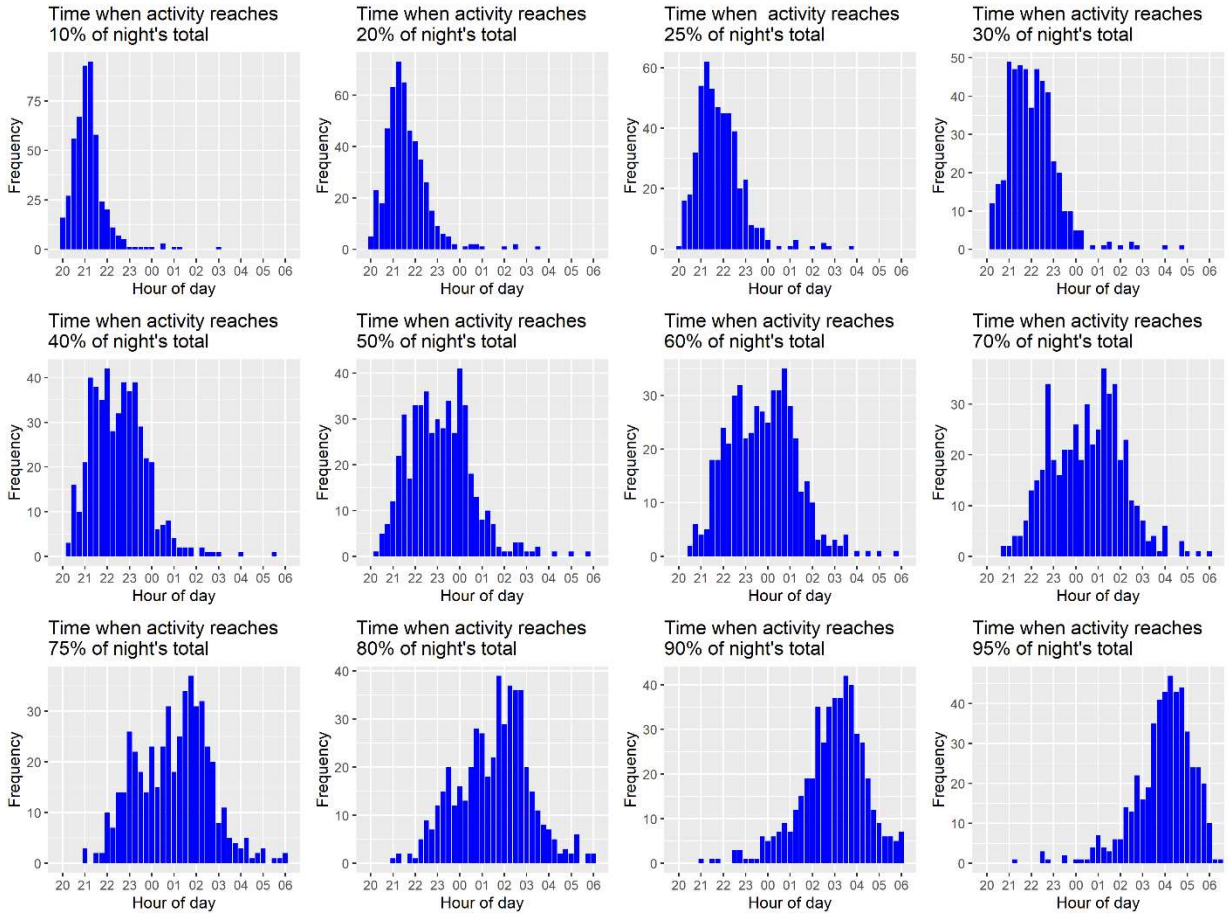

Figure S2.3. Estimated time of different percentiles of a night's count. For each percentile, the bars show the time of night e.g., 10% of the night's total *Cx. tarsalis* count had entered the trap.

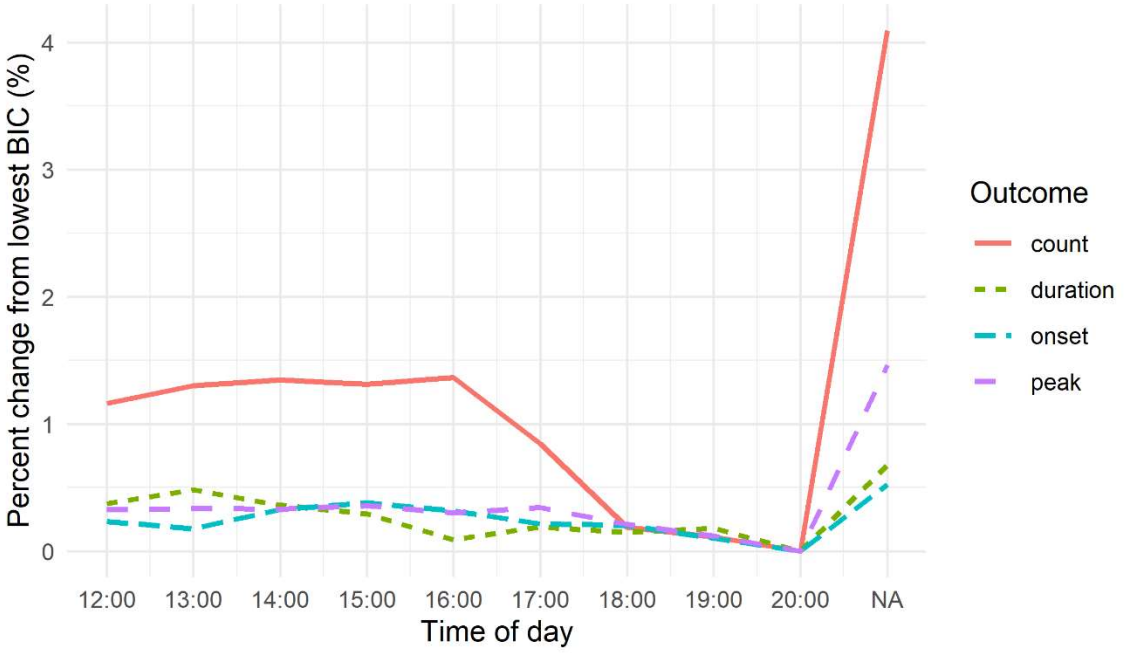

Figure S2.4. Comparison of the Bayesian information criterion for models using weather observed at different hours. The BIC values are evaluated as the percent change from the lowest observed BIC. The *NA* indicator on the x-axis marks models that did not include weather variables as predictors.

2.8 References

Amos, B. A., K. M. Staunton, S. A. Ritchie, and R. T. Cardé. 2020. Attraction versus capture: Efficiency of BG-Sentinel trap rnder semi-field conditions and characterizing response behaviors for female *Aedes aegypti* (Diptera: Culicidae). J. Med. Entomol. 57: 884–892.

Bailey, S. F., D. A. Eliason, and B. L. Hoffmann. 1965. Flight and dispersal of the mosquito *Culex tarsalis* Coquillett in the Sacramento Valley of California. Hilgardia. 37: 73–113.

Bates, D., M. Maechler, B. Bolker, and S. Walker. 2015. Fitting linear mixed-effects models using lme4. J. Stat. Softw. 67: 1–48.

Bidlingmayer, W. L. 1974. The influence of environmental factors and physiological stage on flight patterns of mosquitoes taken in the vehicle aspirator and truck, suction, bait and New Jersey light traps. J. Med. Entomol. 11: 119–146.

Bidlingmayer, W. L. 1985. The measurement of adult mosquito population changes - some considerations. J. Am. Mosq. Control Assoc. 1: 328–348.

Bidlingmayer, W. L., J. F. Day, and D. G. Evans. 1995. Effect of wind velocity on suction trap catches of some Florida mosquitoes. J. Am. Mosq. Control Assoc. 11: 295–301.

Bivand, R. S., E. Pebesma, and V. Gomez-Rubio. 2013. Applied spatial data analysis with

R, 2nd ed. Springer, NY.

Bolling, B. G., C. M. Barker, C. G. Moore, W. J. Pape, and L. Eisen. **2009**. Seasonal patterns for entomological measures of risk for exposure to *Culex* vectors and West Nile virus in relation to human disease cases in northeastern Colorado. J. Med. Entomol. 46: 1519–1531.

California Department of Public Health, Mosquito & Vector Control Association of California, and University of California. **2020**. California Mosquito-Borne Virus Surveillance & Response Plan. Sacramento.

Chuang, T., M. B. Hildreth, D. L. Vanroekel, and M. C. Wimberly. **2011**. Weather and land cover influences on mosquito populations in Sioux Falls, South Dakota. J. Med. Entomol. 48: 669–679.

Ciota, A. T., A. C. Matacchiero, A. M. Kilpatrick, and L. D. Kramer. **2014**. The effect of temperature on life history traits of *Culex* mosquitoes. J. Med. Entomol. 51: 55–62.

Colborn, J. M., K. A. Smith, J. Townsend, D. Damian, R. S. Nasci, and J.-P. Mutebi. **2013**. West Nile virus outbreak in Phoenix, Arizona—2010: Entomological observations and epidemiological correlations. J. Am. Mosq. Control Assoc. 29: 123–132.

Cooperband, M. F., and R. T. Cardé. **2006**. Orientation of Culex mosquitoes to carbon dioxide-baited traps: Flight manoeuvres and trapping efficiency. Med. Vet. Entomol. 20: 11–26.

Cummings, R. F. 1992. The design and use of a modified Reiter gravid mosquito trap for mosquito-borne encephalitis surveillance in Los Angeles County, California. Proc. Pap. Conf. Mosq. Vector Control Assoc. Calif. 60: 170–176.

Cummins, B., R. Cortez, I. M. Foppa, J. Walbeck, and J. M. Hyman. **2012**. A spatial model of mosquito host-seeking behavior. PLoS Comput. Biol. 8: 1002500.

Deichmeister, J. M., and A. Telang. **2011**. Abundance of West Nile virus mosquito vectors in relation to climate and landscape variables. J. Vector Ecol. 36: 75–85.

Endo, N., and E. A. B. Eltahir. **2018**. Modelling and observing the role of wind in *Anopheles* population dynamics around a reservoir. Malar. J. 17: 48.

GADM. **2018**. Database of Global Administrative Areas, version 3.6. (www.gadm.org/data.html).

Gamer, M., J. Lemon, I. Fellows, and P. Singh. **2019**. irr: Various Cooefficients of Interrater Reliability and Agreement.

Giordano, B. V., S. Kaur, and F. F. Hunter. **2017**. West Nile virus in Ontario, Canada: A twelve-year analysis of human case prevalence, mosquito surveillance, and climate data. PLoS One. 12: e0183568.

Goddard, L. B., A. E. Roth, W. K. Reisen, and T. W. Scott. **2002**. Vector competence of California mosquitoes for West Nile virus. Emerg. Infect. Dis. 8: 1385–1391.

Godsey, M. S., K. Burkhalter, M. Delorey, and H. M. Savage. **2010**. Seasonality and time of host-seeking activity of *Culex tarsalis* and floodwater *Aedes* in northern Colorado, 2006-2007. J. Am. Mosq. Control Assoc. 26: 148–159.

Gray, K. M., N. D. Burkett-Cadena, M. D. Eubanks, and T. R. Unnasch. **2011**. Crepuscular Flight Activity of *Culex erraticus* (Diptera: Culicidae). J. Med. Entomol. 48: 167–172.

Groen, T. A., G. L'Ambert, R. Bellini, A. Chaskopoulou, D. Petric, M. Zgomba, L. Marrama, and D. J. Bicout. **2017**. Ecology of West Nile virus across four European countries: Empirical modelling of the *Culex pipiens* abundance dynamics as a function of weather. Parasit Vectors. 10: 1–11.

Gubler, D. J., G. L. Campbell, R. Nasci, N. Komar, L. Petersen, and J. T. Roehrig. **2000**. West Nile virus in the United States: Guidelines for detection, prevention, and control. Viral Immunol.

Hock, J. W. 2015. Collection Bottle Rotator. John W. Hock Co. (https://johnwhock.com/products/programmable-collection/collection-bottle-rotator/).

Hoffmann, E. J., and J. R. Miller. **2003**. Reassessment of the role and utility of wind in suppression of mosquito (Diptera: Culicidae) host Finding: Stimulus dilution supported over flight limitation. J. Med. Entomol. 40: 607–614.

Hribar, L. J. 2017. Influence of meteorological variables on mosquito catch by dry ice-baited light traps in the Florida Keys, USA. Florida Sci. 80: 165–171.

Hribar, L. J., D. J. DeMay, and U. J. Lund. **2010**. The association between meteorological variables and the abundance of *Aedes taeniorhynchus* in the Florida Keys. J. Vector Ecol. 35: 339–346.

Karki, S., G. L. Hamer, T. K. Anderson, T. L. Goldberg, U. D. Kitron, B. L. Krebs, E. D. Walker, and M. O. Ruiz. **2016**. Effect of trapping methods, weather, and landscape on estimates of the *Culex* vector mosquito abundance. Environ. Health Insights. 10: 93–103.

Karki, S., N. E. Westcott, E. J. Muturi, W. M. Brown, and M. O. Ruiz. **2017**. Assessing human risk of illness with West Nile virus mosquito surveillance data to improve public health preparedness. Zoonoses Public Health. 00: 1–8.

Kilpatrick, A. M., and W. J. Pape. **2013**. Predicting human West Nile virus infections with mosquito surveillance data. Am. J. Epidemiol. 178: 829–835.

Kwan, J. L., S. Kluh, M. B. Madon, and W. K. Reisen. **2010**. West Nile virus emergence and persistence in Los Angeles, California, 2003-2008. Am. J. Trop. Med. Hyg. 83: 400–412.

Lacey, E. S., and R. T. Cardé. **2011**. Activation, orientation and landing of female *Culex quinquefasciatus* in response to carbon dioxide and odour from human feet: 3-D flight analysis in a wind tunnel. Med. Vet. Entomol. 25: 94–103.

Lebl, K., K. Brugger, and F. Rubel. **2013**. Predicting *Culex pipiens/restuans* population dynamics by interval lagged weather data. Parasites and Vectors. 6: 1–11.

Liu, A., V. Lee, D. Galusha, M. D. Slade, M. Diuk-Wasser, T. Andreadis, M. Scotch, and P. M. Rabinowitz. **2009**. Risk factors for human infection with West Nile Virus in Connecticut: a multi-year analysis. Int. J. Health Geogr. 8.

Lothrop, H. D., B. Lothrop, and W. K. Reisen. **2002**. Nocturnal microhabitat distribution of adult *Culex tarsalis* (Diptera: Culicidae) impacts control effectiveness. J. Med. Entomol. 39: 574–582.

McDonald, E., S. W. Martin, K. Landry, C. V. Gould, J. Lehman, M. Fischer, and N. P. Lindsey. **2019**. West Nile virus and other domestic nationally notifiable arboviral diseases — United States, 2018. Morb. Mortal. Wkly. Rep. 68: 673–678.

McLean, R. G., S. R. Ubico, D. E. Docherty, W. R. Hansen, L. Sileo, and T. S.

McNamara. **2001**. West Nile virus transmission and ecology in birds. Ann. N. Y. Acad. Sci. 951: 54–57.

Menne, M. J., I. Durre, R. S. Vose, B. E. Gleason, and T. G. Houston. **2012**. An overview of the Global Historical Climatology Network-Daily database. J. Atmos. Ocean. Technol. 29: 897–910.

Moise, I. K., C. Riegel, and E. J. Muturi. **2018**. Environmental and social-demographic predictors of the southern house mosquito *Culex quinquefasciatus* in New Orleans, Louisiana. Parasites and Vectors. 11.

Montarsi, F., L. Mazzon, S. Cazzin, S. Ciocchetta, and G. Capelli. **2015**. Seasonal and daily activity patterns of mosquito (Diptera: Culicidae) vectors of pathogens in northeastern Italy. J. Med. Entomol. 52: 56–62.

Newhouse, V. F., R. W. Chamberlain, J. G. Johnston, and W. D. Sudia. **1966**. Use of dry ice to increase mosquito catches of the CDC miniature light trap. Mosq. News. 30–35.

Pebesma, E. J., and R. S. Bivand. **2005**. Classes and methods for spatial data in R. R News. 5: 9–13.

Pruszynski, C. 2016. The BG-Counter: A new surveillance trap that remotely measures mosquito density in real-time. Wing Beats. 27: 13–18.

R Core Team. **2020**. R: A language and environment for statistical computing.

Reisen, W. K., and H. D. Lothrop. **1995**. Population ecology and dispersal of *Culex tarsalis* (Diptera: Culicidae) in the Coachella Valley of California. J Med Entomol. 32: 490–502.

Reisen, W. K., H. D. Lothrop, and A. R. P. Meyer. **1997**. Time of host-seeking by *Culex tarsalis* (Diptera: Culicidae) in California, J. Med. Entomol.

Reisen, W., H. Lothrop, R. Chiles, M. Madon, C. Cossen, L. Woods, S. Husted, V. Kramer, and J. Edman. **2004**. West Nile virus in California. Emerg. Infect. Dis. 10: 1369–1378.

Reiter, P. 1987. A revised version of the CDC gravid mosquito trap. J. Am. Mosq. Control Assoc. 3: 325–327.

Ripoche, M., C. Campagna, A. Ludwig, N. H. Ogden, and P. A. Leighton. **2019**. Short-term forecasting of daily abundance of West Nile virus vectors *Culex pipiens-restuans* (Diptera: Culicidae) and *Aedes vexans* based on weather conditions in southern Québec (Canada). J. Med. Entomol. 56: 859–872.

Rochlin, I., A. Faraji, K. Healy, and T. G. Andreadis. **2019**. West Nile virus mosquito vectors in North America. J. Med. Entomol. 56: 1475–1490.

Rudolfs, W. 1925. Relation between temperature, humidity and activity of house mosquitoes. J. New York Entomol. Soc. 33: 163–169.

Schwarz, G. 1978. Estimating the dimension of a model. Ann. Stat. 6: 461–464.

Service, M. W. 1980. Effects of wind on the behaviour and distribution of mosquitoes and blackflies. Int. J. Biometeorol. 24: 347–353.

Snyder, R. L. 1984. California Irrigation Management Information System. Am. Potato J. 61: 229–234.

Sudia, W. D., R. W. Emmons, V. F. Newhouse, and R. F. Peters. **1971**. Arbovirus-vector studies in the Central Valley of California, 1969. Mosq. News. 31: 160–168.

Thieurmel, B., and A. Elmarhraoui. **2019**. suncalc: Compute Sun Position, Sunlight Phases, Moon Position and Lunar Phase.

Veronesi, R., G. Gentile, M. Carrieri, B. Maccagnani, L. Stermieri, and R. Bellini. **2012**. Seasonal pattern of daily activity of *Aedes caspius*, *Aedes detritus*, *Culex modestus*, and *Culex pipiens* in the Po Delta of northern Italy and significance for vector-borne disease risk assessment. J. Vector Ecol. 37: 49–61.

Wood, S. N. 2017. Generalized Additive Models: An Introduction with R, 2nd ed. Chapman and Hall/CRC, Boca Raton, FL.

Chapter 3: Spatio-temporal prediction of West Nile virus vector *Culex tarsalis* abundance

Pascale C. Stiles[1], Christopher M. Barker[1]

[1]Davis Arbovirus Research and Training Lab, Department of Pathology, Microbiology, and Immunology, University of California, Davis, CA, 95616

Abstract

West Nile virus (WNV) is a zoonotic arbovirus that cycles between avian hosts and mosquito vectors, particularly mosquitoes in the genus *Culex*, that can spill over to humans through the bites of infected mosquitoes. As there is no licensed vaccine for use in humans, disease prevention relies on mosquito control with entomological surveillance guiding the application of adulticides in an area when risk indicators, particularly mosquito abundance and WNV infection prevalence in mosquitoes, become elevated. Because vector control districts often operate with limited resources, knowledge of where and when upcoming high-risk periods are expected, and the certainty of that estimate, is critical for allocating resources appropriately. We employed a generalized additive model (GAM) to estimate spatio-temporal trends in *Cx. tarsalis* abundance in the Central Valley of California, the region with the highest WNV incidence in the state. The model was validated through a k-fold cross-validation procedure and used to predict weekly *Cx. tarsalis* abundance across the Central Valley for the years 2016-2020 using data observed up to the week prior to that being predicted in order to mimic the progression of knowledge during a surveillance season. The GAM found strong seasonal patterns in abundance, modified by local land use and spatio-temporal anomalies. Additionally, the models maintained a similar predictive accuracy for out-of-sample data compared to that for the training data set. We then predicted *Cx. tarsalis* one week in the future at sites within 10 km of an observed trap within the prior four weeks. We further estimated the uncertainty around these predictions to visualize not only where *Cx. tarsalis* abundance would be expected to be high, but also where lack of surveillance coverage limits the utility of predictions. We observed predictions to be most accurate when the nearest observed trap was within 2 km and one week prior, thus limiting the window of utility for making short-term future predictions of abundance. Ultimately these results provided a step towards improved spatial risk estimation of WNV transmission, specifically of future high-risk periods in a high-incidence region of California.

3.1 Introduction

West Nile virus (WNV; family *Flaviviridae*) is a zoonotic encephalitic arbovirus of annual concern across most of the U.S. WNV is maintained and amplified in bird-mosquito cycles, with incidental spillover to mammalian hosts through bridge vectors, typically within the genus *Culex* (Reisen et al. 2004, Rochlin et al. 2019). There is no licensed vaccine to protect humans against WNV disease, so population-level disease prevention relies on vector control to reduce biting of infectious mosquitoes on humans (Gubler et al. 2000, Rose 2001, Kaiser and Barrett 2019). The need for vector control is assessed through routine surveillance of mosquito populations by local vector control agencies to monitor for increases in mosquito abundance and/or infection prevalence in mosquitoes (California Department of Public Health et al. 2020). Both of these metrics have been associated with detections of human cases (Bolling et al. 2009, Colborn et al. 2013, Kilpatrick and Pape 2013, Karki et al. 2017, Talbot et al. 2019) and are able to be reduced with the timely application of vector control in response to elevated risk levels (Carney et al. 2008, Holcomb et al. 2021). WNV activity in an area is further estimated through detections of WNV through the passive surveillance of dead birds and seroconversions in sentinel chicken flocks in some areas, which can trigger intensified mosquito surveillance efforts (California Department of Public Health et al. 2020).

The California Mosquito-Borne Virus Surveillance and Response Plan (hereafter: Response Plan) delineates a risk assessment for interpreting surveillance observations, incorporating mosquito abundance, mosquito infection prevalence, dead bird infections, sentinel chicken seroconversions, and daily mean temperature through inverse-distance weighting into a risk surface for the state . The Response Plan map is produced weekly using information recorded over the preceding two weeks but lacks a predictive aspect to forecast how WNV activity in an area will evolve in the near-term future. Additionally, there is no measure of uncertainty due to different levels of surveillance coverage, where some risk estimates may be unreliable due to high stochastic variability from small sample sizes.

Although the highest case numbers in California are concentrated in the Los Angeles area of southern California, the highest incidence tends to occur in the rural, sparsely populated areas of the Central Valley (Snyder et al. 2020). Furthermore, WNV risk is heterogeneously distributed within these high-risk counties when incidence is examined on a finer spatial scale (Danforth et al. 2021). The vector *Cx. tarsalis* has been associated with high rates of WNV transmission in regions defined by irrigated agriculture in the United States, which provides key larval habitat for this species (Bailey et al. 1965, Sudia et al. 1971, Reisen et al. 2009, Eisen et al. 2010, Schurich et al. 2014, Kovach and Kilpatrick 2018, Dunphy et al. 2019, Rochlin et al. 2019). In California, the abundance of *Cx. tarsalis* varies seasonally and geographically and is found in high abundance in the Central Valley and irrigated areas of the southern desert (Reisen, Lothrop, Presser, et al. 1995, Barker et al. 2010). *Cx. tarsalis* are also more competent vectors of WNV and more likely to act as bridge vectors through opportunistic feeding than mosquitoes in the *Cx. pipiens* complex (Reisen et al. 2005, 2013, Thiemann et al. 2012, Rochlin et al. 2019), making it more likely that an infectious mosquito comes into contact with a person and thereby contributing to the high incidence observed in *Cx. tarsalis*-dominated areas.

Mosquito abundance forecasts and prediction uncertainty are elements that have not yet been incorporated into the Response Plan's risk assessment. Space-time models such as generalized additive models (GAMs) offer a simple method for producing forecasts based on historical and current trends. GAMs feature the ability to model nonlinear relationships as smooth functions rather than linear coefficients (Wood 2017) and previously have been applied for modeling spatio-temporal trends in mosquito abundance (Hwang et al. 2020, Wang et al. 2020, Holcomb et al. 2021). However, the use of GAMs in this context has been primarily retrospective with the intention of understanding factors affecting mosquito population dynamics. Here, we apply GAMs that incorporate observed surveillance information to forecast weekly *Cx. tarsalis* abundance across unsampled locations of the Central Valley of California for the peak WNV transmission season for five historical surveillance years. This study will provide

a useful tool for understanding WNV risk patterns in areas where surveillance coverage is limited or nonexistent and for identifying where additional vector control activity may be warranted.

3.2 Methods

3.2.1 Study area

This study focused on one of the regions of California where *Cx. tarsalis* is highly abundant. The Central Valley is a large, elongated valley predominantly characterized by irrigated agriculture, including rice, and is bounded by the Sierra Nevada to the east, the Coast Range to the west, the Cascade Mountains to the north, and the Tehachapi Mountains to the south. There are 31 vector control districts that operate throughout the Central Valley (Figure 3.1), of which 20 districts met maintained records of CO_2-baited trap collections in the VectorSurv Gateway database (see acknowledgements).

3.2.2 Mosquito abundance data

Entomological surveillance data relating to adult mosquito abundance for the years 2006-2020 were obtained from the VectorSurv Gateway through data request #53 (VectorSurv 2021). These data encompassed all CO_2-baited trap collections for all districts whose data were available in the database. We focused on CO_2-baited traps as these are a standard method for collecting host-seeking female mosquitoes and readily capture adult *Cx. tarsalis* (Newhouse et al. 1966, Reisen and Pfuntner 1987, Reisen et al. 2000). We excluded traps set by districts outside of the study region as well as traps above 300 m (≈1000 ft) elevation, where the transition to mountainous landscape provides less suitable *Cx. tarsalis* habitat (Barker et al. 2009, Schurich et al. 2014). The elevation at each trap site was drawn from the R package "elevatr", version 0.4.1 (Hollister 2021). Each mosquito collection event was associated with the date of collection, the number of trap-nights for which the trap was operated, and the GPS coordinates of the trap. We used the collection date to estimate the epidemiologic week of collection using the R package "lubridate", version 1.7.10 (Grolemund and Wickham 2011).

Because of low surveillance numbers during the winter months, any observations occurring during week 53 were treated as week 52. We then created an indicator for the week since the start of the study period (year-week) by multiplying the epidemiologic week by the number of years since 2006.

3.2.3 Environmental data

Trap coordinates were projected to NAD83/California Albers (EPSG: 3310) and a range of buffers were applied to each unique trap location during each year: 0.1 km, 0.5 km, 1 km, 2 km, and 5 km. We estimated the proportion coverage between 0 (no coverage within each buffer of the trap) to 1 (full coverage within each buffer of the trap) of land use categories from the USDA Cropland data for each of the years 2008-2020. These data have 30-meter resolution and incorporate the National Land Cover Database as the non-agricultural layers (Homer et al. 2015, USDA National Agricultural Statistics Service Cropland Data Layer 2020). Cropland data prior to 2008 were at a coarser resolution, so these years were excluded from the study. Land use types were categorized into seven groups relevant for discriminating *Cx. tarsalis* habitat and abundance: cover crops, developed land, orchards and vineyards, rice fields, row crops, wetlands, and unsuitable habitat, such that the sum of proportions of the seven groups within each buffer zone equaled 1 (Table S3.1). We separated rice fields from other irrigated agriculture because of its singular relationship with *Cx. tarsalis* habitat (Hoy et al. 1971, Pitcairn et al. 1994). Temperature data were derived from the North American Land Data Assimilation System dataset (Xia et al. 2012). We calculated the daily mean temperature for each day of the study period, which we then aggregated by week to estimate the mean temperature for the two weeks prior to the week of mosquito collection. The raster pixel values for mean temperature during the week of the collection event and the two weeks prior to the collection event were extracted at each trap location using the R package "raster", version 3.4-5 (Hijmans 2020).

3.2.4 Statistical analyses

To model the relative abundance of *Cx. tarsalis*, we fitted a negative binomial GAM for the Central Valley using the R package "mgcv", version 1.8-34 (Wood 2011, 2017). The model structure for establishing smooth functions of seasonality followed the structure introduced by Holcomb et al. (2021), which allowed the nonlinear effects of epidemiologic week to vary by percent coverage of each land use category. The model included an offset for the number of trap-nights of collection, the combined effects of [X, Y] point location of the trap and year-week to capture overall spatio-temporal trends at each site, and the average temperature over the two weeks prior to the week of trapping. In addition, the model contained a seasonal term for each of the land use groups to capture the seasonality of *Cx. tarsalis* abundance within different ecologic zones. We used the Akaike information criterion (AIC) to select the buffer zone for land use that produced the best-fitting model. We also used the AIC to evaluate whether certain similar land use categories within the best-fitting buffer zone could be grouped for a more parsimonious model.

The final model was validated by training 10 individual models with a random subset of 90% of the data, withholding the remaining 10% for testing. We estimated the Dawid-Sebastiani scores (DSS) and logarithmic scores (LS) of the predicted values using the R package "surveillance", version 1.19.1 (Czado et al. 2009). The DSS and LS are penalties comparing the expectation of the probability mass function for the negative binomial distribution to the observed value at a given set of covariates and are minimized when the expectation matches the true value (Gneiting and Raftery 2007, Czado et al. 2009, Paul and Held 2011). The mean DSSs LSs of predicting the training versus testing subsets were compared through paired sample *t*-tests to examine the ability of the models to predict *Cx. tarsalis* abundance at sites that were not recorded, where p-values below 0.05 would indicate a differing predictive ability. We used both scores to confirm that the chosen score did not impact the observed results.

We tested the predictive ability of the final model by repeating the 10-fold cross-validation process for a series of models iteratively adding weeks of data and randomly withholding 10% of the traps operated during the final week included in the data from model fitting. We repeated this process for each week from the beginning of April through the end of October for each of the years 2009-2020. The mean DSSs and LSs of predicting the training versus testing subsets were compared as before. We started with the year 2009 because at least one year of data was required to estimate a seasonal trend. We also compared the mean fitted *Cx. tarsalis* abundance from the 10 models at the traps run during the week following the last week in the model to the observed abundance at each of those locations. This allowed us to assess the utility of the model at predicting abundance at unmeasured locations and understand how increasing data availability impacted model prediction.

Finally, we predicted weekly abundance per CO_2-baited trap-night on a 2.5-km uniform spatial grid for the beginning of April through the end of October (weeks 14-44) for each of the years 2016-2020 by sequentially fitting models using data observed up to the week before the week being predicted. Weekly predictions were made by taking the mean estimated abundance from 1,000 random draws of the posterior distribution of the model, a multivariate normal distribution, and a 95% prediction interval around the mean was calculated from the 2.5% and 97.5% quantiles of the estimates (Wood 2017). To reduce prediction error, we restricted predictions to points within 10 km of observed trapping locations in the four weeks prior to the prediction week. We restricted predictions within a buffer of 10 km from observed surveillance locations based on a conservative estimate of *Cx. tarsalis* flight range (Dow et al. 1965, Reisen et al. 1992, Reisen and Lothrop 1995). All statistical analyses were conducted in R (version 4.0.5) (R Core Team 2021).

3.3 Results

Between 2008 and 2020, 161,257 trapping events were sampled from 10,511 unique trapping locations within the study area (Table 3.1). We observed that 4,188 (39.84%) of these

unique locations were sampled in more than one year, with 106 (1.01%) being sampled in all years. There were higher concentrations of traps around the populated areas of the Central Valley (Figure 3.1). Agriculture of all types covered almost half of the land within 1 km of trap locations while developed areas covered the highest single proportion of land within the 1 km trap buffer, on average (Table 3.1). Overall, there was a distinct seasonal trend in *Cx. tarsalis* abundance (Figure 3.2). Mean abundance across all years peaked between epidemiologic weeks 28-39, corresponding to approximately the beginning of July through the end of September, with smaller early-season peaks in weeks 14 and 18.

The AIC indicated that the best buffer zone for estimating land use around the trap sites was 1 km. The more parsimonious models combining the non-rice agriculture categories or open water and wetlands were not better fitting than the full model, so all seven land use variables were retained for the final model. All smooth terms included in the final model were highly significant (p-value < 0.0001) and the AIC of the model without the separate seasonal trends by land use indicated that model fit was improved by including the land use stratification. The smooth function estimates are presented in Figure 3.3. Variability in *Cx. tarsalis* abundance was explained largely by the spatio-temporal terms and seasonal variation in rice fields and wetlands. In terms of model validation, the differences in the paired mean LSs and DSSs for the training data versus the testing data were not statistically different (Table 3.2) and there was no difference in model residuals between the testing and training data (Figure S3.1).

When predicting at trap sites withheld from model-fitting, we observed no differences in the LS or DSS trends between training, testing, and prediction data (Figure 3.4). LSs in all years were higher in the middle of the prediction season, corresponding to the period of greatest *Cx. tarsalis* abundance, and did not vary across years, indicating that accumulating data history did not improve model fitting. This trend was not observed with the DSSs. The average predicted counts from the 10 validation models for each prediction week tended to be similar during the weeks with the highest average *Cx. tarsalis* abundance, but the model did not capture the high

early-season abundance during 2017, instead predicting high early-season counts in 2018 (Figure 3.5). When examining scores for observations within 10 km of a trap in the prior four weeks, LSs indicated that the model performed better at predicting abundance when predictions were within 1 week of another trap within 5 km or within 2 weeks of a trap within 1 km, limiting the window of utility for model predictions of *Cx. tarsalis* abundance. However, this pattern was not observed for the DSSs (Figure 3.6).

Prediction points were an average of 4.62 (SD: 2.60) km from the nearest trap operated during the prior four weeks and the nearest traps were set an average of 1.64 (SD: 0.95) weeks prior to the prediction week. The land cover composition in the immediate surroundings of the prediction points (i.e., within 1 km) was generally similar to that of the trap sites, although the prediction locations had lower proportion coverage of developed land due to the higher density of observed trap locations near developed areas (Figure S3.2). There was overall moderate correlation (0.45) by the Spearman's rank correlation coefficient between the predicted abundance and the observed abundance at the nearest trap to the prediction point. Correlation coefficients were highest between predicted and observed points when the predictions were closest in both space and time to the nearest observed trap and decreased as the predictions became farther from the nearest trap (Figure 3.7).

The overall predicted spatio-temporal patterns of *Cx. tarsalis* abundance showed low estimated abundance coinciding with low trap coverage in the early part of the season, with a peak of both coverage and predicted abundance in the middle part of the season, and then with a decline in surveillance at the end of the season (Figure 3.8). The highest abundance was predicted to occur in the northern extent of the primary Central Valley corridor (Sutter-Yuba MVCD and Yolo County) as well as to the southwest of the Central Valley (Fresno Westside MAD and western Merced County MAD). Urban centers throughout the valley stood out as regional pockets with lower predicted abundance. As a measure of uncertainty around the predicted estimates, the width of the 95% prediction interval was greatest at points with the highest

predicted abundance (Figure 3.8). There was variation among years in the extent of surveillance coverage in the four weeks prior to prediction as well as the magnitude of predicted abundance (Fig S3.3). The weekly prediction and prediction interval rasters for all years are available as supplementary geoTIFF files.

3.4 Discussion

Our study demonstrated an efficient method for utilizing antecedent surveillance observations to both spatially and temporally predict *Cx. tarsalis* abundance at unmeasured locations. This species is an important vector of WNV in rural areas of the western United States (Reisen et al. 2009, Kovach and Kilpatrick 2018, Dunphy et al. 2019, Rochlin et al. 2019) and abundance estimates are a key feature of local WNV risk assessments (California Department of Public Health et al. 2020). Our approach modelled the spatial heterogeneity in entomological surveillance coverage and assessed the ability to generate short-term future abundance estimates based on current data. We evaluated the large geographic area of the Central Valley, which has the highest human WNV disease incidence in the state (Snyder et al. 2020). This region is ecologically diverse and includes extremely productive habitat for *Cx. tarsalis*, particularly irrigated agriculture such as rice and vegetated wetlands (Hoy et al. 1971, Pitcairn et al. 1994, Kwasny et al. 2004).

There was variability in surveillance coverage both within and among districts. WNV vector surveillance typically is concentrated around inhabited areas where preventative measures would be most beneficial, and this was reflected in the distribution of unique trap locations throughout the study area and study period. However, the modelling approach we used allowed us to estimate *Cx. tarsalis* abundance at areas that were not sampled. Cross-validations evaluated the ability of the model to predict abundance at unmeasured sites and times by comparing fitted model abundance estimates to the observed counts in both the modelled training data and the withheld testing data. That there was no significant difference in DSSs or LSs between the training and testing data for any of the ten fitted cross-validation

models indicated that the model could be used to incorporate sites without surveillance coverage within the Central Valley, for example through historical data. We also saw no difference in DSSs or LSs in the weekly model cross-validation over time, meaning that the addition of surveillance years did not improve model estimation. The increased scores during the period of greatest *Cx. tarsalis* abundance reflected greater variability in counts at the maxima of the distribution, whereas the fitted distributions better captured observed *Cx. tarsalis* counts during the low periods of the season.

We saw a clear seasonal trend in *Cx. tarsalis* abundance throughout the study area. The main peak in mean abundance occurred during the summer with negligible counts recorded during the winter. This is consistent with the seasonal patterns of *Cx. tarsalis* abundance observed in California (Reisen and Reeves 1990, Reisen et al. 1992, Barker et al. 2010) and elsewhere in the United States (Snow and Pickard 1956, Bolling et al. 2009, Fauver et al. 2016, Vincent et al. 2020). The smaller springtime peaks in abundance are associated with the flooding of managed wetlands in conjunction with warming temperatures triggering oviposition by overwintering females (Kwasny et al. 2004, Reisen and Wheeler 2019).

In our model, variations in *Cx. tarsalis* abundance were strongly driven by seasonal effects in rice fields and in wetlands, which are two habitats most associated with high *Cx. tarsalis* counts in California (Sudia et al. 1971, Pitcairn et al. 1994, Wekesa et al. 1996). Accordingly, we also observed the highest predicted *Cx. tarsalis* abundance during the middle of the surveillance season where rice is cultivated in Yolo County and Sutter-Yuba MVCD and around a cluster of national wildlife refuges in the later part of the season in western Merced County MAD and Fresno Westside MAD (US Fish and Wildlife Service 2021). There was a lower seasonal effect in urban areas on *Cx. tarsalis* abundance, which was expected as this has been found in lower numbers within urbanized environments (Reisen and Reeves 1990, Schurich et al. 2014). Furthermore, incursions into populated areas are generally limited to the urban periphery as *Cx. tarsalis* flight dispersal is typically within 2 km of larval emergence sites,

although dispersal up to 25 km has been observed downwind (Bailey et al. 1965, Dow et al. 1965, Reisen et al. 1992, Reisen and Lothrop 1995). On a small scale, this limited incursion was observed by interpolating *Cx. tarsalis* counts from traps placed throughout a city, with higher abundance observed at the edges (Nielsen et al. 2008).

The predicted surfaces reflected how *Cx. tarsalis* abundance varies over the course of a season and from year to year. By refitting models sequentially adding observed weeks of data, we were able to simulate the progression of surveillance-based knowledge of *Cx. tarsalis* activity. This approach used past and current information to infer spatial patterns in the near-term future, which has not previously been attempted. We saw overall low estimated abundance during the early weeks of each season for the districts that conducted surveillance during that time. Surveillance coverage intensified into the middle of the season when estimated abundance was highest across the valley, followed by a waning of estimated abundance towards the conclusion of the season. Other studies mapping *Cx. tarsalis* abundance have not considered temporal trends, have been limited to suitability models, or have encompassed a limited spatial domain (Tachiiri et al. 2006, Nielsen et al. 2008, Larson et al. 2010). One study that did account for seasonality only assessed predictions at the trap locations that provided observations for model fitting (Schurich et al. 2014).

Our spatio-temporal models for risk-mapping improved on the Response Plan for estimating vector abundance, which uses retrospective data to estimate the current week's risk and does not incorporate environmental factors other than temperature. Our resolution was also higher than the Response Plan, which allowed us to visualize spatial heterogeneity between primary *Cx. tarsalis* habitat around irrigated agriculture and wetlands and the less suitable urban and suburban cores. We were further able to visualize uncertainty around the estimates, which was highest in areas with greatest predicted *Cx. tarsalis* abundance due to a combination of larger standard errors for higher predicted counts, thus increasing the margin of error, and lower trap densities in areas where *Cx. tarsalis* abundance is greatest, thus reducing the sample

size for estimating spatio-temporal effects. The latter explanation is corroborated by comparing the landscape composition of the observed trap sites to that of the prediction sites, where the observed traps had a higher proportion of developed land within 1 km of the site than the prediction points. We retained similarity to the Response Plan by only predicting abundance for zones within 10 km of traps run in the prior four weeks, which allowed risk estimation to evolve as more information about the observed trap counts was known.

The predicted abundance across the 2.5 km gridded surface was only moderately correlated with the observed abundance at the prediction point's nearest trap, but this was expected as the nearest trap could be a minimum of one week prior to prediction, and week to week changes in abundance estimates could be quite large. Furthermore, we did not account for the application of vector control during the study period. Elevated abundance estimates of *Cx. tarsalis* trigger the intensification of adult mosquito control measures aimed at reducing the risk of WNV transmission to humans and have been shown to be effective, if temporally limited (Elnaiem et al. 2008, Holcomb et al. 2021). However, these applications could reduce observed *Cx. tarsalis* counts during the weeks being predicted, which the model would not have captured, thus reducing the correlation between observed and predicted abundance. However, as these models were intended to provide a basis for WNV risk estimation in the near-term future, the absence of a vector control term in the model means that districts can assess abundance as a risk indicator in the absence of intervention.

Although this study encompassed most of the primary *Cx. tarsalis* range in California, there are populations in southern California, notably in the Coachella Valley and Orange County, that we did not include in our analyses. These regions feature different landscape composition, different seasonality, and *Cx. tarsalis* distribution concentrated around wetlands as opposed to the widespread distribution around irrigated agriculture in the Central Valley (Walton et al. 1990, Reisen, Lothrop, and Hardy 1995). Therefore, models for *Cx. tarsalis* in the

Central Valley would not necessarily be applied for *Cx. tarsalis* abundance elsewhere in the state.

Overall, our study demonstrated the utility of routine surveillance data combined with environmental information at estimating the spatio-temporal abundance of *Cx. tarsalis*, an important vector of WNV in the western United States. The models developed here will serve as a starting point for improved spatio-temporal risk assessments for WNV transmission. The standardized approach for evaluating the contribution of land cover around a trap means that the model could be further developed into a tool to produce mosquito abundance estimates that integrate and extend existing surveillance data, providing a basis for risk estimates at unobserved locations and/or future time periods. Ultimately this knowledge, alongside data-based limits on uncertainty, will help direct vector control resources to areas of need.

3.5 Acknowledgements

The authors acknowledge the following mosquito control districts for the usage of routine arbovirus surveillance data: Butte County Mosquito and Vector Control, Consolidated Mosquito Abatement, Delano Mosquito Abatement, Delta Mosquito and Vector Control, East Side Mosquito Abatement, Fresno Mosquito and Vector Control, Fresno Westside Mosquito Abatement, Glenn County Mosquito and Vector Control, Kern County Mosquito and Vector Control, Kings Mosquito Abatement, Madera County Mosquito and Vector Control, Merced County Mosquito Abatement, Placer Mosquito and Vector Control, Sacramento-Yolo Mosquito and Vector Control, San Joaquin County Mosquito and Vector Control, Shasta Mosquito and Vector Control, Sutter-Yuba Mosquito and Vector Control, Tulare Mosquito Abatement, Turlock Mosquito Abatement, Westside Mosquito and Vector Control.

3.6 Tables and figures

Table 3.1. Descriptive statistics for traps in the Central Valley.

Factor	Values
Sample size (trap-nights)	161,257
Unique trap sites	10,511
Mean *Cx. tarsalis* abundance per trap-night (SD)	29.6 (152.2)
Mean weekly average temperature in °C (range)	25.3 (0.7-39.7)
Mean percent cover crops coverage within 1 km of traps (SD)	15.3% (18.5%)
Mean percent developed area coverage within 1 km of traps (SD)	34.2% (34.2%)
Mean percent orchards and vines coverage within 1 km of traps (SD)	18.2% (23.3%)
Mean percent rice field coverage within 1 km of traps (SD)	0.4% (3.6%)
Mean percent row crops coverage within 1 km of traps (SD)	3.9% (9.1%)
Mean percent wetlands coverage within 1 km of traps (SD)	2.0% (5.8%)
Mean percent unsuitable habitat coverage within 1 km of traps (SD)	26.1% (24.3%)

Table 3.2. Mean logarithmic and Dawid-Sebastiani scores from k-fold cross-validation. The final model was evaluated through 10-fold cross-validation, randomly withholding 10% of the data for testing and fitting a training model to the remaining 90% of the data.

	Dawid-Sebastiani score		Logarithmic score	
Model number	Training	Testing	Training	Testing
1	9.80	9.75	3.47	3.46
2	10.37	9.35	3.47	3.49
3	10.37	10.40	3.47	3.46
4	10.32	10.45	3.47	3.48
5	10.25	10.52	3.47	3.47
6	9.80	9.23	3.47	3.46
7	10.20	9.93	3.47	3.48
8	10.31	10.66	3.47	3.45
9	10.27	9.21	3.47	3.46
10	10.25	10.97	3.47	3.47
Average of all models	10.19	10.05	3.47	3.47
Paired *t*-test statistic (*P*-value)	-0.79 (0.45)		-0.77 (0.46)	

Table S3.1. USDA Cropland data categories and groups for analysis.

USDA category	Group for analysis
Alfalfa	Cover crops
Almonds	Orchards and vineyards
Apples	Orchards and vineyards
Apricots	Orchards and vineyards
Aquaculture	Unsuitable habitat
Asparagus	Row crops
Avocados	Orchards and vineyards
Background	Unsuitable habitat
Barley	Cover crops
Barren	Unsuitable habitat
Blueberries	Row crops
Broccoli	Row crops
Buckwheat	Cover crops
Cabbage	Row crops
Camelina	Cover crops
Caneberries	Row crops
Canola	Cover crops
Cantaloupes	Row crops
Carrots	Row crops
Cauliflower	Row crops
Celery	Row crops
Cherries	Orchards and vineyards
Chickpeas	Row crops
Christmas trees	Unsuitable habitat
Citrus	Orchards and vineyards
Clover, wildflowers	Cover crops
Corn	Row crops
Cotton	Row crops
Cucumbers	Row crops
Barley/corn	Cover crops
Barley/sorghum	Cover crops
Corn/soybeans	Row crops
Durum wheat/sorghum	Cover crops
Lettuce/barley	Row crops

USDA category	Group for analysis
Hops	Row crops
Lentils	Row crops
Lettuce	Row crops
Millet	Cover crops
Mint	Row crops
Misc. fruits, vegetables	Row crops
Mixed forest	Unsuitable habitat
Mustard	Cover crops
Nectarines	Orchards and vineyards
Undefined	Unsuitable habitat
Oats	Cover crops
Olives	Orchards and vineyards
Onions	Row crops
Open water	Unsuitable habitat
Oranges	Orchards and vineyards
Other crops	Row crops
Other hay, non-alfalfa	Cover crops
Other small grains	Cover crops
Other tree crops	Orchards and vineyards
Peaches	Orchards and vineyards
Peanuts	Row crops
Pears	Orchards and vineyards
Peas	Row crops
Pecans	Orchards and vineyards
Peppers	Row crops
Perennial ice, snow	Unsuitable habitat
Pistachios	Orchards and vineyards
Plums	Orchards and vineyards
Pomegranates	Orchards and vineyards
Pop or orn corn	Row crops
Potatoes	Row crops
Prunes	Orchards and vineyards
Pumpkins	Row crops
Radishes	Row crops

Lettuce/cantaloupe	Row crops
Lettuce/cotton	Row crops
Lettuce/durum wheat	Row crops
Oats/corn	Cover crops
Soybeans/oats	Row crops
Triticale/corn	Cover crops
Winter wheat/corn	Cover crops
Winter wheat/cotton	Cover crops
Winter wheat/sorghum	Cover crops
Winter wheat/soybeans	Cover crops
Deciduous forest	Unsuitable habitat
Developed, high intensity	Developed land
Developed, low intensity	Developed land
Developed, medium intensity	Developed land
Developed, open space	Developed land
Dry beans	Row crops
Durum wheat	Cover crops
Eggplants	Row crops
Evergreen forest	Unsuitable habitat
Fallow/idle cropland	Unsuitable habitat
Flaxseed	Cover crops
Forest	Unsuitable habitat
Garlic	Row crops
Gourds	Row crops
Grapes	Orchards and vineyards
Grassland/pasture	Unsuitable habitat
Greens	Row crops
Herbaceous wetlands	Wetlands
Herbs	Row crops
Honeydew melons	Row crops

Rapeseed	Cover crops
Rice	Rice fields
Rye	Cover crops
Safflower	Cover crops
Shrubland	Unsuitable habitat
Sod, grass seed	Cover crops
Sorghum	Cover crops
Soybeans	Cover crops
Speltz	Cover crops
Spring wheat	Cover crops
Squash	Row crops
Strawberries	Row crops
Sugar beets	Row crops
Sugarcane	Row crops
Sunflower	Row crops
Sweet corn	Row crops
Sweet potatoes	Row crops
Switchgrass	Cover crops
Tobacco	Row crops
Tomatoes	Row crops
Triticale	Cover crops
Turnips	Row crops
Vetch	Cover crops
Walnuts	Orchards and vineyards
Water	Unsuitable habitat
Watermelons	Row crops
Wetlands	Wetlands
Winter wheat	Cover crops
Woody wetlands	Wetlands

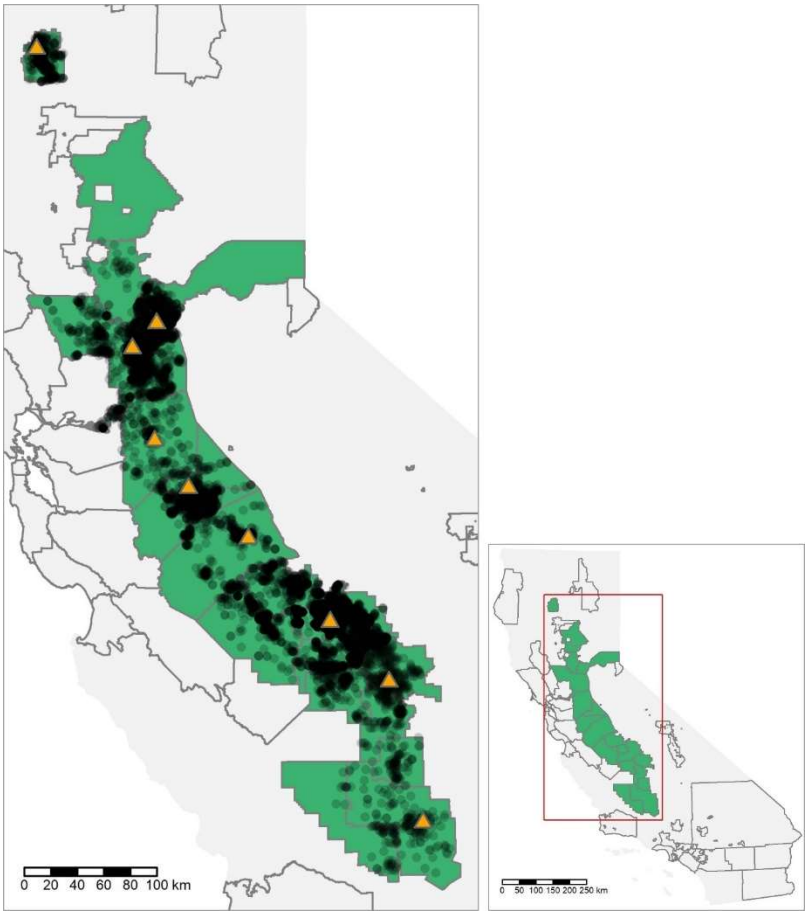

Figure 3.1. Map of the study area in California. Vector control district boundaries are shown with dark grey borders with the study districts highlighted in green. Unique trapping locations are indicated by transparent black circles. Areas with the highest trap density show up in darker black. Major urban centers (from north to south: Redding, Roseville, Sacramento, Stockton, Modesto, Merced, Fresno, Visalia, Bakersfield) are denoted by orange triangles. State boundaries were obtained from the Database of Global Administrative Areas (GADM 2018) and mosquito and vector control district boundary shapefiles were obtained from the Mosquito and Vector Control Association of California (Mosquito & Vector Control Association of California 2017).

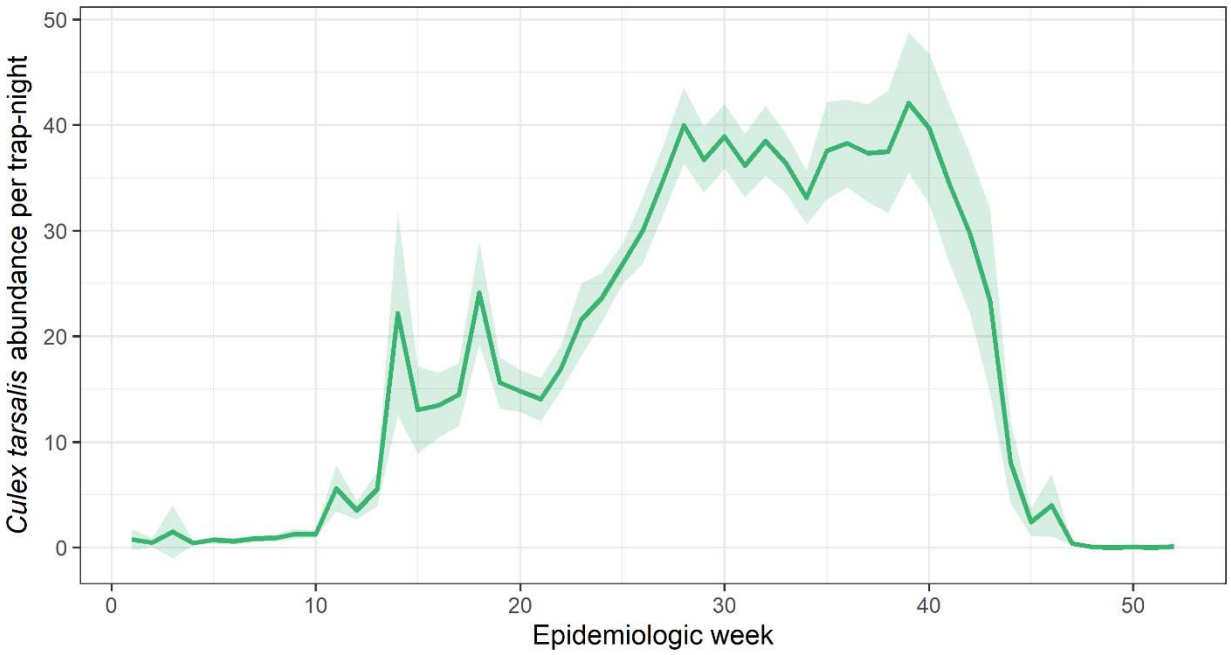

Figure 3.2. Seasonal trend of *Culex tarsalis* abundance in the Central Valley. The solid lines show the weekly mean *Cx. tarsalis* abundance per trap-night across all sites and years within the study region. The shaded band shows the 95% confidence interval around the mean.

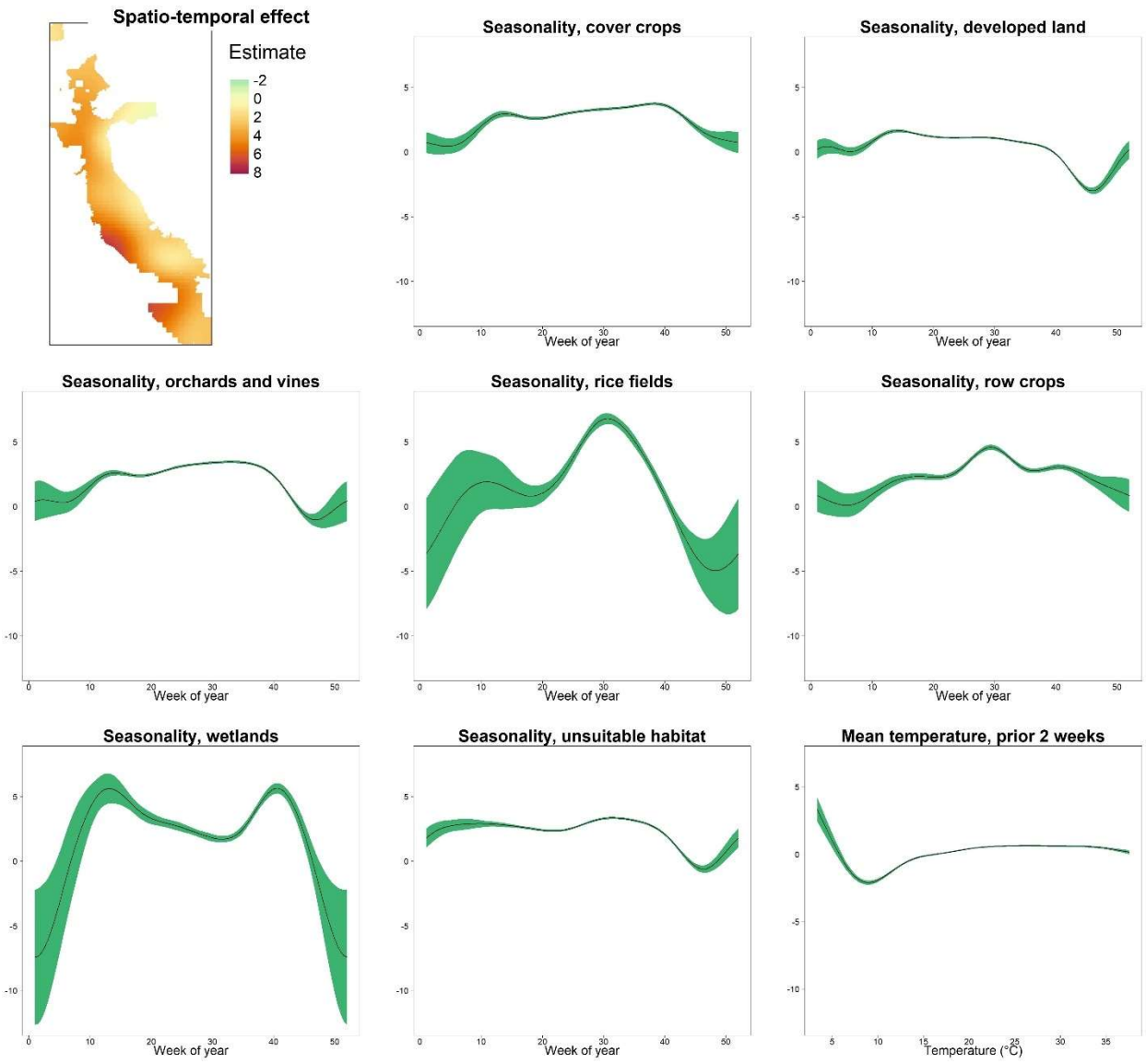

Figure 3.3. Generalized additive model (GAM) smooth functions. The spatio-temporal effect is depicted on a gradient from lowest (green) to highest (red). This image shows a representative time point of the spatio-temporal surface, the middle of July for 2020. For the one-dimensional smooths (green confidence interval bands), the y-axis represents the effect on *Cx. tarsalis* abundance for each unit of the x-axis.

Figure 3.4. Weekly mean Dawid-Sebastiani scores (DSS) and log scores (LS) from 10 cross-validation models per week.

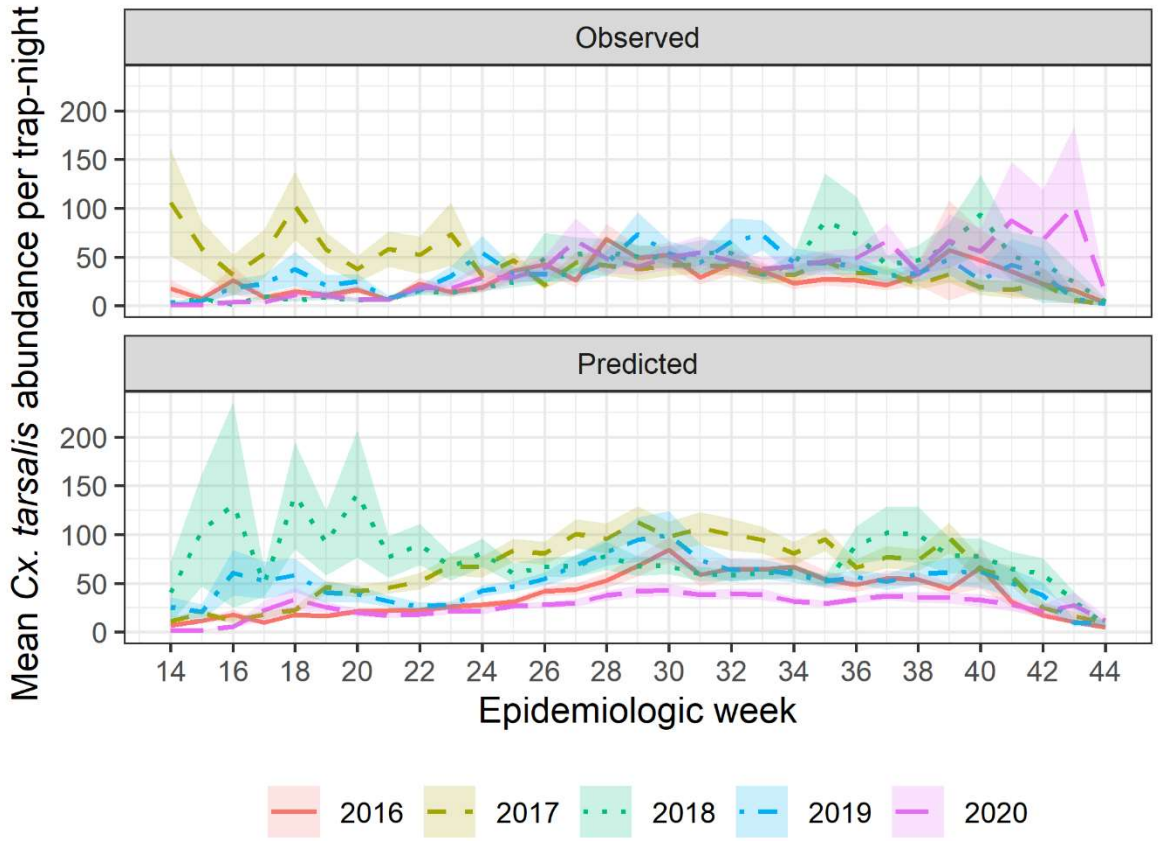

Figure 3.5. Comparison of weekly average observed and fitted *Culex tarsalis* abundance at surveillance locations for the years 2016-2020. The solid and dashed lines represent the mean abundance per week and year and the shaded bands show the 95% confidence interval around the means. We focused here on the years 2016-2020 because these were the years for which gridded surfaces were predicted.

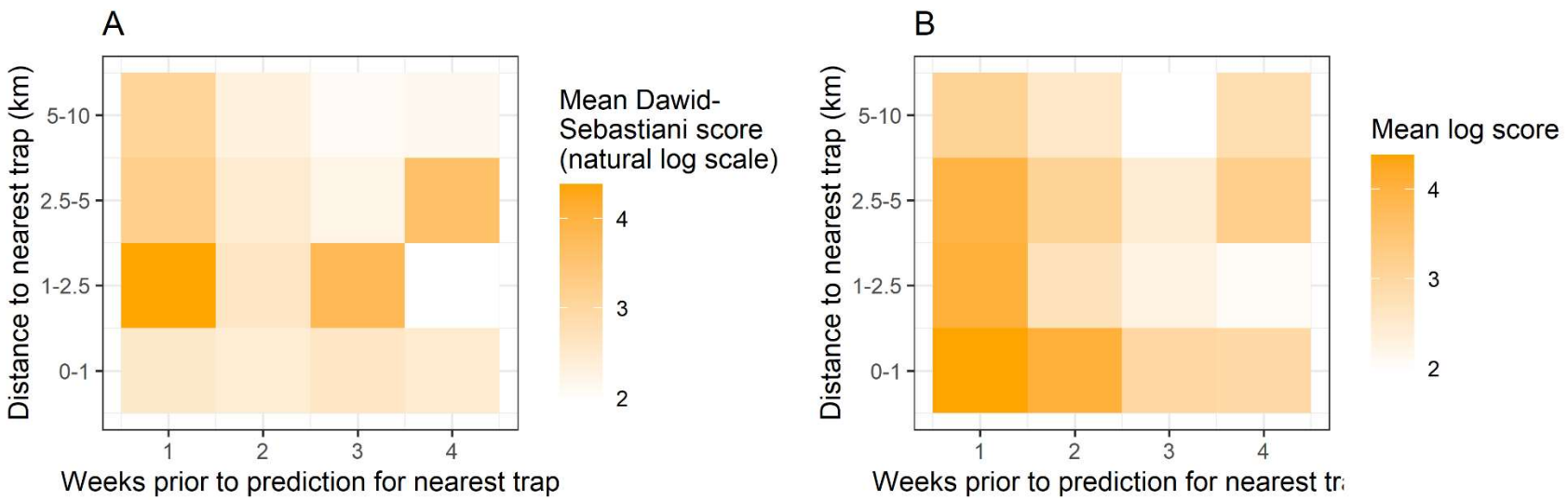

Figure 3.6. Mean Dawid-Sebastiani scores (DSS) are shown in Panel A and log scores (LS) in Panel B for weekly predictions made at traps within different spatial and temporal ranges from traps run during the prior four weeks. The lower-left pixels represent instances where the closest trap was within 1 km and 1 week prior to the fitted trap whereas the upper-right pixels represent instances where the closest trap was 5-10 km from and 4 weeks prior to the fitted trap. Lower values indicated better fits. Note that the DSSs are shown on the natural log scale.

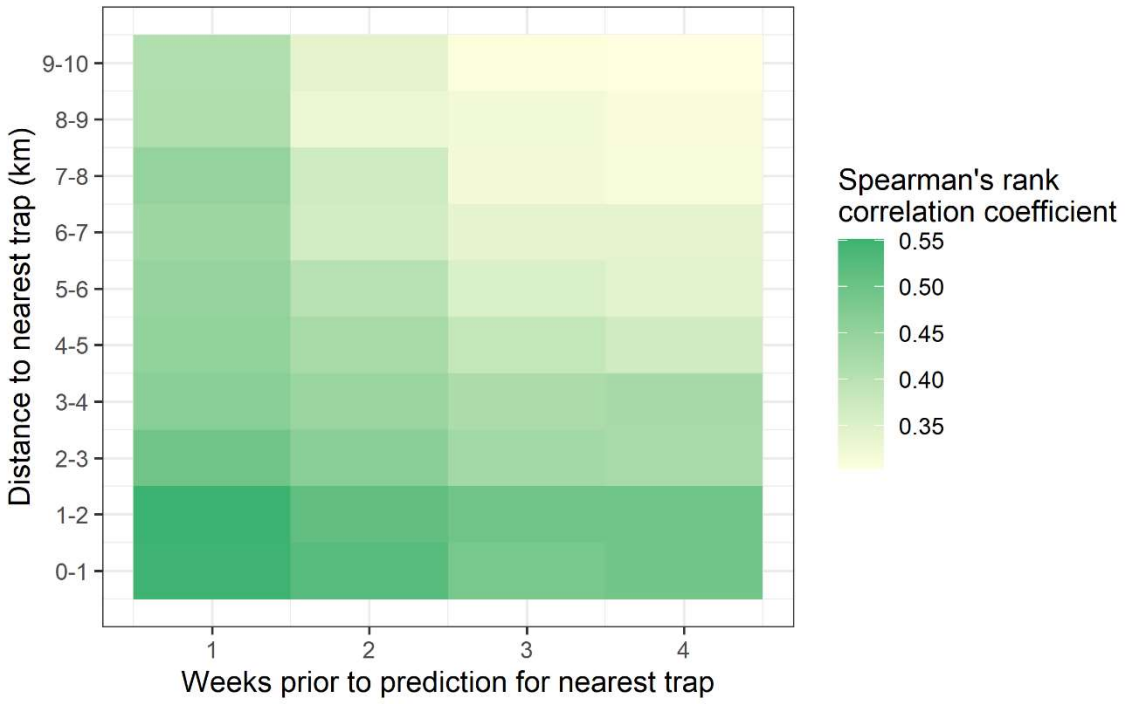

Figure 3.7. Spearman's rank correlation coefficient between predicted abundance and observed abundance at the nearest traps to the prediction location. Correlations were assessed for predictions where the nearest trap was a range of distances and weeks prior from the prediction locations and prediction weeks. The lower-left pixel represents instances where the closest trap was within 1 km of and 1 week prior to the prediction whereas the upper-right pixel shows instances where the closest trap was over 9 km from and 4 weeks prior to the prediction.

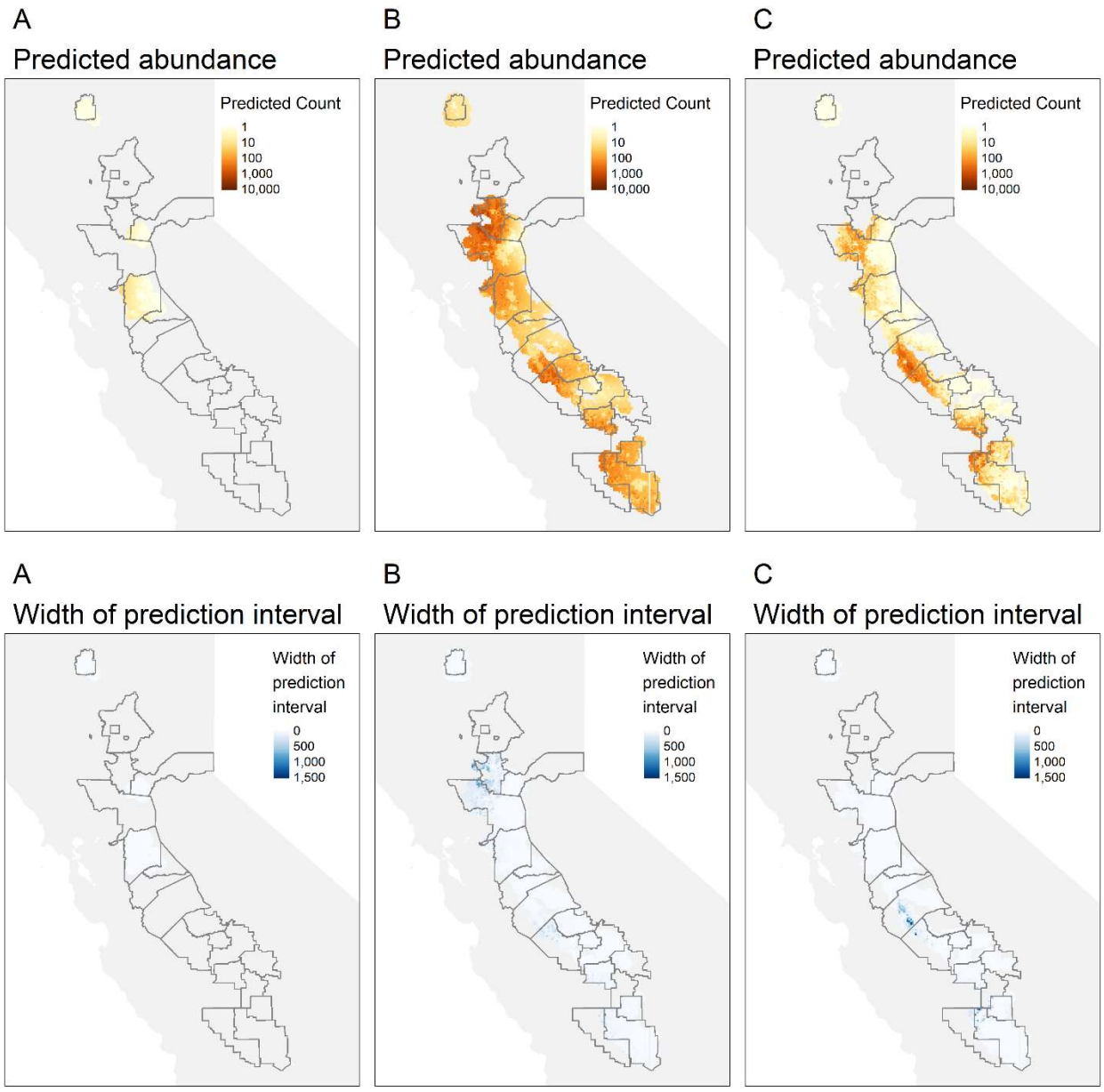

Figure 3.8. Gridded predictions and estimates of predictive uncertainty, shown as the width of the 95% prediction intervals. Predictions were made on a uniform 2.5-km grid for points within 10 km of a traps operated within four weeks prior to the prediction week. Column (A) shows the beginning (Week 14, March 29-April 4), column (B) the middle (Week 29, July 12-18), and column (C) the end (Week 44, October 25-31) of the season in 2020. State boundaries were obtained from the Database of Global Administrative Areas (GADM 2018) and mosquito and vector control district boundary shapefiles were obtained from the Mosquito and

Vector Control Association of California (Mosquito & Vector Control Association of California 2017).

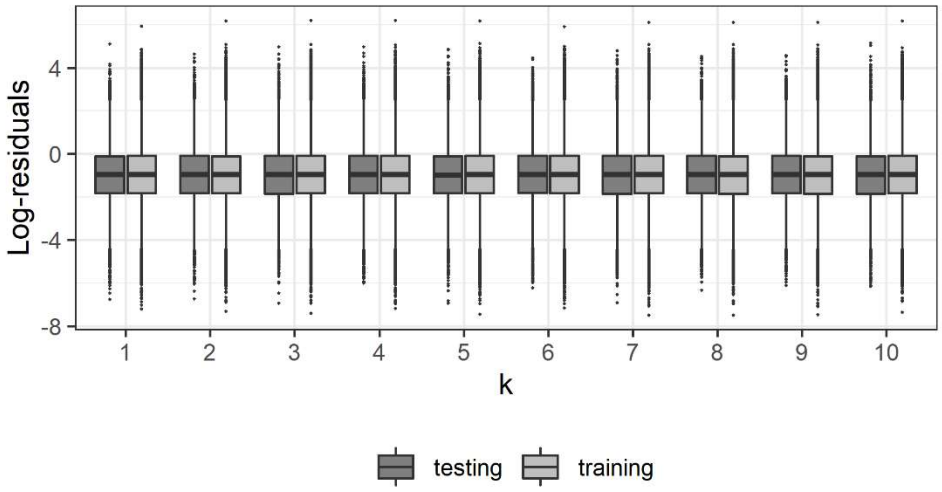

Figure S3.1. K-fold cross-validation model residuals. The model was evaluated through 10-fold cross-validation, randomly withholding 10% of the data for testing and fitting a training model to the remaining 90% of the data. The log-residuals were calculated by subtracting the natural log of the model fitted value from the natural log of the observed *Cx. tarsalis* count.

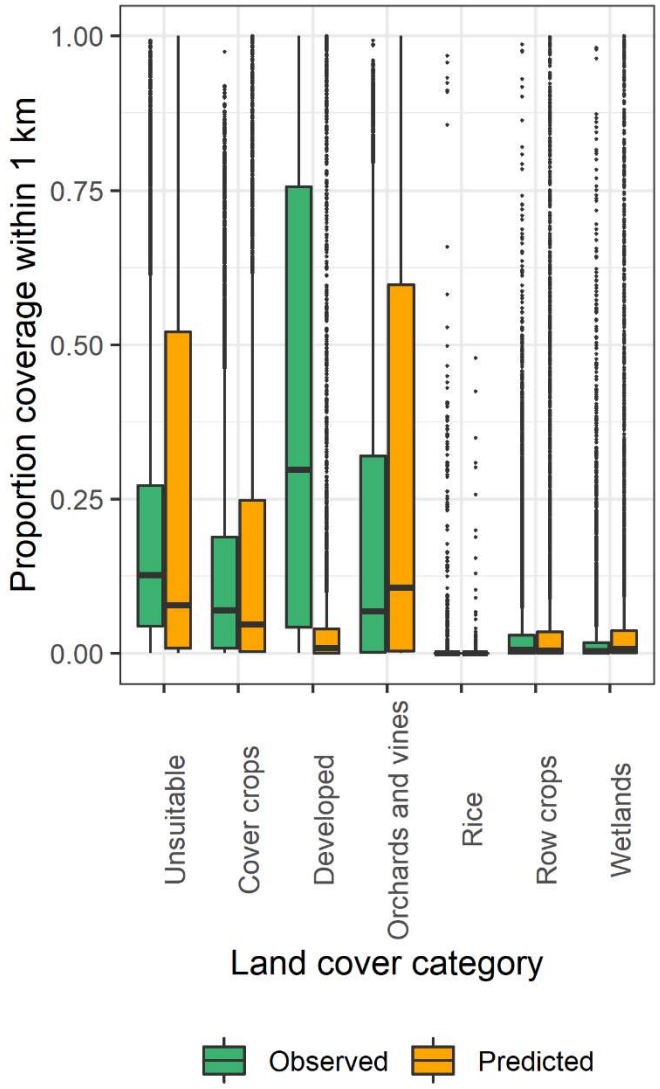

Figure S3.2. Comparison of land cover composition surrounding observed trap sites and prediction points for the years 2016-2020. The prediction locations were less likely to be surrounded by developed area within 1 km than the trap sites that were used to fit the models.

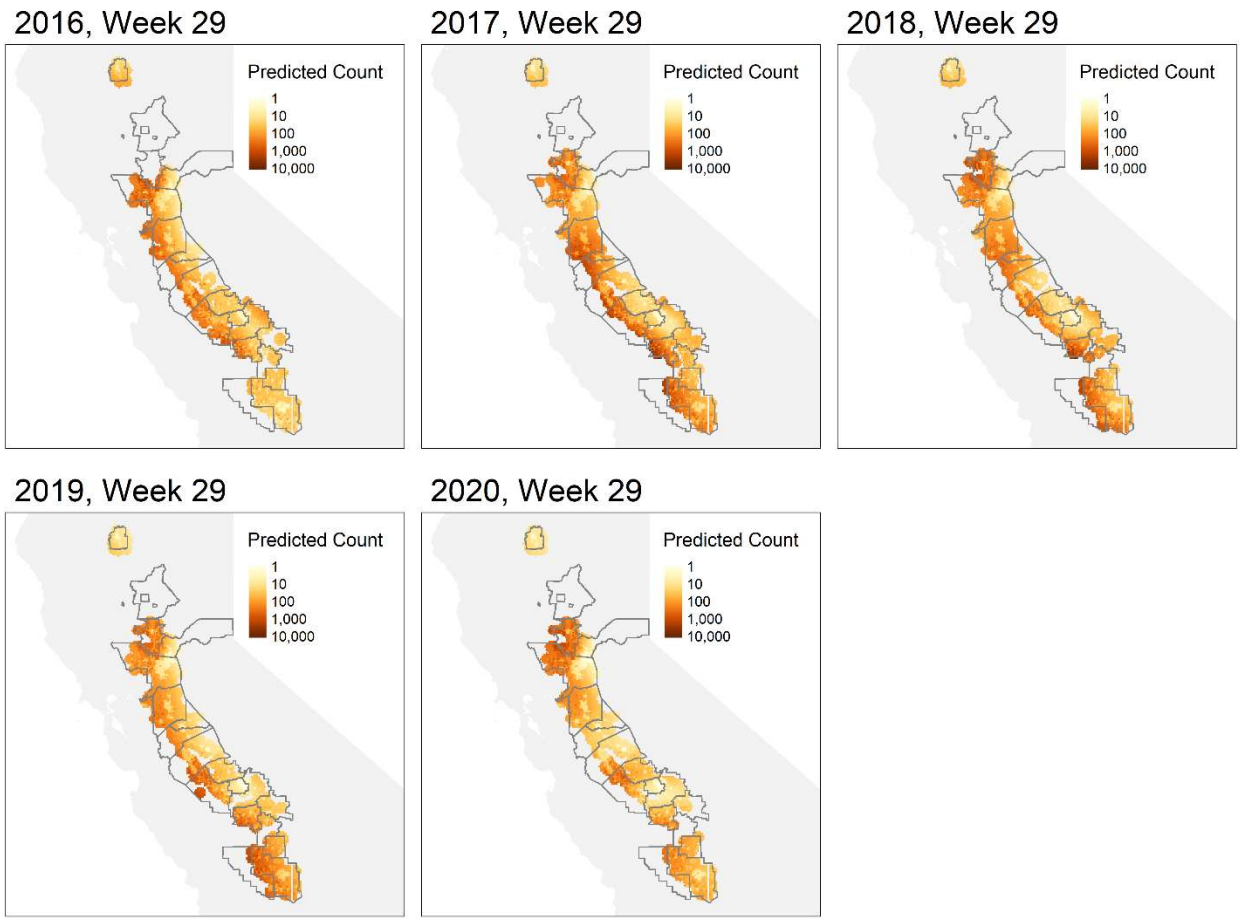

Figure S3.3. Prediction rasters for the middle of the season (Week 29) for each of the years 2016-2020. Predictions were made for points within 10 km of a trap run in the four weeks prior to the prediction week. State boundaries were obtained from the Database of Global Administrative Areas (GADM 2018) and mosquito and vector control district boundary shapefiles were obtained from the Mosquito and Vector Control Association of California (Mosquito & Vector Control Association of California 2017).

3.7 References

Bailey, S. F., D. A. Eliason, and B. L. Hoffmann. **1965**. Flight and dispersal of the mosquito *Culex tarsalis* Coquillett in the Sacramento Valley of California. Hilgardia. 37: 73–113.

Barker, C. M., B. G. Bolling, W. C. Black, C. G. Moore, and L. Eisen. **2009**. Mosquitoes and West Nile virus along a river corridor from prairie to montane habitats in eastern Colorado. J. Vector Ecol. 34: 276–293.

Barker, C. M., B. F. Eldridge, and W. K. Reisen. **2010**. Seasonal abundance of *Culex*

tarsalis and *Culex pipiens* complex mosquitoes (Diptera: Culicidae) in California. J. Med. Entomol. 47: 759–768.

Bolling, B. G., C. M. Barker, C. G. Moore, W. J. Pape, and L. Eisen. **2009**. Seasonal patterns for entomological measures of risk for exposure to *Culex* vectors and West Nile virus in relation to human disease cases in northeastern Colorado. J. Med. Entomol. 46: 1519–1531.

California Department of Public Health, Mosquito & Vector Control Association of California, and University of California. **2020**. California Mosquito-Borne Virus Surveillance & Response Plan. Sacramento.

Carney, R. M., S. Husted, C. Jean, C. Glaser, and V. Kramer. **2008**. Efficacy of aerial spraying of mosquito adulticide in reducing incidence of West Nile virus, California, 2005. Emerg. Infect. Dis. 14: 747–754.

Colborn, J. M., K. A. Smith, J. Townsend, D. Damian, R. S. Nasci, and J.-P. Mutebi. **2013**. West Nile virus outbreak in Phoenix, Arizona—2010: Entomological observations and epidemiological correlations. J. Am. Mosq. Control Assoc. 29: 123–132.

Czado, C., T. Gneiting, and L. Held. **2009**. Predictive model assessment for count data. Biometrics. 65: 1254–1261.

Danforth, M. E., M. Fischer, R. E. Snyder, N. P. Lindsey, S. W. Martin, and V. L. Kramer. **2021**. Characterizing areas with increased burden of West Nile virus disease in California, 2009–2018. Vector-Borne Zoonotic Dis.

Dow, R. P., W. C. Reeves, and R. E. Bellamy. **1965**. Dispersal of female *Culex tarsalis* into a larvicided area. Am. J. Trop. Med. Hyg. 14: 656–670.

Dunphy, B. M., K. B. Kovach, E. J. Gehrke, E. N. Field, W. A. Rowley, L. C. Bartholomay, and R. C. Smith. **2019**. Long-term surveillance defines spatial and temporal patterns implicating *Culex tarsalis* as the primary vector of West Nile virus. Sci. Rep. 9: 6637.

Eisen, L., C. M. Barker, C. G. Moore, W. J. Pape, A. M. Winters, and N. Cheronis. **2010**. Irrigated agriculture is an important risk factor for West Nile virus disease in the hyperendemic Larimer-Boulder-Weld area of North Central Colorado. J. Med. Entomol. 47: 939–951.

Elnaiem, D. A., K. Kelley, S. Wright, R. Laffey, G. Yoshimura, M. Reed, G. Goodman, T. Thiemann, L. Reimer, W. K. Reisen, D. Brown, and D. A. Elnaiem. **2008**. Impact of aerial spraying of pyrethrin insecticide on Culex pipiens and Culex tarsalis (Diptera: Culicidae) abundance and West Nile virus infection rates in an urban/suburban area of Sacramento County, California. J. Med. Entomol. 45: 751–757.

Fauver, J. R., L. Pecher, J. A. Schurich, B. G. Bolling, M. Calhoon, N. D. Grubaugh, K. L. Burkhalter, L. Eisen, B. G. Andre, R. S. Nasci, A. LeBailly, G. D. Ebel, and C. G. Moore. **2016**. Temporal and spatial variability of entomological risk indices for West Nile virus infection in northern Colorado: 2006-2013. J. Med. Entomol. 53: 425–434.

GADM. **2018**. Database of Global Administrative Areas, version 3.6. (www.gadm.org/data.html).

Gneiting, T., and A. E. Raftery. **2007**. Strictly proper scoring rules, prediction, and estimation. J. Am. Stat. Assoc. 102: 359–378.

Grolemund, G., and H. Wickham. **2011**. Dates and times made rasy with lubridate. J. Stat. Softw. 40: 1–25.

Gubler, D. J., G. L. Campbell, R. Nasci, N. Komar, L. Petersen, and J. T. Roehrig. **2000**. West Nile virus in the United States: Guidelines for detection, prevention, and control. Viral Immunol.

Hijmans, R. J. 2020. raster: Geographic data analysis and modeling. R package version 3.4-5. (https://cran.r-project.org/package=raster).

Holcomb, K., R. Reiner, and C. Barker. **2021**. Spatio-temporal impacts of aerial insecticide applications on West Nile virus vectors. Parasit. Vectors. 14: 120.

Hollister, J. W. 2021. elevatr: Access elevation data from various APIs. R package version 0.4.1. (https://cran.r-project.org/package=elevatr).

Homer, C. G., J. Dewitz, L. Yang, S. Jin, P. Danielson, Xian, J. Coulston, N. Herold, J. Wickham, and K. Megown. **2015**. National Land Cover Database for the conterminous United States – representing a decade of land cover change information. Photogramm. Eng. Remote Sensing. 81: 345–353.

Hoy, J. B., A. G. O'Berg, and E. E. Kauffman. **1971**. The mosquitofish as a biological control agent against *Culex tarsalis* and *Anopheles freeborni* in Sacramento Valley rice fields. J. Am. Mosq. Control Assoc. 31: 146–152.

Hwang, M.-J., H.-C. Kim, T. A. Klein, S.-T. Chong, K. Sim, Y. Chung, and H.-K. Cheong. **2020**. Comparison of climatic factors on mosquito abundance at US Army Garrison Humphreys, Republic of Korea. PLoS One. 15: e0240363.

Kaiser, J. A., and A. D. T. Barrett. **2019**. Twenty years of progress toward West Nile virus vaccine development. Viruses. 11: 823.

Karki, S., N. E. Westcott, E. J. Muturi, W. M. Brown, and M. O. Ruiz. **2017**. Assessing human risk of illness with West Nile virus mosquito surveillance data to improve public health preparedness. Zoonoses Public Health. 00: 1–8.

Kilpatrick, A. M., and W. J. Pape. **2013**. Predicting human West Nile virus infections with mosquito surveillance data. Am. J. Epidemiol. 178: 829–835.

Kovach, T. J., and A. M. Kilpatrick. **2018**. Increased human incidence of West Nile virus disease near rice felds in California but not in southern United States. Am. J. Trop. Med. Hyg. 99: 222–228.

Kwasny, D. C., M. Wolder, C. R. Isola, and J. Pickering. **2004**. Technical guide to best management practices for mosquito control in managed wetlands.

Larson, S. R., J. P. DeGroote, L. C. Bartholomay, and R. Sugumaran. **2010**. Ecological niche modeling of potential West Nile virus vector mosquito species in Iowa. J. Insect Sci. 10: 1–17.

Mosquito & Vector Control Association of California. **2017**. MVCAC Webmap. (https://www.arcgis.com/home/webmap/viewer.html?webmap=604a0fe9f2b74e98a53b53d192b2ac67&extent=-131.4442,32.5803,-108.7025,41.6862).

Newhouse, V. F., R. W. Chamberlain, J. G. Johnston, and W. D. Sudia. **1966**. Use of dry ice to increase mosquito catches of the CDC miniature light trap. Mosq. News. 30–35.

Nielsen, C. F., M. V. Armijos, S. Wheeler, T. E. Carpenter, W. M. Boyce, K. Kelley, D. Brown, T. W. Scott, and W. K. Reisen. **2008**. Risk factors associated with human infection during the 2006 West Nile virus outbreak in Davis, a residential community in northern California. A. J. Trop. Med. Hyg. 78: 53–62.

Paul, M., and L. Held. **2011**. Predictive assessment of a non-linear random effects model for

multivariate time series of infectious disease counts. Stat. Med. 30: 1118–1136.

Pitcairn, M. J., L. T. Wilson, R. K. Washino, and E. Rejmankova. **1994**. Spatial patterns of *Anopheles freeborni* and *Culex tarsalis* (Diptera: Culicidae) larvae in California rice fields. J. Med. Entomol. 31: 545–553.

R Core Team. **2021**. R: A language and environment for statistical computing.

Reisen, W., H. Lothrop, R. Chiles, M. Madon, C. Cossen, L. Woods, S. Husted, V. Kramer, and J. Edman. **2004**. West Nile virus in California. Emerg. Infect. Dis. 10: 1369–1378.

Reisen, W. K., B. D. Carroll, R. Takahashi, Y. Fang, S. Garcia, V. M. Martinez, and R. O. B. Quiring. **2009**. Repeated West Nile Virus epidemic transmission in Kern County, California, 2004-2007. J. Med. Entomol. 46: 139–157.

Reisen, W. K., Y. Fang, and V. M. Martinez. **2005**. Avian host and mosquito (Diptera: Culicidae) vector competence determine the efficiency of West Nile and St. Louis encephalitis virus transmission. J Med Entomol. 42: 367–375.

Reisen, W. K., and H. D. Lothrop. **1995**. Population ecology and dispersal of *Culex tarsalis* (Diptera: Culicidae) in the Coachella Valley of California. J Med Entomol. 32: 490–502.

Reisen, W. K., H. D. Lothrop, and J. L. Hardy. **1995**. Bionomics of *Culex tarsalis* (Diptera: Culicidae) in relation to arbovirus transmission in southeastern California. J. Med. Entomol. 32: 316–327.

Reisen, W. K., H. D. Lothrop, S. B. Presser, M. M. Milby, J. L. Hardy, M. J. Wargo, and R. W. Emmons. **1995**. Landscape ecology of arboviruses in southern California: Temporal and spatial patterns of vector and virus activity in Coachella Valley, 1990–1992. J. Med. Entomol. 32: 255–266.

Reisen, W. K., H. D. Lothrop, and T. Thiemann. **2013**. Host selection patterns of *Culex tarsalis* (Diptera: Culicidae) at wetlands near the Salton Sea, Coachella Valley, California, 1998–2002. J. Med. Entomol. 50: 1071–1076.

Reisen, W. K., R. P. Meyer, R. F. Cummings, and O. Delgado. **2000**. Effects of trap design and CO2 presentation on the measurement of adult mosquito abundance using Centers for Disease Control-style miniature light traps. J. Am. Mosq. Control Assoc. 16: 13–18.

Reisen, W. K., M. M. Milby, and R. P. Meyer. **1992**. Population dynamics of adult *Culex* mosquitoes (Diptera: Culicidae) along the Kern River, Kern County, California, in 1990. J. Med. Entomol. 29: 531–543.

Reisen, W. K., and A. R. Pfuntner. **1987**. Effectiveness of five methods for sampling adult *Culex* mosquitoes in rural and urban habitats in San Bernardino County, California. J. Am. Mosq. Control Assoc. 3: 601–606.

Reisen, W. K., and W. C. Reeves. **1990**. Bionomics and ecology of *Culex tarsalis* and other potential mosquito vector species., pp. 254–329. *In* Epidemiol. Control Mosquito-Borne Arboviruses California, 1943-1987. California Mosquito and Vector Control Association, Sacramento, CA.

Reiesn, W. K., and S. S. Wheeler. 2019. Overwintering of West Nile virus in the United States. J. Med. Entomol. 56: 1498-1507.

Rochlin, I., A. Faraji, K. Healy, and T. G. Andreadis. **2019**. West Nile virus mosquito vectors in North America. J. Med. Entomol. 56: 1475–1490.

Rose, R. I. 2001. Pesticides and public health: Integrated methods of mosquito management. Emerg. Infect. Dis. 7: 23.

Schurich, J. A., S. Kumar, L. Eisen, and C. G. Moore. **2014**. Modeling *Culex tarsalis* abundance on the Northern Colorado Front Range using a landscape-level approach. J. Am. Mosq. Control Assoc. 30: 7–20.

Snow, W. E., and E. Pickard. **1956**. Seasonal history of *Culex tarsalis* and associated species in larval habitats of the Tennessee Valley region. Mosq. News. 16: 143–148.

Snyder, R. E., T. Feiszli, L. Foss, S. Messenger, Y. Fang, C. M. Barker, W. K. Reisen, D. J. Vugia, K. A. Padgett, and V. L. Kramer. **2020**. West Nile virus in California, 2003–2018: A persistent threat. PLoS Negl. Trop. Dis. 14: e0008841.

Sudia, W. D., R. W. Emmons, V. F. Newhouse, and R. F. Peters. **1971**. Arbovirus-vector studies in the Central Valley of California, 1969. Mosq. News. 31: 160–168.

Tachiiri, K., B. Klinkenberg, S. Mak, and J. Kazmi. **2006**. Predicting outbreaks: A spatial risk assessment of West Nile virus in British Columbia. Int. J. Health Geogr. 5: 1–21.

Talbot, B., M. Caron-Lévesque, M. Ardis, R. Kryuchkov, and M. A. Kulkarni. **2019**. Linking bird and mosquito data to assess spatiotemporal West Nile virus risk in humans. Ecohealth. 16: 70–81.

US Fish and Wildlife Service. **2021**. National Wildlife Refuge System. (https://www.fws.gov/refuges/).

USDA National Agricultural Statistics Service Cropland Data Layer. **2020**. Published crop-specific data layer. USDA-NASS. (https://nassgeodata.gmu.edu/CropScape/).

VectorSurv. **2021**. Vectorborne Disease Surveillance System. (https://vectorsurv.org/).

Vincent, G. P., J. K. Davis, M. J. Wittry, M. C. Wimberly, C. D. Carlson, D. L. Patton, and M. B. Hildreth. **2020**. Epidemic West Nile virus infection rates and endemic population dynamics among South Dakota mosquitoes: A 15-yr study from the United States Northern Great Plains. J. Med. Entomol. 57: 862–871.

Walton, W. E., E. T. Schreiber, and M. S. Mulla. **1990**. Distribution of *Culex tarsalis* larvae in a freshwater marsh in Orange County, California. J. Am. Mosq. Control Assoc. 6: 539–543.

Wang, J.-N., J. Hou, J.-Y. Zhong, G.-P. Cao, Z.-Y. Yu, Y.-Y. Wu, T.-Q. Li, Q.-M. Liu, and Z.-Y. Gong. **2020**. Relationships between traditional larval indices and meteorological factors with the adult density of *Aedes albopictus* captured by BG-mosquito trap. PLoS One. 15: e0234555.

Wekesa, J. W., B. Yuval, and R. K. Washino. **1996**. Spatial distribution of adult mosquitoes (Diptera: Culicidae) in habitats associated with the rice agroecosystem of Northern California. J. Med. Entomol. 33: 344–350.

Wood, S. N. 2011. Fast stable restricted maximum likelihood and marginal likelihood estimation of semiparametric generalized linear models. J. R. Stat. Soc. Ser. B (Statistical Methodol. 73: 3–36.

Wood, S. N. 2017. Generalized Additive Models: An Introduction with R, 2nd ed. Chapman and Hall/CRC, Boca Raton, FL.

Xia, Y., K. Mitchell, M. Ek, J. Sheffield, B. Cosgrove, E. Wood, L. Luo, C. Alonge, H. Wei, J. Meng, B. Livneh, D. Lettenmaier, V. Koren, Q. Duan, K. Mo, Y. Fan, and D. Mocko. **2012**. Continental-scale water and energy flux analysis and validation for

the North American Land Data Assimilation System project phase 2 (NLDAS-2): 1. Intercomparison and application of model products. J. Geophys. Res. Atmos. 117: D03109.

Conclusions and Summary

The maintenance and amplification cycle of West Nile virus (WNV) between avian reservoir hosts and mosquito vectors makes prediction of high-risk periods notoriously difficult in time and space. However, previous studies have linked certain environmental indicators with increased risk for human infections. This dissertation made use of routinely collected entomological data combined with easily accessible environmental data to provide tools for improving the estimation of WNV transmission risk and decision-making to enact vector control with the goal of human WNV disease prevention.

Chapter 1 examined the direct relationship between an entomological risk indicator, the vector index (VI), and human WNV disease incidence. The VI combines mosquito abundance and mosquito infection prevalence and is commonly used by vector control districts as a guideline for enacting vector control when the VI becomes elevated. However, a specific VI threshold indicating the transition between minimal and high risk of WNV transmission to humans has not yet been established. I utilized eleven years of historical entomological surveillance and reported human case data from six mosquito and vector control districts across California with two objectives. First, I examined the empirical relationship between the antecedent city-level weekly VI and the cumulative WNV disease incidence during the following three weeks. I used receiver operating characteristic (ROC) curve analyses, a method typically employed for establishing diagnostic testing thresholds, to determine the VI threshold which best predicted whether the observed incidence was higher than the typical three-week average for a given city. These thresholds varied depending on vector control district jurisdiction and the species and trap type data from which the VI was estimated. The thresholds were also dependent on the distribution of VIs for a given species and trap type. For example, in rural districts where *Culex tarsalis* is the predominant vector, I observed higher VI thresholds for *Cx. tarsalis* than for the *Cx. pipiens* complex, the predominant vector in urban areas. Furthermore,

the sensitivities and specificities of the estimated thresholds for predicting high-risk periods were highest for the dominant vector species in a given district.

The second aim of Chapter 1 was to evaluate the effect of spatial scale on the ability of the VI to predict human WNV disease incidence, because vector control operations typically work at the level of a small city, but WNV case occurrence can be sporadic at that scale. The same negative binomial regression model was applied to the same weekly data as the ROC analyses but was aggregated at four control-relevant spatial scales: district-wide, census county division, city, and zip code. Through ROC analysis of the modelled outcome, a positive predictive value of 0.17, sensitivity of 0.80, and specificity of 0.54 was found using city-level data, demonstrating a good balance between being small enough to be operationally relevant but large enough to have enough data to produce accurate predictions of high-risk periods.

Chapter 2 focused on the direct association between daily weather conditions and mosquito host-seeking activity to understand how single-day weather anomalies during trapping events could be introducing bias in trap counts used to estimate mosquito abundance. As mosquito abundance is a core component of the VI, misrepresentations of this metric could influence risk perception and the need for mosquito control efforts. For this chapter, mosquitoes and weather information were collected at ten trap sites around the rice-growing area of western Placer County, northern Sacramento County, and eastern Yolo County for two months during the peak mosquito season. This region was characterized by large populations of *Cx. tarsalis*, the rural WNV vector in California. A novel mosquito trap was used at each of the ten sites that featured a sensor to detect mosquito-sized objects entering the trap and recorded these counts every fifteen minutes to evaluate four outcomes: the overnight *Cx. tarsalis* count, the time when *Cx. tarsalis* host-seeking activity began, the time when the middle of *Cx. tarsalis* host-seeking activity occurred in a night, and the hour with the highest *Cx. tarsalis* count.

Each of these outcomes were related through statistical models to the wind speed and temperature recorded at a range of times in the afternoon leading to the host-seeking night. I

found both wind speed and temperature at 20:00h, or just prior to the onset of host-seeking, on average, to be significant predictors of all four outcomes. Notably, increasing wind speed was associated with lower overnight *Cx. tarsalis* activity whereas increasing temperature was associated with increased activity. What's more, there was little information loss using weather recorded earlier in the day, giving the opportunity for vector control districts to use this information to prepare for the upcoming evening. By evaluating the hour with the highest *Cx. tarsalis* count overnight, I identified predictable factors to guide the timing of adulticide applications that would have the maximum impact on a local vector population and thereby reduce the overall risk of WNV transmission.

Chapter 3 spatially estimated and predicted WNV risk. Spatial risk was depicted previously through the VectorSurv Gateway, the database for vector-borne disease surveillance in California, but these maps lacked both an estimate of uncertainty and the ability to predict risk in the near-term future. I focused initially on the prediction of *Cx. tarsalis* abundance in the Central Valley of California as the first element of a WNV risk estimation plan. The Central Valley experiences the highest WNV incidence in the state and has widespread distribution of *Cx. tarsalis* produced by irrigated agriculture. I used a spatio-temporal generalized additive model (GAM) to describe the nonlinear weekly seasonal trends of *Cx. tarsalis* abundance in a range of environments using thirteen years' worth of entomological surveillance data collected by vector control districts in the Central Valley. Overall, the model captured strong seasonal patterns in abundance, modified by local land use and ephemeral spatio-temporal anomalies. Models maintained a similar predictive accuracy for out-of-sample data compared to that for the training data set.

I used historical trap count data to mimic the progression of a surveillance season by fitting the model in series, sequentially adding weeks of data, and predicting weekly abundance across a 2.5 km grid of the Central Valley within 10 km of an observed trap for the week after the final week in the data used to fit that week's model. Overall, I observed an expected spatio-

temporal trend in *Cx. tarsalis* abundance across the predicted surface, with the highest abundance predicted to occur mid-summer around the rice growing areas of the northern Central Valley and around the wetland preserves of the southwestern Central Valley in all years. I also saw higher uncertainty around these high abundance areas where trap coverage was sparse.

Taken together, these three chapters provide a basis for improving WNV risk estimation through entomological surveillance. I worked closely with vector control districts across California to ensure that I were asking the right questions and working with data in a reproducible and generalizable way. Through this dissertation, I have shown how the VI could be used effectively as a threshold for identifying future high-risk periods but was most useful when tailored to the surveillance circumstances of the area being evaluated. I identified how the VI may be biased due to variability in the trap counts used to estimate mosquito abundance and thereby helped to improve the efficiency of vector control measures. Finally, I established a simple spatio-temporal model for *Cx. tarsalis* abundance that could be developed into a tool for enhanced spatial WNV risk estimation. Ultimately, these chapters will inform efforts to prevent human WNV disease through a more complete understanding of the link between WNV vector dynamics and the risk of human disease, improving the ability to predict risk and target mosquito control.